(12)

NAVSWC TR 91-645

PERFORMANCE OF REINFORCED POLYMER ABLATORS EXPOSED TO A SOLID ROCKET MOTOR EXHAUST

BY C. BOYER T. BURGESS J. BOWEN K. DELOACH
WEAPONS SYSTEMS DEPARTMENT

I. TALMY D. HAUGHT J. DUFFY J. ZAYKOSKI
WEAPONS RESEARCH AND TECHNOLOGY DEPARTMENT

OCTOBER 1992

NAVAL SURFACE WARFARE CENTER
Dahlgren, Virginia 22448-5000 • Silver Spring, Maryland 20903-5000

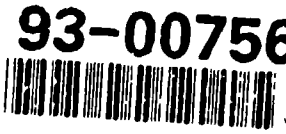

NAVSWC TR 91-645

PERFORMANCE OF REINFORCED POLYMER ABLATORS EXPOSED TO A SOLID ROCKET MOTOR EXHAUST

BY C. BOYER T. BURGESS J. BOWEN K. DELOACH
WEAPONS SYSTEMS DEPARTMENT

I. TALMY D. HAUGHT J. DUFFY J. ZAYKOSKI
WEAPONS RESEARCH AND TECHNOLOGY DEPARTMENT

OCTOBER 1992

NAVAL SURFACE WARFARE CENTER
Dahlgren, Virginia 22448-5000 • Silver Spring, Maryland 20903-5000

FOREWORD

The U.S. Navy is attempting to identify new ablators that can be used to protect guided missile launchers and ships' structures in order to increase the number of tactical missiles that can be launched prior to ablator refurbishment. A Navy/Industrial team was formed to participate in this task and consisted of representatives from Codes H13 and R31 at the Naval Surface Warfare Center Dahlgren Division (NSWCDD); FMC Corporation in Minneapolis, Minnesota (launcher manufacturer); 17 domestic ablator developers and manufacturers; and 1 Canadian composite developer. This task began in October 1990 as a joint effort funded by the Independent Exploratory Development (IED) Program and the MK 41 Vertical Launching System (VLS) Program Offices to identify and evaluate off-the-shelf ablators not currently used to protect Navy launchers. The task has been expanded to include: modifying existing ablator designs and evaluating these modified materials in FY 92; and developing and testing new ablators in FY 93.

The authors would like to acknowledge the support of this task by both the NSWCDD Independent Exploratory Development Program Office, Dr. Glen Moore (H023) and the MK 41 VLS Program Office, Mr. Mike Puig (G205). Thanks are extended to: Mr. C. Juhl, Mr. E. Hemmelman, and Mr. D. Dalenberg of ICI Fiberite, Inc.; Mr. S. Stephenson of Fiber Materials, Inc.; Mr. B. Hecht of Haveg Division of Ametek, Inc.; Mr. J. Hartman of Structural Polymer Systems, Inc.; Dr. J. Sakonia and Dr. S. Gonczy of Allied Signal, Inc.; Mr. H. Weatherly of American Poly-Therm Co., Inc.; and Mr. J. White of Swedlow, Inc. for providing the ablator samples at no cost to the Government. Dr. M. Norr (R34) is thanked for the scanning electron microscopy analysis and Dr. S. Dallek (R33) for the thermogravimetric analysis.

This report has been reviewed by Raymond W. Mattozzi, Head, Ship Engineering Branch, and Frank H. Maillie, Head, Combat System Safety and Engineering Division.

Approved by:

David Malyevac

DAVID S. MALYEVAC, Deputy Department Head
Weapons Systems Department

ABSTRACT

Summarized in this report is the effort by the Naval Surface Warfare Center Dahlgren Division (NSWCDD) and FMC Corporation (a launcher manufacturer) to identify new high performance ablators suitable for use on Navy guided missile launchers (GML) and ships' structures. The goal is to reduce ablator erosion by 25 to 50 percent compared to that of the existing ablators such as MXBE350 (rubber-modified phenolic containing glass fiber reinforcement). This reduction in erosion would significantly increase the number of new missiles with higher-thrust, longer-burn rocket motors that can be launched prior to ablator refurbishment. In fact, there are a number of new Navy missiles being considered for development and introduction into existing GML: e.g., the Antisatellite Missile (ASM) and the Theater High-Altitude Area Defense (THAAD) Missile.

The U.S. Navy experimentally evaluated the eight best fiber-reinforced, polymer composites from a possible field of 25 off-the-shelf ablators previously screened by FMC Corporation. They were tested by the Navy in highly aluminized solid rocket motor exhaust plumes to determine their ability to resist erosion and to insulate. Izod impact tests were conducted to characterize their flexibility and resistance to cracking. Finally, these materials were studied using scanning electron microscopy (SEM) and thermogravimetric analysis (TGA) to better understand the macroscopic behavior they demonstrated. Each of these new ablators tested at NSWCDD was only comparable to or significantly inferior to the existing in-service ablator MXBE350 when it came to erosion resistance in the presence of flows producing high convective heating and also heavily laden with aluminum-oxide particles. Hence the Navy and FMC are working with both domestic and foreign composite developers to modify existing ablator designs in hopes of achieving the desired performance improvements in 1992.

CONTENTS

ILLUSTRATIONS

ILLUSTRATIONS (Continued)

TABLES

INTRODUCTION

New ablative materials are being identified that can be used to replace those now protecting certain Navy guided missile launchers (GML) and ships' structures in order to increase the number of tactical missiles that can be launched prior to ablator refurbishment. These new materials will have to be more resistant to the heat transfer and erosion produced by new higher-thrust, longer-burn rocket motors being considered for introduction into fleet use. They must also be sufficiently flexible so as to bend with the launcher structure during missile firings, when necessary. The new ablators must also be capable of meeting these requirements in reasonable at-sea environments.

A new higher-performance ablator could be used to line the interior of the MK 41 Vertical Launching System (VLS) uptake extension section in order to protect it from the highly erosive exhaust plume of the MK 104 rocket motor used with STANDARD Missile-2 Block II (SM-2 Blk II), or the EX 72 rocket motor booster used with the SM-2 Blk IV. There are also other growth missiles being considered for launch from the VLS such as a new Antisatellite Missile (ASM) or even a Theater High-Altitude Area Defense (THAAD) Missile. It is likely that the rocket motors associated with these missiles will produce greater ablator erosion in the VLS gas management system (GMS) than the SM-2 Blk II or the SM-2 Blk IV. Other launchers could also benefit from introducing a new, thinner ablator to reduce total launcher weight, such as the MK 141 Harpoon launcher, or a more erosion-resistant ablator that could be used on the MK 13 GML.

This report will summarize a three-step investigation underway to identify such an ablator or ablators. The first step is to identify and evaluate all existing domestic ablators, not currently in use by the Navy on GML, that have the potential to meet all four of the following design goals:

1. 25 to 50 percent reduction of erosion,
2. reduction of thermal diffusivity,
3. adequate flexibility, and
4. capability of surviving realistic at-sea environments.

That task was performed in FY 91 and is reported here. The second step is to cooperate with the domestic ablator manufacturers in early FY 92 to modify and improve the best ablator concepts identified during FY 91, and to evaluate them. Furthermore, existing ablators developed by our Allies, such as France and West Germany, will also be evaluated. The second step is now underway, and a brief

summary of the progress will be given. Finally, if none of the above ablators meets all of the performance objectives, then work will begin in the latter half of FY 92, with the assistance of R31, to develop a totally new ablator concept.

A Navy/industrial team was formed to participate in this task and consisted of representatives from Codes H13 and R31 at the Naval Surface Warfare Center Dahlgren Division (NSWCDD), FMC Corporation in Minneapolis, Minnesota, seventeen domestic ablator developers and manufacturers, and one Canadian developer. This task began in October 1990 as a joint effort funded by the Independent Exploratory Development (IED) Program and the MK 41 VLS Program Office to identify and evaluate off-the-shelf ablators not currently used to protect Navy launchers. The task has been expanded to include modifications to existing ablator concepts in FY 92 and the development of new ablators in FY 92 and FY 93.

The approach taken in FY 91 was to identify new ablators and to develop an understanding of why these materials behave as they do, to become an educated consumer of these materials, instead of just measuring the performance of these materials. FMC Corporation and NSWCDD began contacting all of the known domestic ablator developers and manufacturers (as well as five Navy, NASA, and Air Force agencies) and describing the Navy's new ablator performance objectives. The goal of this survey was to identify all of the attractive existing ablators that could be evaluated. First, FMC conducted cost-efficient, subscale tests using a liquid-fueled rocket motor, whose plume was seeded with solid aluminum oxide particles, in order to identify the most promising ablator concepts. The best concepts were then tested by H13 personnel in more expensive, more realistic static solid-propellant rocket motor firings using MK 36 MOD 5 Sidewinder rocket motors. Scientists from R31 then assisted in the evaluation of the microscopic changes in these materials to gain a better understanding of why they performed the way they did. Each of these new ablators tested at NSWCDD was only comparable to or significantly inferior to the existing in-service ablator MXBE350, the benchmark in this test, in regard to the erosion resistance in the presence of flows producing high convective heating and also heavily laden with aluminum oxide particles. Thus, it was necessary to evaluate modified versions of the best FY 91 ablators, in hopes of finding the desired ablators.

SELECTION OF CANDIDATE ABLATORS

FMC and NSWCDD contacted ablator developers and manufacturers in FY 91 and asked for recommendations for materials that had the potential to meet the four design goals. Included in this list of companies were:

Aerospace Corporation,
Allied Signal, Inc.,
American Poly-Therm Co., Inc. (AP),
BP Chemicals,
Dow Corning Corp.,
Ferro Composites Division of Structural Polymer Systems, Inc.,
Fiber Materials, Inc. (FMI),
ICI Fiberite, Inc.,
Haveg Division of Ametek, Inc.,
Lanxide, Inc.,
Lockheed Missiles and Space Company,
LTV Missiles Division,
Martin Marietta Manned Space Systems,
Mortile Industries of Ontario, Canada,
Mosites Rubber Company,
Shin-Etsu,
Swedlow, Inc., and
Textron Speciality Materials, Inc.

Twenty-five new ablators not currently used by the Navy in GML were identified by FMC and NSWCDD as having the potential to meet the design goals. Finally, four additional in-service ablators were also included as benchmarks against which the new materials were compared. Twenty of these materials were reinforced phenolic resins, seven more contained elastomer matrices, and two additional ones were reinforced-ceramic matrix materials. The manufacturers provided, free of charge, the samples of all of these ablators for testing at FMC and, later, at NSWCDD.

The purpose of the FMC tests was to reduce the number of ablators that were to be tested in the more expensive solid rocket motor firings at NSWCDD. Hence FMC conducted subscale tests of all of the new materials and the four in-service benchmark materials.[1] These cost-effective tests consisted of exposing the samples to the supersonic exhaust plume of a kerosene-oxygen torch, simulating a liquid-fueled rocket motor. The plume was seeded with solid aluminum oxide particles, 3.6 percent by weight.[2,3] Four-inch square, half-inch thick test samples were located three inches from the exit plane of the rocket motor nozzle. The motor performance was adjusted to produce a measured convective heat flux of 650 BTU/ft^2-sec, reproducing the convective heating measured in the MK 41 VLS uptake extension section.

The FMC test facility is a useful tool for screening ablators; however, its limitations must be taken into account to properly extrapolate FMC test data to conditions observed in a solid rocket motor exhaust. There are several salient differences in the environment between those in the FMC liquid-fueled motor exhaust plume and those in an actual solid rocket motor plume. First, the percentage of aluminum oxide particles in a high-performance solid rocket motor is an order of magnitude greater than in the FMC subscale plume. Second, the aluminum oxide particles in an actual solid rocket motor exhaust are more likely to be liquid than

solid; whereas, they are solid in the FMC plume. These two differences produce competing effects on the ablator erosion. The erosion is increased as the percentage of aluminum oxide in the flow increases, but the erosion may decrease if the particles are liquid instead of the more abrasive solid ones. Third, the FMC plume is an oxidizing environment; whereas the solid rocket motor plume inside the VLS is fuel-rich once the oxygen is purged from the GMS, soon after the rocket motor is ignited. This difference between the two environments can result in significantly different erosion results when testing carbon containing materials or materials that produce carbonaceous chars.

The performance of each of these materials was ranked relative to that of MXBE350 using the following ablator data measured by FMC:

1. maximum erosion depth,
2. maximum back-wall temperature achieved after the test,
3. weight loss, and
4. appearance of the ablator heated surfaces during motor burn.

The seven best materials were chosen for further testing at NSWCDD:

1. FR1 by FMI,
2. CD208 by Haveg,
3. FM16771 by both Fiberite and American Poly-Therm,
4. FTR402 by FMI,
5. CA6304 by Ferro, and
6. Blackglas™ 6241 by Allied Signal, Inc.

After reviewing these test results, FMI suggested that NSWCDD also test two densified ablators, BLM/E and C^3, which were thought to be more erosion resistant than FR1 and FTR402. Finally, the glass-reinforced, rubber-modified phenolic ablator MXBE350, currently in use in the MK 41 VLS, was also included as a benchmark for testing at NSWCDD. A brief description of these materials is provided in Table 1, along with a summary of the tests in which they were evaluated.

These materials included a variety of matrices, reinforcement materials and reinforcement geometries. In this group are phenolic, modified-phenolic, densified-phenolic, and ceramic matrices. The reinforcement compositions include glass, carbon, and ceramic fibers, as well as a mixture of these fibers. The reinforcement geometry includes a continuous mat, chopped rovings, chopped fibers, and two-dimensional weaves. These materials represent an extensive cross section of the types of materials currently available from domestic manufacturers.

Additional information on the composition, physical properties, and physical characteristics of the ablators tested by NSWCDD are included in the following paragraphs. Some of this data is not presented because it was either proprietary or

not available from the manufacturer. It should be noted that all of the samples were nominally 10-inches square and 0.75-inch thick.

1. MXBE350 was developed by ICI Fiberite, Inc., 501 West Third St., Winona, MN 55987, and these samples were manufactured by Swedlow, Inc., 12122 Western Avenue, Garden Grove, CA 92641.

a. constituents:[4]
   1) 15 percent glass powder
   2) 43 percent glass mat
   3) 14 percent acrylonitrile-butadiene rubber
   4) 28 percent phenol-formaldehyde resin
b. virgin specific gravity (g/cc): 1.72[4]
c. virgin thermal conductivity at 20°C (cal/cm-s-K): 0.0015[4]
d. virgin specific heat at 20°C (cal/gm-K): 0.30[4]
e. compressive modulus (Mpsi): 1.2-1.6[5]
f. compressive strength (psi): 47005
g. cure temperature (°C):
h. MXBE350 was intended for use in the MK 41 VLS uptake.

2. FM16771 was developed by ICI Fiberite, Inc., and these samples were manufactured by both Fiberite and American Poly-Therm Co., Inc., 2000 Flightline Drive, Lincoln, CA 95648.

a. constituents:
   1) - percent single-stage resin
   2) - percent 1-inch chopped glass roving
b. specific gravity (g/cc): 1.84-1.92[6]
c. virgin thermal conductivity at 20°C (cal/cm-s-K):
d. virgin specific heat at 20°C (cal/gm-K):
e. compressive modulus (Mpsi):
f. compressive strength (psi): 16,400[6]
g. cure temperature (°C):

3. CA6304 was developed and manufactured by Ferro Composites Division of Structural Polymer Systems, Inc., 5915 Rodeo Road, Los Angeles, CA 90016.

a. constituents:[7]
   1) - percent phenolic resin
   2) - percent elastomer modifier
   3) - percent 1583 woven fiberglass
b. specific gravity (g/cc): 1.40-1.65[7]
c. virgin thermal conductivity at 20°C (cal/cm-s-K):
d. virgin specific heat at 20°C (cal/gm-K):
e. compressive modulus (Mpsi):
f. compressive strength (psi):

g. cure temperature (°C): 163[7]
h. CA6304 was intended for use as an external insulator where aerodynamic heating is a problem.[7]

4. FTR402 was developed and manufactured by FMI, 5 Morin St., Biddeford, ME 04005.

a. constituents:[8]
   1) - percent phenolic resin
   2) - percent unknown modifier
   3) - percent 2-D glass weave
b. specific gravity (g/cc):
c. virgin thermal conductivity at 20°C (cal/cm-s-K):
d. virgin specific heat at 20°C (cal/gm-K):
e. compressive modulus (Mpsi):
f. compressive strength (psi):
g. cure temperature (°C): 163[8]
h. FTR402 was intended for use as a fire resistant composite in aircraft interiors.[8]

5. BLM/E, a densified ablator that was reimpregnated with a structural epoxy, was developed and manufactured by FMI.

a. constituents:[9]
   1) - percent phenolic resin
   2) - percent chopped carbon fibers
   3) - percent epoxy impregnated into the pyrolyzed resin
b. specific gravity (g/cc):
c. virgin thermal conductivity at 20°C (cal/cm-s-K):
d. virgin specific heat at 20°C (cal/gm-K):
e. compressive modulus (Mpsi):
f. compressive strength (psi):
g. pyrolysis temperature (°C): 1100[9]
h. BLM/E is a research material.[9]

6. C3 was developed and manufactured by FMI. It was produced by pyrolyzing an FMI ablator CP1, a 2-D carbon weave impregnated with a phenolic matrix, and then reimpregnating it with the same phenolic.

a. constituents:[9]
   1) - percent phenolic resin
   2) - percent 2-D carbon weave
   3) - percent phenolic impregnated into the pyrolyzed resin
b. specific gravity (g/cc):
c. virgin thermal conductivity at 20°C (cal/cm-s-K):
d. virgin specific heat at 20°C (cal/gm-K):

e. compressive modulus (Mpsi):
f. compressive strength (psi):
g. pyrolysis temperature (°C):
h. C3 is a research material.[9]

7. FR1 was developed and manufactured by FMI.

a. constituents:[9]
   1) - percent phenolic resin
   2) - percent modifier
   3) - percent chopped ceramic fibers
b. specific gravity (g/cc):
c. virgin thermal conductivity at 20°C (cal/cm-s-K):
d. virgin specific heat at 20°C (cal/gm-K):
e. compressive modulus (Mpsi):
f. compressive strength (psi):
g. pyrolysis temperature (°C):
h. FR1 was originally intended to protect hardware from extreme thermal and erosive environments.[9]

8. Blackglas™ ceramic matrix composite 6241 was developed and manufactured by Allied Signal, Inc., 101 Columbia Road, Morristown, NJ 07962-1021. At the request of the manufacturer, the test results for this material are not being reported.

a. constituents:[10]
   1) 56-62 percent densified silicon carboxide matrix
   2) 44-38 percent carbon coated 2-D Nicalon weave[11]
b. specific gravity as tested (g/cc): 1.75-1.99[11]
c. virgin thermal conductivity at 20°C (cal/cm-s-K): 0.0024[12]
d. virgin specific heat at 20°C (cal/gm-K): 0.19[12]
e. compressive modulus (Mpsi): not determined
f. compressive strength (psi): not determined
g. pyrolysis temperature (°C): <1000[10]
h. Blackglas™ ceramic is intended for fabricating radomes and structural composites, which operate in the range of temperatures of 400-1200°C.[10]

9. CD208 was developed and manufactured by the Haveg Division of Ametek, Inc., 900 Greenbank Road, Wilmington, DE 19808.

a. constituents:
   1) - percent H41N phenolic resin
   2) - percent talc filler
   3) - percent chopped glass fibers
   4) - percent chopped carbon fibers
   5) - percent chopped ceramic fibers

b. specific gravity (g/cc):
c. virgin thermal conductivity at 20°C (cal/cm-s-K):
d. virgin specific heat at 20°C (cal/gm-K):
e. compressive modulus (Mpsi):
f. compressive strength (psi):
g. cure temperature (°C):
h. This material was derived from Haveg H41N, which is currently being used on Navy GML.

NSWCDD ABLATOR TEST FACILITY

The NSWCDD tests were conducted in the ablator test facility at the Terminal Range, NSWCDD. This test facility, shown in Figure 1, consists of a live MK 36 MOD 5 Sidewinder rocket motor, a rocket motor restraint stand, an ablator mounting frame, a T-plate for rigidly restraining both the restraint stand and mounting frame, four ablator samples, an instrumentation system, an instrumentation bunker, and a personnel shelter. This test configuration has been used for over 12 years.

The three-foot standoff distance between the rocket nozzle exit plane and the test ablators has been used frequently, thus an extensive amount of ablator erosion data has been collected at this distance.[13] Four ablators are mounted on an aluminum plate, as shown in Figure 1, so that their inside corners meet on the axis of the rocket; furthermore, the front surface of the ablators is normal to the rocket motor axis. This ensures that the heating and flow conditions on the front of each of the four ablators is the same. This arrangement results in an ablator erosion pattern similar to that in Figure 2, where the maximum erosion does not occur along the centerline of the rocket motor. Figure 2 is a three-dimensional plot of the surface of a piece of Ferro CA6304 ablator after a Sidewinder rocket firing, where the erosion was maximum at a radius of approximately 2.75 inches from the centerline of the rocket motor, with decreasing erosion observed both inside and outside of that radius. An erosion pattern of this shape implies a radial heat flux distribution similar to that in Figure 3 (G. Soo Hoo, H13), if it is assumed the erosion is due only to thermal effects, with no mechanical abrasion.

This heat flux distribution is difficult to understand without an explanation such as that provided by Soo Hoo, Moore, and Anderson.[14] At this standoff distance, the supersonic underexpanded Sidewinder plume impinging on the originally flat ablator surface produces a

> "maximum static pressure on the plate (not) at the center of jet impingement, but rather on a circle (at some distance) from the center of impingement. Corresponding to the off-axis peak in the plate static

pressure distribution, the flow has been observed to have a recirculation region inward of the maximum static pressure. (Figure 4) shows the general flow pattern that exists in the central stagnation region. Flow exiting the nozzle is diverted from the center of the plate by the stagnation bubble.. Inside the bubble, a vortical flow develops such that velocities along the plate are directed toward the centerline and velocities along the centerline are opposite in direction to the jet itself...Additional considerations have to be made for a jet which contains particulate matter. For instance, the use of metal additives to increase the performance of solid propellant rocket motors yields condensed metal oxide combustion products in the exhaust gases...Thus when considering ablation and erosion of the plate surface, the kinetic energy flux due to particles impacting the plate must be considered in addition to the effects of heat transfer from the gases... (Small) particles closely follow the fluid flow and are turned away from the plume centerline and are caught up in the flow along the edges of the stagnation bubble. The intermediate (size)...particles located near the centerline traverse the plate standoff shock, but they are decelerated sufficiently to become entrained in the recirculatory flow. The intermediate sized particles initially found further out radially along the exit plane, however, travel an almost direct route to impact the plate. The large...particles also possess the momentum to traverse across both the normal shock and the recirculatory flow to directly impact the plate...The stagnation bubble alters the particle trajectories such that the maximum kinetic energy flux occurs away from the centerline at the extremities of the recirculatory flow."

A subsequent analysis by Soo Hoo predicted the particle kinetic energy distribution on a flat ablator for the MK 36 rocket motor with a three-foot standoff (see Figure 5). There is no significant particle kinetic energy flux inside a radius of one inch; it peaks at approximately 2.5 inches and then decreases with increasing radius. This energy flux distribution is reasonably consistent with the total energy flux in Figure 3 and with the erosion pattern in Figure 2.

Considering both the gaseous flow pattern and the particle energy flux distribution, it becomes apparent that the NSWCDD test configuration permits the Navy to evaluate the erosion produced by two different flow impingement conditions. From the centerline out to a 4-inch radius, the erosion and heating is primarily due to the gaseous convective heating and particle kinetic energy flux, of which both are significant and of comparable magnitude. Outside the four-inch radius, the total energy flux decreases rapidly and becomes more dependent on convective heating from tangential and obliquely impinging flows.

TEST PROCEDURES

A Standard Operating Procedure (SOP)[15] for conducting this test and the Procedures for Testing Ablative Samples with Sidewinder Rocket Motors (Appendix A) provide the detailed instructions required to prepare for and conduct this test, as well as the responsibilities of the project, instrumentation, and test personnel. The procedures in this appendix reflect the lessons learned during the testing conducted in FY 91, and a discussion of the significant changes made from the procedures used last year will be briefly discussed in the Conclusions and Recommendations section of this report.

Three types of data were measured by H13 during and immediately after the Sidewinder tests:

1. erosion of the entire heated surface,
2. back-wall temperature histories, and
3. a visual inspection of the heated surface after the test.

Additional data was gathered at a later date by R31 using scanning electron microscopy (SEM), thermogravimetric analysis (TGA), and Izod impact tests.

The four, 10-inch square samples were attached to the 24-inch square, 0.75-inch thick aluminum backing plates using a trowelable FMI ablator FLEXFRAM 605TH as an adhesive. The two-inch border all the way around the four ablator samples, Figure 1, was also filled with the same FLEXFRAM ablator to:

1. protect the exposed edges of the adhesive, which bonds the samples to the aluminum plate, from the exhaust plume, and

2 help thermally insulate the aluminum plate from the exhaust plume.

It was important that the back-wall temperature of the ablators not be biased by any heat absorbed by the aluminum plate. Once the FLEXFRAM had cured, the total thickness of the samples, the FLEXFRAM, and the aluminum plate were measured at the NSWCDD Gauge Lab. Measurements were made over the entire front surface of each sample using the one-inch grid shown in Figure 6. Extreme care was taken when locating each measurement point to insure that it could again be located exactly after the test, since the difference between the pretest and posttest thickness measurements determined the erosion at that gauge point.

The back-wall temperature history of each sample during and after the rocket motor firing was a qualitative indication of its combined thermal diffusivity and the magnitude of its endothermic decomposition reaction. In this report, no attempt was made to extrapolate measured back-wall temperature data to a particular launcher/

rocket motor combination. Back-wall ablator temperatures were measured using OMEGA CO1-K type-K thermocouples attached directly to the back of the ablator using OMEGABOND 200, a high-thermal conductivity epoxy that had a service temperature of 500°F. The thermocouple was attached to the ablator after the aluminum plate and four ablators were gauged for pretest thickness. There was a 1.5-inch hole in the aluminum plate behind each of the four test plates at a radius of 2.5 inches (see Figure 7) to allow access to the back of the ablator and to minimize heat transfer between the thermocouple and the aluminum backing plate.

The aluminum plate with four ablator samples was bolted to the test stand (see Figure 1) and precisely aligned, with the assistance of a small wattage laser mounted in an actual, inert MK 36 rocket motor. The laser was mounted in the motor case such that its beam was collinear with the axis of the motor case. The four ablators were centered on the rocket motor axis using this laser beam to align the rocket motor axis with the four inside corners of the ablators. The thermocouple reference junctions in Figure 7, one for each of the four ablator thermocouples, were wrapped in NEXTEL cloth and placed in the sealed metal container on the back of the test stand (see Figure 8). The leads from these reference junctions were wrapped with NEXTEL cloth and suspended from the test stand to keep them directly behind the center of the aluminum plate for protection from the rocket motor exhaust shown in Figure 9, as viewed from behind the test stand.

Two VHS video cameras and 35mm still photography were used to record the test hardware before, during, and after the tests. The exhaust plume was opaque and prevented a detailed observation of the heated surfaces of the ablators during the test. However, much information could be gleaned from both the videos and stills taken during the tail-off of the motor burn and after the test.

The aluminum oxide from the rocket exhaust was removed from the heated surface of each of the ablators after the test samples cooled down, but before the post-test thickness measurements were made. Care was taken to try to remove only the oxide and not the sublayer of ablator char. If the oxide could not be lifted off by hand, the plastic end of a screwdriver was tapped against the oxide to break it free from the char. The posttest thickness of the aluminum plate and samples were measured at the NSWCDD Gauge Lab, using the grid in Figure 6, taking care to use the same pretest gauging points. The procedures for removing the aluminum oxide and for gauging ablator thickness were changed after the tests reported here, and will be discussed later in the Recommendations and Conclusions section.

Five static rocket motor tests were conducted at NSWCDD in the spring and early summer of 1991 and the results of these tests will now be discussed. A summary of the materials tested is presented in Figure 10 and Table 1. The five tests will be referred to as SW1 through SW5; the plate in the upper left-hand corner in each test is labeled 1, the plate in the upper right-hand is 2, and so forth, as shown in Figure 10.

TEST RESULTS

The data documenting the ablator performance, recorded both during and after these five tests, include:

1. photographs of the appearance of the ablators,
2. erosion over the entire heated surface,
3. back-wall temperature histories,
4. compression modulus,
5. Izod impact strength,
6. SEM photographs, and
7. TGA measurements.

The first four categories of data were measured by H13, while the last three were measured by R31. The first three categories document the macroscopic behavior and character of the ablators; the fourth and fifth describe the mechanical properties of the virgin material; and the sixth and seventh provide insight into the microscopic and macromolecular nature of these ablators, which dictate the macroscopic behavior. The test team felt that the last two categories of data are particularly helpful to them as they tried to become educated consumers, a step beyond being just cut-and-try users.

GENERAL APPEARANCE AND EROSION

Virtually all of the ablators experienced an erosion pattern similar to that shown in Figure 2, where the maximum erosion occurs at approximately 2.75 inches from the center of impingement. Some ablators delaminated faster than they eroded, and have a different shape surface after the test. Most of the ablators were coated, to some extent, with a layer of aluminum oxide after the test similar to that shown in Figure 11. The aluminum oxide coating was relatively thin from the center of impingement out to about a radius of four inches. From four inches to the outside edges of the ablator, the coating became thicker and was on the order of 80 mil thick. The aluminum oxide coating was usually robust and broke off the surface in large pieces, as can be seen in Figure 12 next to a lens cover from the still camera. There were exceptions to this, and they will be dealt with later as each material is discussed separately. Many of the ablators continued to burn after the end of motor burn; e.g., MXBE350 for less than 5 seconds, FTR402 for about 5 seconds, FM16771 for 10 seconds, CD208 for 12 seconds, FR1 for 15 seconds, and BLM/E for approximately 25 seconds. C^3 and CA6304 did not burn after the test.

Three erosion statistics were derived from the 121 thickness measurements (Figure 6) made before and after the test. The maximum erosion was recorded; it always appeared inside the four-inch radius. The average central erosion was determined by averaging the 17 erosion values on or inside the four-inch radius. The average central erosion was a qualitative indication of the resistance of the ablator to the erosion, produced by the high convective heating from recirculating gas flows and by the near perpendicular impingement of aluminum oxide particles. The average peripheral erosion was evaluated by calculating the mean of the 28 erosion values outside the four-inch radius, and on or inside the seven-inch radius. The average peripheral erosion was an indication of the resistance of the ablator to lower levels of convective heating produced by tangential or obliquely impinging gas flows containing little or no oxide particles.

The in-service ablator MXBE350 had a very thick coating of aluminum oxide outside the four-inch radius and a much thinner coating inside that radius. The coating was firmly attached to the char, because it wrapped itself around the glass fibers at the heated surface, which were uncovered when the ablator matrix decomposed. When this coating was removed after the test, it took some of the decomposed ablator with it, leaving the fiber reinforcement exposed (see the left side of Figure 13). A three-dimensional plot of the surface of the MXBE350 sample from test SW2 is presented in Figure 14; note that the coating had already been removed when this data was measured. A contour plot of the MXBE350 surface after test SW2 is presented in Figure 15. The average peripheral erosion in the annulus between the four- and the seven-inch radii for MXBE350 in tests SW1, SW2, and SW5 were 90, 80, and 100 mils, respectively; see Table B-1. The average central erosion for each of these tests was 320, 290, and 300; see Table B-2. The maximum erosion for MXBE350 for each of these tests was 510, 420, and 430 mils ,respectively; see Table B-4.

After the testing, FM16771 was covered with a coating of aluminum oxide similar to that on MXBE350; i.e., thin inside the 4-inch radii and much thicker outside. Apparent in Figure 16 is a circumferential variation in the erosion in the annulus between the radii of two and three inches, similar to what is shown in Figure 15. This is a common but unexplained observation in restrained Sidewinder tests at this standoff distance.[13] It is speculated this is caused by the star perforation design of the propellant grain in the MK 36 MOD 5 motor. The average peripheral erosion of the Fiberite material from tests SW1 and SW3 was 20 and 30 mils, respectively; whereas, in the American Poly-Therm material from tests SW3 and SW4, it was 30 and 40 mils, respectively. The average central erosion of the Fiberite materials was 320 and 280 mils; for the American Poly-Therm ablators, it was 270 and 320 mils. Finally, the maximum erosion in the Fiberite version was 520 and 470 mils, in comparison to the American Poly-Therm materials' erosion of 460 and 440 mils. The erosion of both versions of FM16771 was similar. The erosion measured inside the four-inch radius, for both versions of FM16771, is comparable to that of MXBE350; there was much less erosion outside the four-inch radius.

CA6304 was only slightly coated (if at all) with aluminum oxide after the motor firings. In the peripheral region, the heated surface was flat (see Figure 17), and the original weave pattern could be recognized. Posttest photographs indicate that some of the laminates may have peeled away, taking with them the aluminum oxide coating. CA6304 experienced equal or greater erosion than MXBE350 in all three categories. In the peripheral region, CA6304 had average erosions of 110 and 130 mils; average central erosions of 330 and 340 mils were measured, and maximum central erosions of 510 and 560 mils were recorded.

FTR402 performed comparably to, or worse than MXBE350 on the basis of erosion. In the outer region, average erosions of 70 to 90 mils were recorded; inside the four-inch radius, average central erosion was on the order of 360 to 370 mils, and the maximum erosion was approximately 510 to 520 mils. There was only a very thin coating of aluminum oxide, but it was firmly attached to the peripheral surface.

Another FMI material, BLM/E, was also tested and exhibited very low erosion, generally much lower than MXBE350. Its average peripheral erosion was negligible, its average central erosion was 210 mils, and its maximum erosion was 360 mils. It also exuded a thick, brown, uncharred liquid from its lower corners after the test was over. The brown liquid may have been the structural epoxy used in the densification of BLM/E.

One sample of C^3 was evaluated in test SW4, and it experienced the maximum surface recession seen in this series of Sidewinder tests. This surface recession was attributed to delamination, which occurred at such a dramatic rate as to be observed from the personnel shelter hundreds of feet away, as shown in Figure 9. The large black squares above the test stand are pieces of this material and another ablator, both of which came apart layer-by-layer during the test. At the end of the test, the C^3 is shown in the upper right-hand corner of Figure 18. The surface of the C^3 was almost entirely flat, with the exception of a slight mound near the center of impingement, and there was hardly any aluminum oxide on the surface. The absence of aluminum oxide is probably due to the fact that the delamination process continuously removed it as soon as it was deposited. Figure 19 is an example of the debris around the test stand after test SW4. The average peripheral erosion was 560 mils; the average central erosion was 490 mils (this average was affected by the mound of ablator remaining near the center of impingement), and the maximum erosion was 610 mils.

FR1 performed very well from the erosion standpoint (as shown in Appendix B), and in all cases, it performed as well as or better than MXBE350. The average peripheral erosion ranged from 10 mils of increase in surface height in test SW3 to 30 mils of erosion in SW2. The average central erosions were 240 and 270 mils, while the maximum erosions were 460 to 470 mils. Immediately after test SW2, the heated surface appeared relatively flat outside the four-inch radius. At the time the photograph in Figure 20 was taken, less than 10 minutes after the motor firing, one of the corners had lifted up. That corner lowered somewhat after the entire

sample cooled down. One possible explanation for this phenomenon is that the back of the FR1 expanded as the heat from the middle of the sample reached the back surface. At the same time, the exposed front surface began contracting as it cooled down, as it lost heat to the air in front of the sample. Thickness measurements in Figures 21 and 22, with the aluminum oxide removed, revealed that the FR1 remained distorted even after it cooled down. If the FR1 lifted off of the aluminum backing plate, the reported erosion measurements for test SW2 were in error by the distance it raised from the aluminum plate. Finally, this material also exhibited a radial layer of aluminum oxide after the test, especially near the outer edges of the sample, as shown in Figure 20.

Finally, the erosion measured in CD208 (Figure 23) was comparable or less than that of MXBE350; however, that is a qualified statement. The average peripheral erosion for CD208 was between -10 mils (SW3), due to expansion and/or distortion, and 20 mils; average central erosions of 150 (SW3), 220, and 300 mils were observed; and the maximum erosions of 320 (SW3), 420, and 530 mils were measured. These apparent erosions exhibited a much wider range of variation than was observed for any other material. One possible explanation for this large variation in erosion was apparent after looking at the upper right-hand ablator sample in test SW3 (Figure 24). There was a small pit or depression at a radius of two to three inches from the center of impingement. A cross section of this sample, cut along the diagonal from the center of impingement to the opposite corner, revealed a cavity parallel to the heated surface. There was a cavity inside the CD208 sample in test SW3. It could be argued the thickness of this cavity should be added to the erosion if the cavity first appeared during the test. Discussions with Haveg[16] indicated that these samples were not made using the same procedures employed in production; i.e., the sample was not cured under compression. Furthermore, an examination of the R31 SEM data, which will be discussed later, offered another possible explanation for the cavity in this sample of CD208.

A comparison of the average peripheral erosion data in Figure 25 indicates that CD208, FR1, and FM16771 were more erosion resistant in the outer regions of flow impingement than MXBE350. The heating in this region is probably more convective in nature, and the aluminum oxide particle kinetic energy heating is less significant than inside the four-inch radius. FTR402 erosion is comparable to that of MXBE350 under these circumstances, and the CA6304 is less erosion resistant.

None of the new ablators is significantly different from MXBE350 in terms of average or maximum erosion in the central region of impingement, where the convective and aluminum oxide particle kinetic energy heating are both high and comparable. Figures 26 and 27 summarize these categories of erosion for the six best-performing ablators. The data in Figures 26 and 27 are reported in the same order from left to right as in Figure 25, and use the same graphic shading patterns as well. The variation in the performance of CD208 is the largest of the ablators that is reported.

BACK-WALL HEATING

All of the back-wall temperature history data that was recorded is presented in Figures 28, 29, and 30. The fiducial time was motor ignition time, and all of the materials reached their peak back-wall temperature well after the end of the motor burn. It should be noted that significantly different back-wall soak temperatures were recorded for each different material in any one test; this indicated that the thermocouples recorded the ablator temperatures and not those of the aluminum plate. The temperature data in tests SW1 and SW3 were lost due to the thermocouple leads being destroyed by the rocket exhaust plume; see Figure 9. The thermocouple leads were not adequately insulated in test SW1; the insulation on the leads was increased somewhat in test SW2, and all of the data were recorded. In test SW3, the leads were insulated as in test SW2, but the hot plume did more damage to the leads than in any other test, and again the data was lost. After test SW3, the NEXTEL insulation on the thermocouple leads was again increased, and there were no problems with the instrumentation on tests SW4 or SW5.

Unfortunately, for purposes of this survey the peak back-wall temperatures of all of the off-the-shelf ablators were, at best, comparable to or higher than those of the in-service ablator MXBE350, which was 95-120°F; see Appendix C. This indicated that none of the ablators was a better insulator than MXBE350. Thermocouples on the back of FM16771 and CA6304 recorded comparable temperature rises of 125 to 130°F. CD208, FTR402, and FR1 experienced significantly higher temperature rises than MXBE350; i.e., 165, 170, and 190°F, respectively. C^3, as expected, had a very high back surface temperature rise of 425°F, partially due to the delamination already described. The ablator BML/E exhibited the highest recorded back-wall temperature rise of 450°F. The bar chart in Figure 31 compared the maximum back-wall temperature rise of all of these materials and presented the data in the same left-to-right order as used in the erosion bar charts. The same shading patterns for the bars were also used to facilitate a comparison of the ablators' performance.

FLEXIBILITY

Virgin samples of the best performing ablators (from the standpoint of average peripheral erosion) were evaluated in Izod impact testing by R31; their impact strengths were measured and reported here. The impact strength was not intended to be a measure of flexibility, but it did give an indication of the resistance of the virgin material to crack propagation. The results of this test are presented in the bar chart in Figure 32. Relative to MXBE350, only FM16771 had a higher impact strength, while CD208 and FR1 had strengths nearly an order of magnitude lower.

The compression modulus of the same four ablators and MXB360 were measured by H13 in a four-point bend test fixture. Emphasis was placed on the compression characteristics of these composites because of the current interest in

finding an improved VLS uptake ablator. In the VLS uptake, the ablator is attached to a steel wall, and the neutral axis is in the steel. Hence, the ablator is entirely in compression when the uptake flexes during a missile's firing. MXBE350 is similar to MXB360; i.e., the only difference between the two is that the matrix of the former contains a rubber modifier, 33 percent by weight, whereas the latter does not. As expected, MXB360 was much more rigid than MXBE350 (see Figure 33). Both the Fiberite (F) and the American Poly-Therm (AP) versions of FM16771 were tested, with significantly different results. The Fiberite version was much more rigid than MXBE350, and the American Poly-Therm version had a modulus similar to that of MXBE350. FR1 had a modulus comparable to that of MXBE350, while CD208 was nearly twice as rigid as MXBE350.

Knowledge of the compression modulus alone does not provide adequate information to determine whether or not an ablator is sufficiently flexible to meet the requirements of a particular application; e.g., the ablator in the VLS extension uptake section.[5] A corresponding minimum compression strength is a second parameter that must be considered. Hence, the compression strength of the materials tested here must also be measured to determine whether or not any of them would be flexible enough for use in the VLS uptake.

SCANNING ELECTRON MICROSCOPY

R31 performed scanning electron microscopy (SEM) evaluations of MXBE350, FM16771 (both Fiberite and American Poly-Therm versions), FR1 and CD208 ablators. The fracture surfaces of virgin and charred regions were examined for all the samples after the NSWCDD test. The FR1 samples were evaluated after both FMC and NSWCDD tests. The SEM micrographs of all samples are presented on Figures 34-40. The purpose of this investigation was to derive possible correlations between microstructure and macroscopic performance of the materials during the tests: erosion resistance, heat transfer, and flexibility. Unfortunately, the charred surfaces of the NSWCDD-tested materials were significantly damaged by removal of the aluminum oxide coating regardless of how carefully it was done. As a result of that, only limited information could be gained from the evaluation of the charred areas. In the future, the procedure for evaluation of erosion microstructure of the charred surfaces after the NSWCDD test will be changed to permit both examinations to be more informative. A detailed description of the new procedure is discussed in the Conclusions and Recommendations section.

Fracture surfaces of the virgin areas of the MXBE350 and FM16771 (both Fiberite and American Poly-Therm) samples exhibited pull-out of the reinforcing fibers (Figures 34A, 35A, and 36A). This type of fracture behavior is an indication of increased toughness of materials and correlates very well with the Izod test data where these materials demonstrated the highest impact strength. Contrary to that, the FR1 and CD208 samples (Figures 37 and 38) did not show any noticeable fiber pull-out and, correspondingly, had low Izod impact strength. The presence of

reinforcing fibers of irregular shape and high amount of glass droplets was determined in the structure of the FR1 ablator (Figure 37) The SEM micrographs of the virgin CD208 material (Figure 38) show smaller diameter silica and aluminosilicate fibers and much larger diameter carbon fibers. They also reveal the absence of the matrix around reinforcing fibers in some areas, which probably represents internal voids such as those already discussed relative to the CD208 sample in test SW3 (Figure 24). This condition could be caused by incomplete mixing of the resin and reinforcing fibers during manufacturing. The defects found in the FR1 and CD208 ablators could also contribute to the low values of impact strength.

The charred areas of the MXBE350 and FM16771 samples (Figures 34B, and 35B, and 36B) appear to be very dense with slight traces of the residual silica-rich glass fibers, which were melted during the test, and infiltrated carbon char from matrix decomposition. The SEM micrographs of the charred area of the CD208 sample (Figure 39) do not show any indications of a matrix present. The melt from silica and aluminosilicate fibers bonded the carbon fibers, holding them together. The results of the NSWCDD and FMC tests are compared in Figures 40A and 40B for the FR1 ablator. The glass fiber reinforcement was still clearly distinguished in the charred region of the sample subjected to the NSWCDD test. Contrary to that, no fibers were found in the charred area of the material after the FMC test. The droplets of solidified glass melt from the fibers are clearly identified in the SEM micrograph (Figure 40B). These differences can be an indication of more severe conditions; e.g., higher heating, in the FMC tests or the result of removing the aluminum oxide from the charred surface of the NSWCDD samples.

THERMOGRAVIMETRIC ANALYSIS

The TGA results from the R31 evaluation of MXBE350, FR1, CD208, and FM16771 were summarized in Figure 41. The heating rate was 20°C/minute, and the environment used in the test was helium. The MXBE350 decomposed significantly over a very narrow range of temperatures and reached the lowest residual mass of the four materials tested. The sudden weight loss beginning at about 350°C was due to the decomposition and low char yield of the rubber modifier; the modifier is less thermally stable than the more highly cross-linked phenolic matrix. The other materials decomposed more gradually over a wider range of temperatures and achieved higher residual masses; CD208 had the highest, followed by FM16771 and FR1.

CORRELATION BETWEEN THE FMC AND NSWCDD RESULTS

The FMC tests were a crucial step in the ablator screening process; they provided a cost effective means of evaluating and reducing the original long list of ablators being considered. Thus, this reduced the number of more expensive, more realistic NSWCDD solid rocket motor tests that had to be performed. At the end of

the FY 91 testing, it was appropriate to determine whether or not the FMC liquid-fueled rocket exhaust tests produced the same trends in erosion and back-wall heating that were observed in the NSWCDD solid rocket motor tests. If not, then the FMC test procedures or methods of interpreting the FMC test results would have to be modified before continuing with the FY 92 testing. It was not unreasonable to anticipate that the two tests might yield somewhat different results, considering the known differences in the natures of the two plumes. The FMC plume was an oxidizing environment, and the NSWCDD plume was not. The aluminum oxide particles in the FMC plume were solid and more abrasive than those in the NSWCDD plume, which were largely molten liquid. The molten particles were hotter and more likely to be in kinetic equilibrium with the gas flow than were the solid particles in the FMC plume. The particles in the FMC test were larger, 5 to 100 microns in diameter,[1] than those in the NSWCDD test, which were smaller than 10 microns in diameter.[14] The gas flow patterns in each plume also had the potential to affec the heating and erosion of the ablative samples, and nothing guaranteed the two were similar.

A plot of the measured NSWCDD average peripheral erosion (the abscissa) versus the measured FMC maximum erosion (the ordinate) in Figure 42 indicated that there was a reasonable correlation between the two. However, similar plots of NSWCDD maximum erosion versus FMC maximum erosion (Figure 43), and of NSWCDD average central erosion versus FMC maximum erosion (Figure 44), showed little correlation among all the data as a whole. In fact, Figures 43 and 44 may imply that the rubber-modified ablators, MXBE350 and CA6304, should have been compared only with each other and not to the remaining materials discussed here, which were not rubber-modified. Similarly the unmodified ablators should have been compared only with the other unmodified ablators. This is logical, considering that rubber-modified ablators tend to be much softer and more susceptible to mechanical erosion by solid particles than would be expected of the unmodified ablators.

The plot in Figure 45 of the maximum back-wall temperatures measured by NSWCDD (the abscissa) and those measured by FMC (the ordinate) revealed absolutely no correlation between the two measurements. The FMC thermocouples were attached to the metal backing plate, where the NSWCDD thermocouples were attached to the ablator and isolated from the aluminum backing plate. It is conceivable that the FMC torch was able to heat the backing plate from both the side and the back, since there was no protection around the periphery of the sample. The lack of correlation in back-wall temperatures could also have been due to a difference in the ablator erosion patterns between the two tests. The FMC erosion is a relatively narrow and deep cavity directly over the thermocouple, in comparison to the pattern described earlier for the NSWCDD tests. Finally, the flow dynamics of the two plumes could well have been entirely different, thus affecting the radial heat flux distribution and the relative contributions of convective, particle kinetic, and particle thermal heating.

COMPARISON OF CURRENT AND PREVIOUS EROSION RESULTS

The maximum erosion measured during the present MXBE350 tests compares favorably with that measured during the 1979 tests.[13] The two sets of data are plotted together in Figure 46. The three pieces of data for MXBE350 at a standoff distance of three feet (three from this test series and one from Reference 13) are reasonably similar. The two maximum erosion measurements from this test, made without rigorous wire brushing, were within approximately 15 percent of, and only slightly higher than, the earlier MXBE350 data.[13] The variation between the two tests could have been due to the differences in the materials caused by changes in the formulation over the last twelve years, or perhaps were due to the processing variations between manufacturers. It should also be noted that erosion for MXBE350 and MX3360 are comparable at both 0.5- and 3-foot standoffs. This is different from the FMC test results, which indicate that the rubber-modified MXBE350 eroded more than twice as much as the unmodified MXB360.[1,3]

CONCLUSIONS AND RECOMMENDATIONS

A number of the ablators demonstrated relatively high erosion resistance, good insulation properties, or flexibility when compared to the in-service ablator MXBE350 (the benchmark for this study). However, under the conditions of highly convective heating from flows heavily laden with aluminum oxide particles, the erosion resistance of these new ablators was only comparable to or significantly inferior to the benchmark. Hence the Navy and FMC are now working with both domestic and foreign composite developers to modify existing ablator designs in hopes of achieving the desired performance in 1992.

The work with domestic ablator developers began with a series of meetings, one manufacturer at a time, to discuss the performance of their materials in the FY 91 FMC and NSWCDD tests. Furthermore, R31 personnel made recommendations in those meetings to each manufacturer as to how to improve their materials and what new approaches could be taken. As a result of these five separate meetings, forty-three new ablator concepts were proposed. Some of these concepts differed by only one design feature; the purpose of these materials was to evaluate the effect of one change at a time on erosion, back-wall temperature, and flexibility. The remaining materials represented the best educated guesses at how to improve ablator performance. Some of the innovative concepts included: polyimide matrices; silicone matrices; sandwich constructions, such as an erosion resistant layer on top of an insulating layer; various reinforcement geometries; new reinforcement materials; and finally, new filler materials. The exact descriptions of these materials were not published here, because many were considered proprietary by the manufacturers.

A number of manufacturers in allied countries were contacted to determine if significantly better ablators existed overseas. Specifically the following companies were contacted: Israeli Military Industries (IMI); two West German companies, Brandenburger and Fratherm; and two French companies, SNPE and SEP. During FY 92 Brandenburger submitted two materials, Fratherm one, and SNPE one. It was interesting to note that some of the concepts recommended by R31 are already in production in Western Europe; e.g., polyimide matrices and a sandwich construction.

The NSWCDD test procedures have been modified to take advantage of the lessons learned during FY 92; see Appendix A. These modifications include:

1. Weigh each of the ablator samples individually both before and after each test, with the adhesive removed.
2. Allow R31 to remove portions of the posttest ablator samples for use in SEM evaluations before and after the aluminum oxide coating is removed.
3. Gauge the thickness of the samples both before and after the test with the aluminum mounting plate and the adhesive removed.
4. Measure the ablator thickness both with and without the aluminum oxide coating.
5. Measure the ablator thickness with the char scraped off with a wire brush.

There are also changes that need to be made to the FMC tests and/or the interpretation of the FMC data in order to maximize the amount of useful information that can be gained from those tests. FMC could improve the erosion measurements by measuring sufficient data so that an average surface recession could be calculated in lieu of just measuring the maximum erosion; e.g., using a laser-based sensor to measure erosion. Changes are necessary to the procedure used by FMC to measure back-wall temperature during and after the test, such as:

1. Measure the back-wall temperature in tests with just convective heating; do not seed the plume with aluminum oxide particles,
2. Add a protective frame around the periphery of the test sample to reduce the possibility of the plume wrapping around the ablator and heating the backing plate, or
3. Thermally isolate the back-wall thermocouple from the the backing plate to reduce spurious heating from the rear.

Finally, it is recommended that FMC modify the types of particles it is injecting into the plume. Smaller particles would be more realistic; aluminum particles would be more likely to melt in the plume and strike the test samples as molten particles. Both of these modifications would result in more realistic particle erosion, due to particle thermal energy and the abrasion.

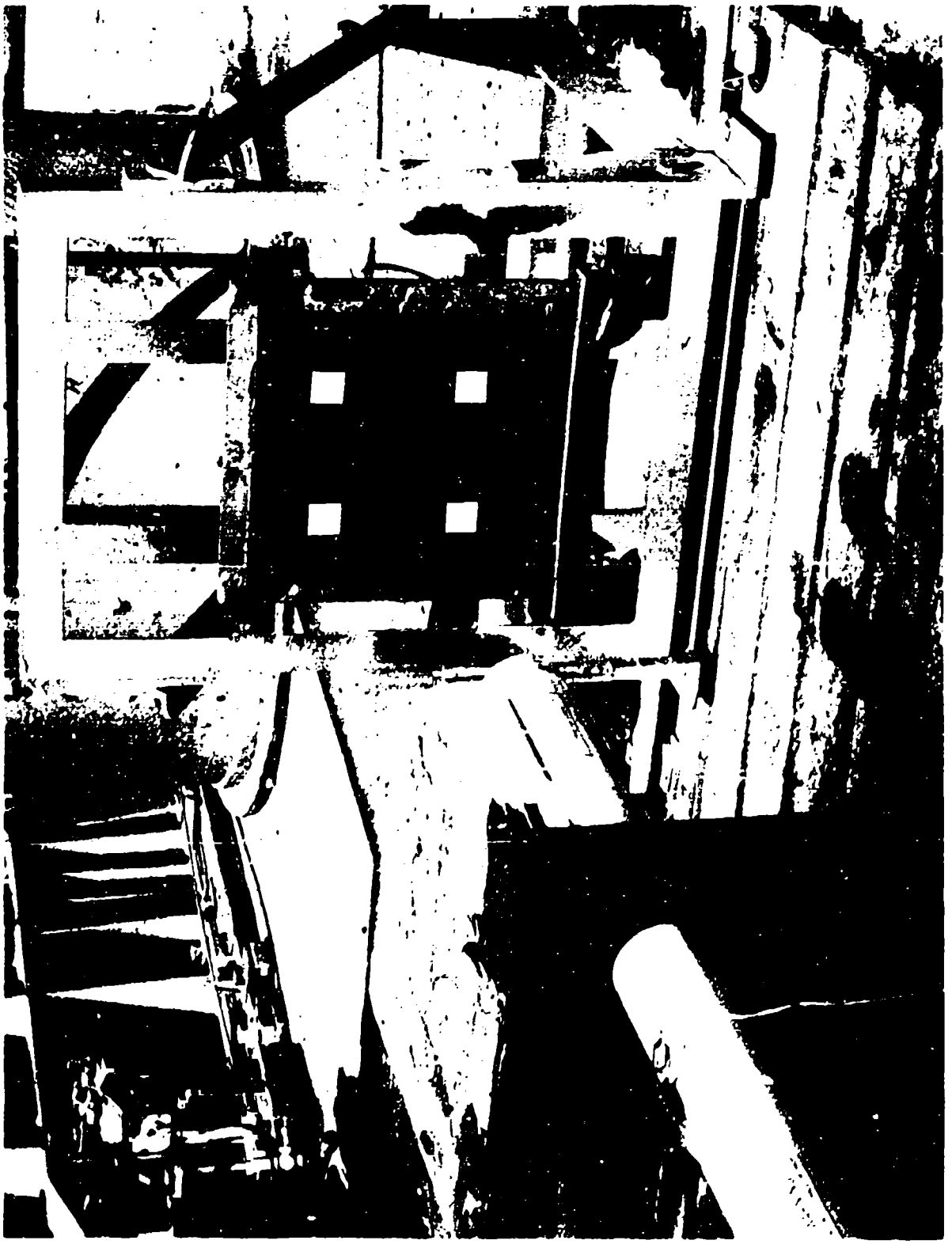

FIGURE 1. NSWCDD ROCKET MOTOR TEST FIXTURE

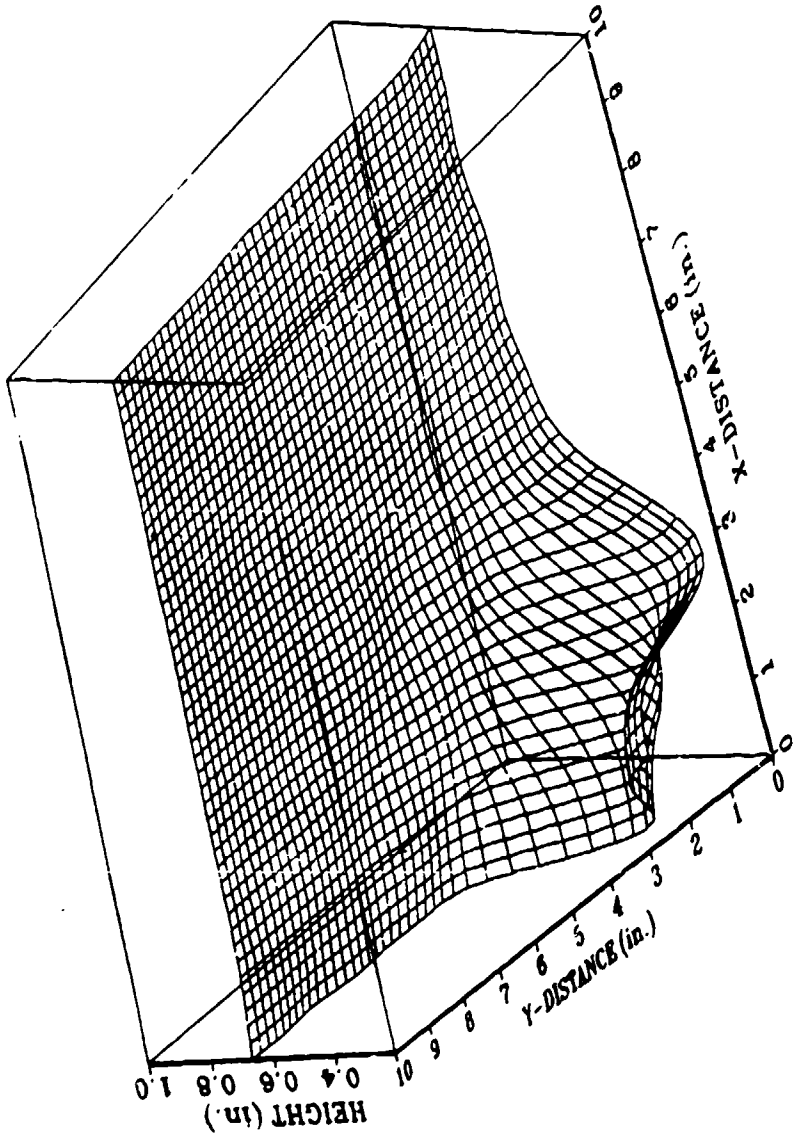

FIGURE 2. TYPICAL EROSION PATTERN (CA6304)

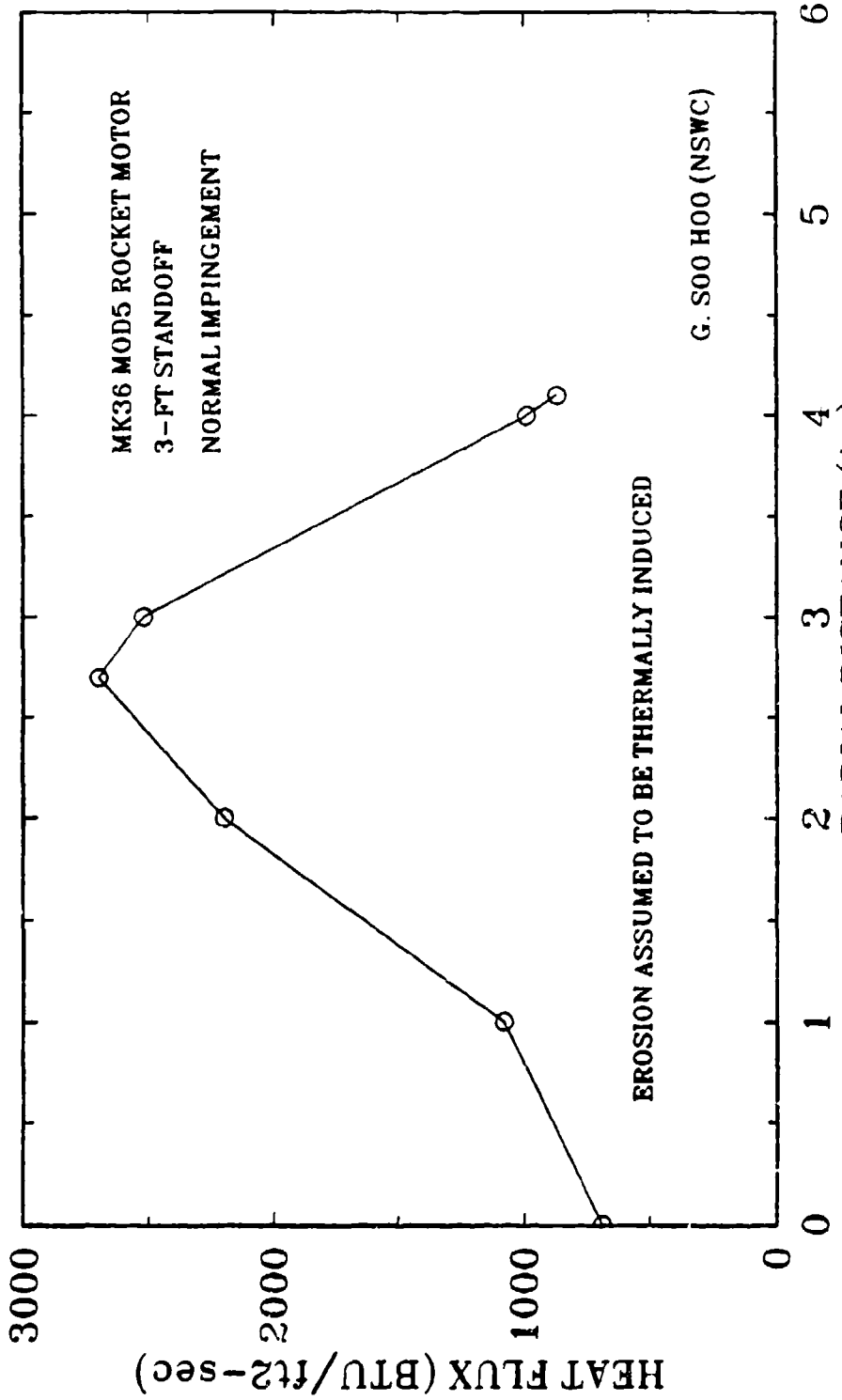

FIGURE 3. TOTAL HEAT FLUX DISTRIBUTION

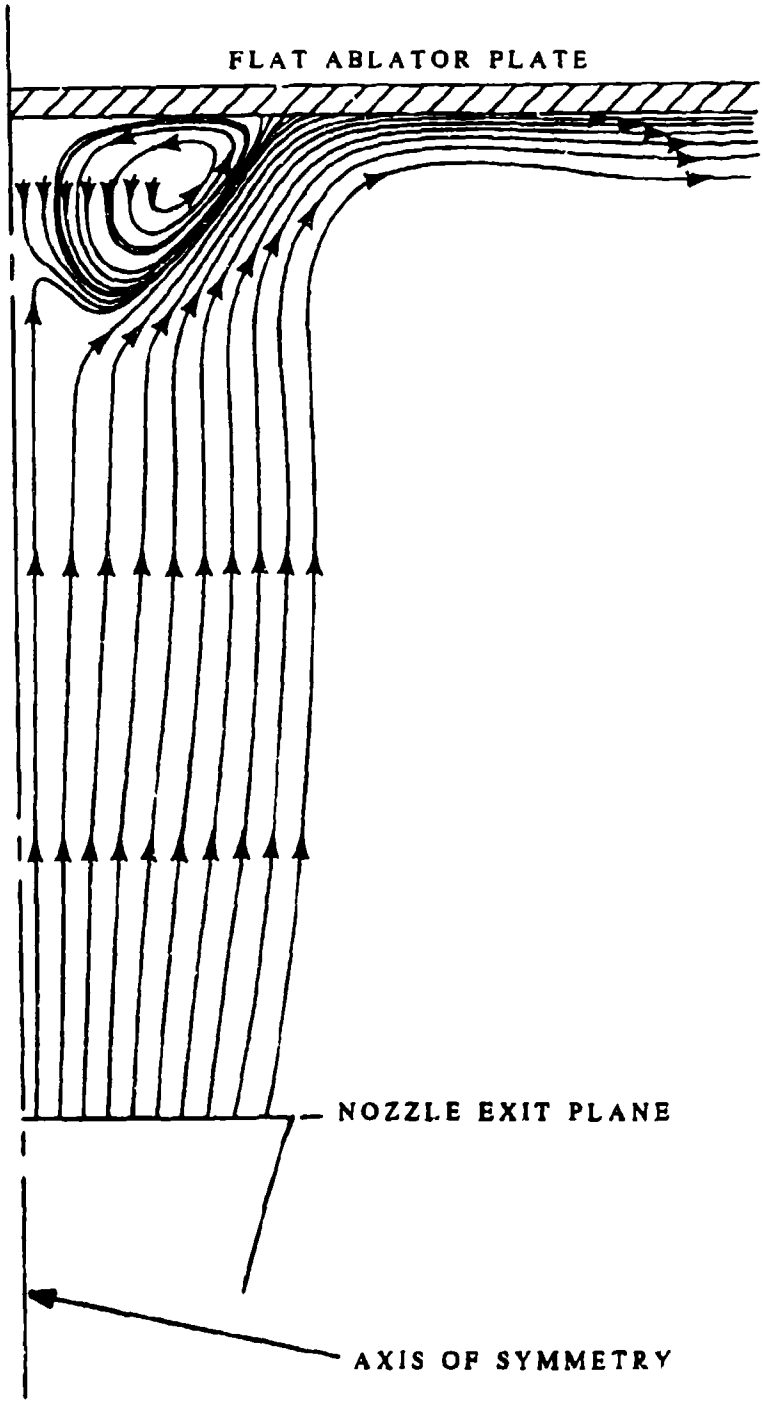

FIGURE 4. GAS-PHASE EXHAUST FLOW

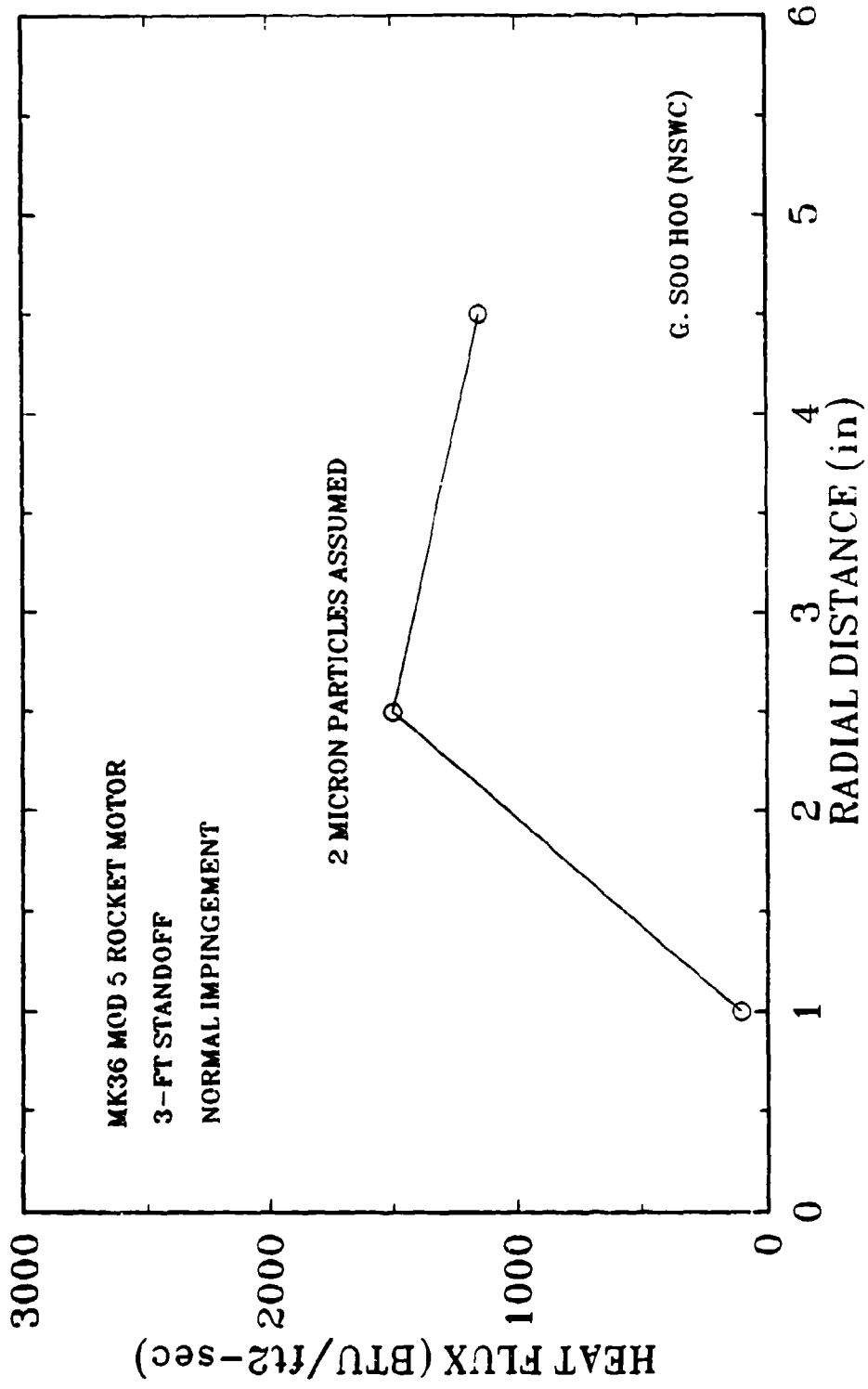

FIGURE 5. CALCULATED PARTICLE KINETIC ENERGY

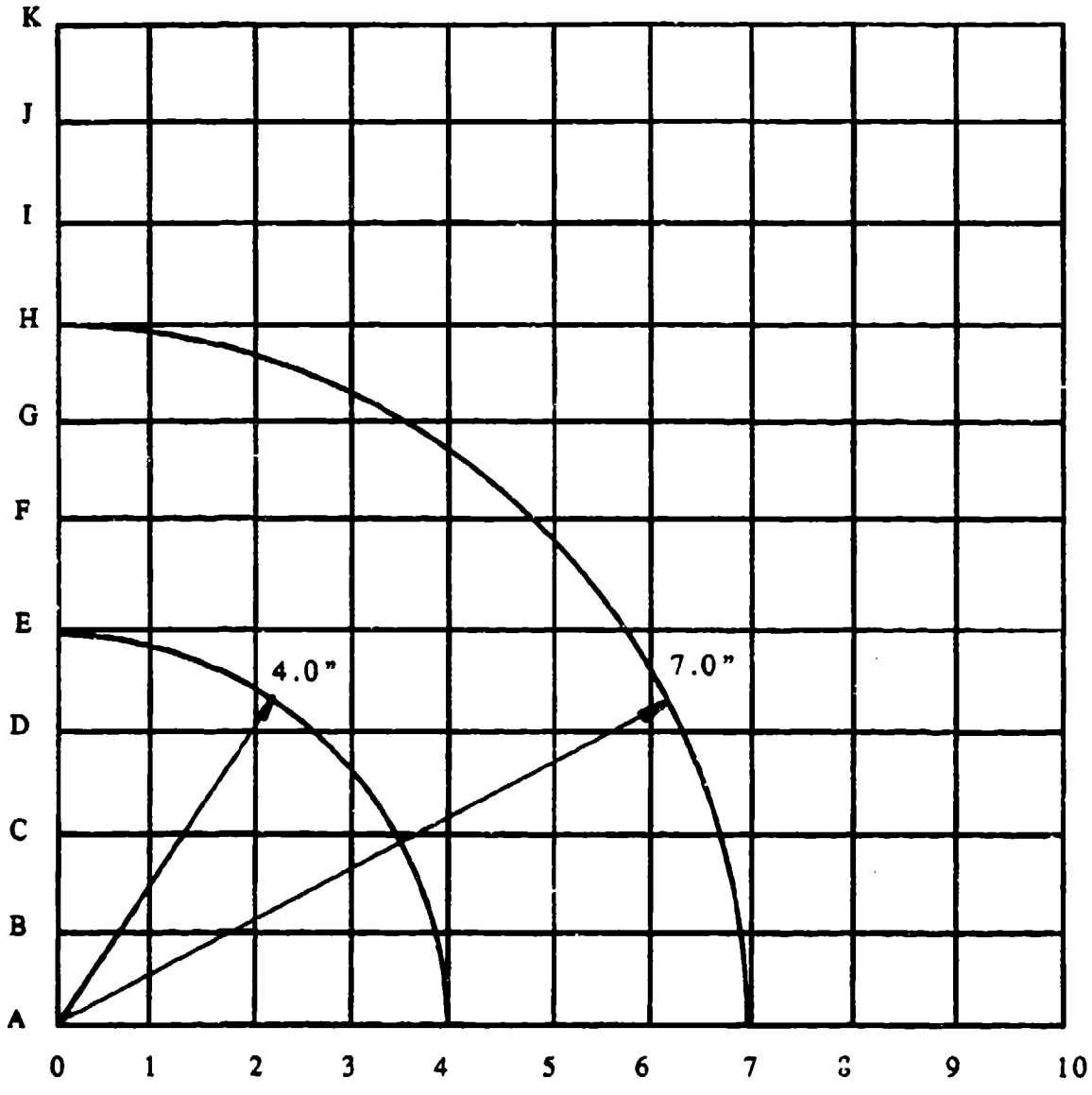

FIGURE 6. EROSION MEASUREMENT GRID

FIGURE 7. BACK SIDE OF ALUMINUM PLATE

FIGURE 8. BACK VIEW OF ABLATOR MOUNTING FRAME

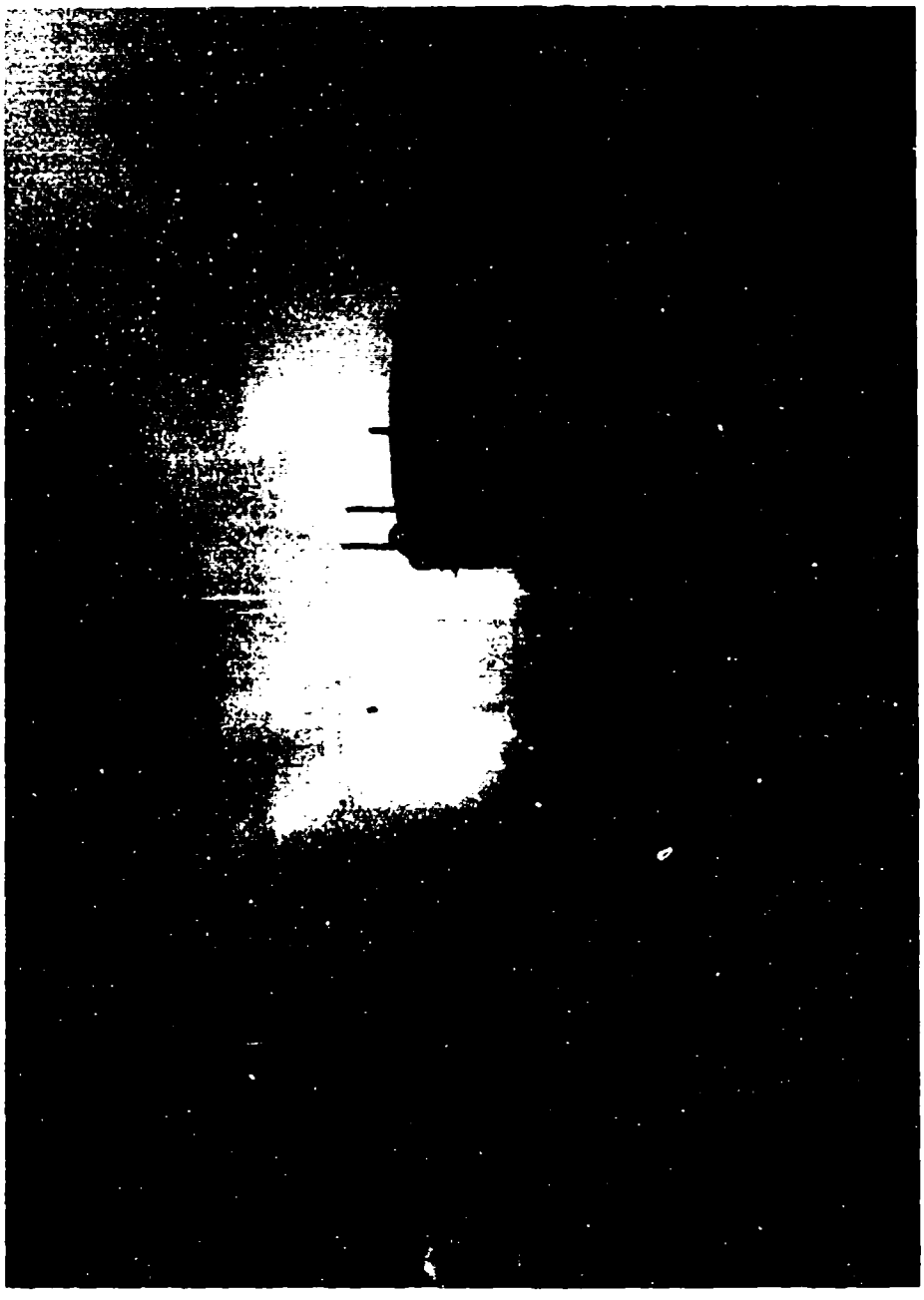

FIGURE 9. MOTOR EXHAUST ENGULFING TEST FIXTURE

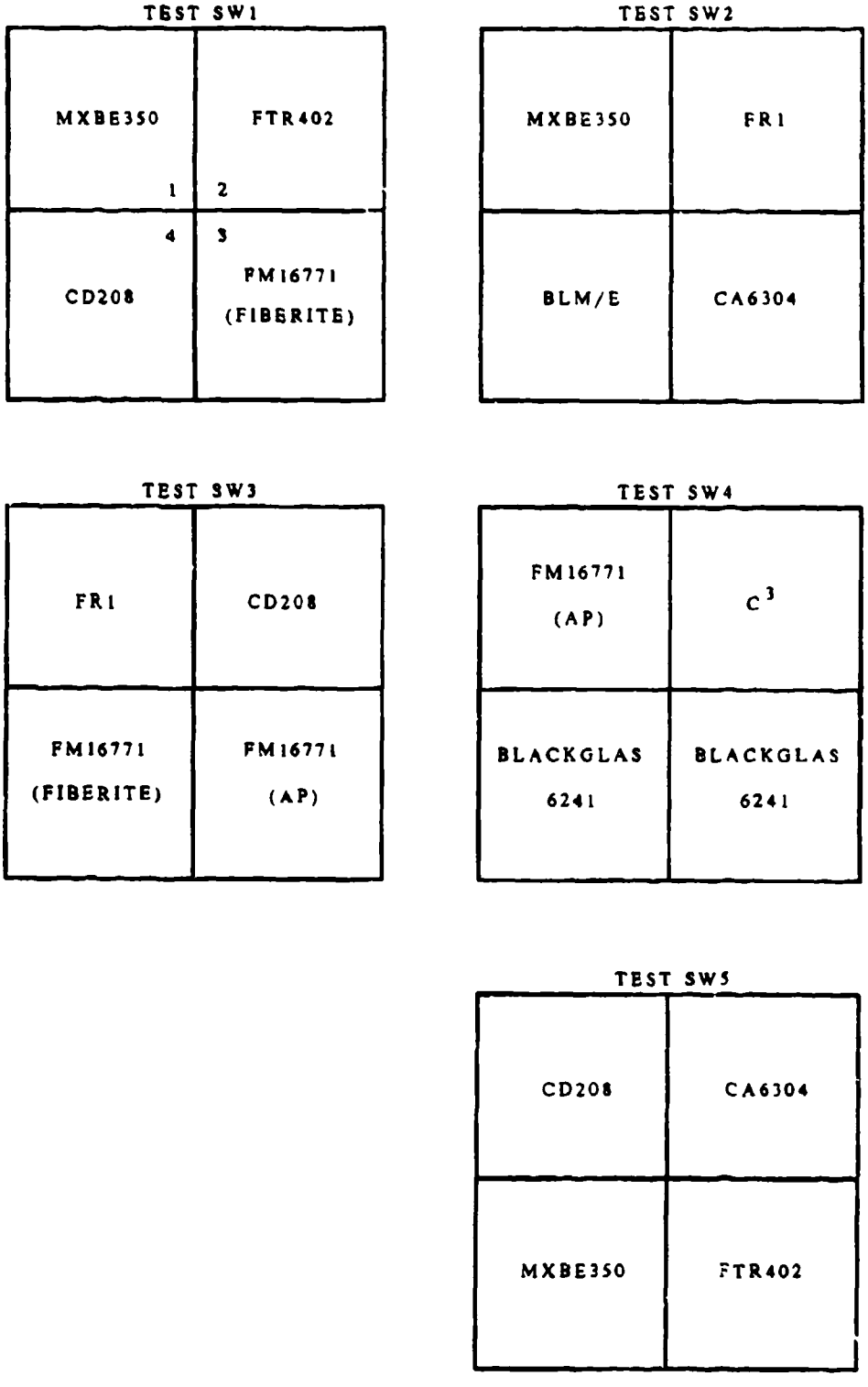

FIGURE 10. ABLATOR SAMPLE LOCATIONS IN TESTS SW1 THROUGH SW5

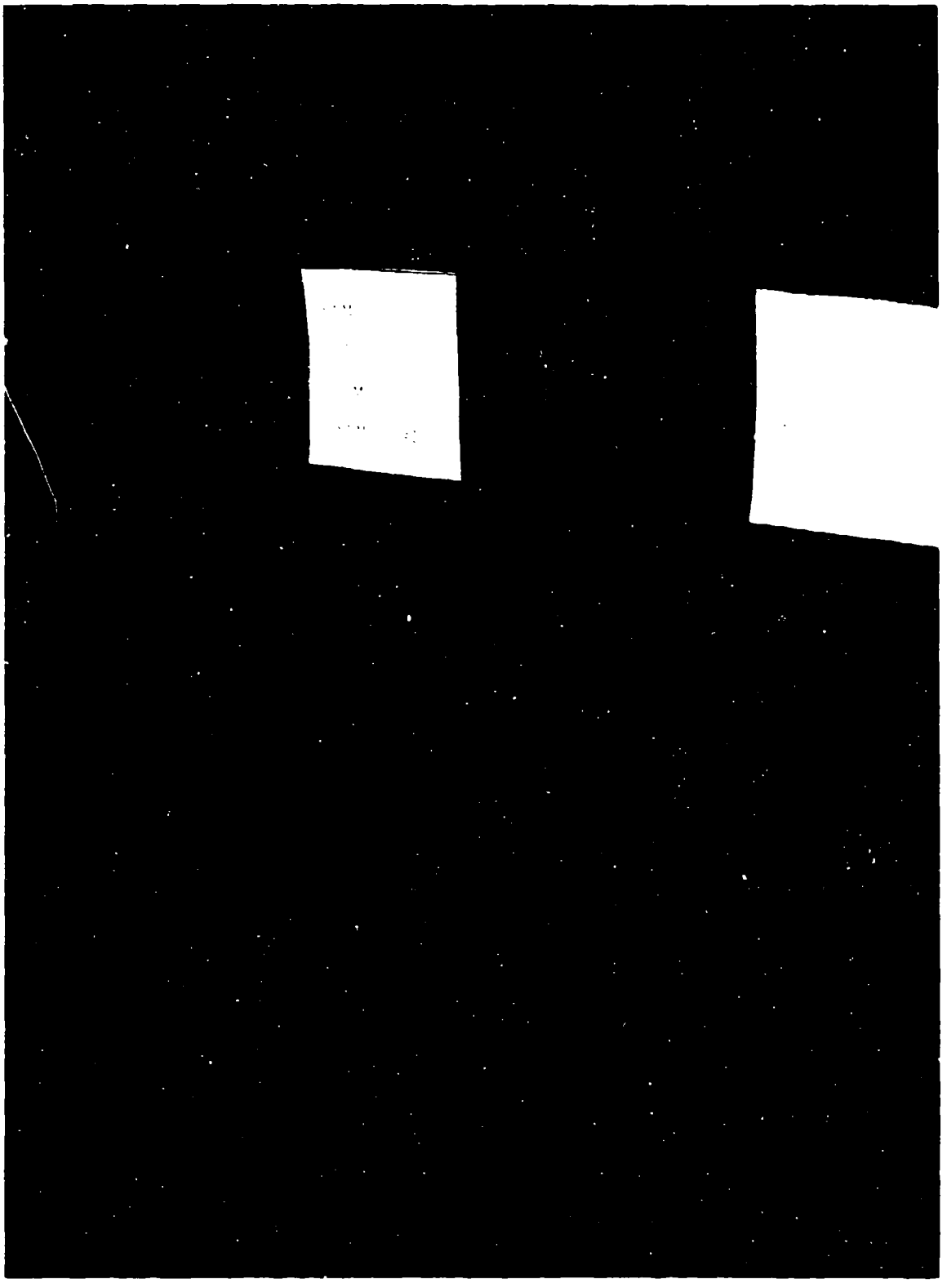

FIGURE 11. POSTTEST VIEW OF ABLATORS (SW3)

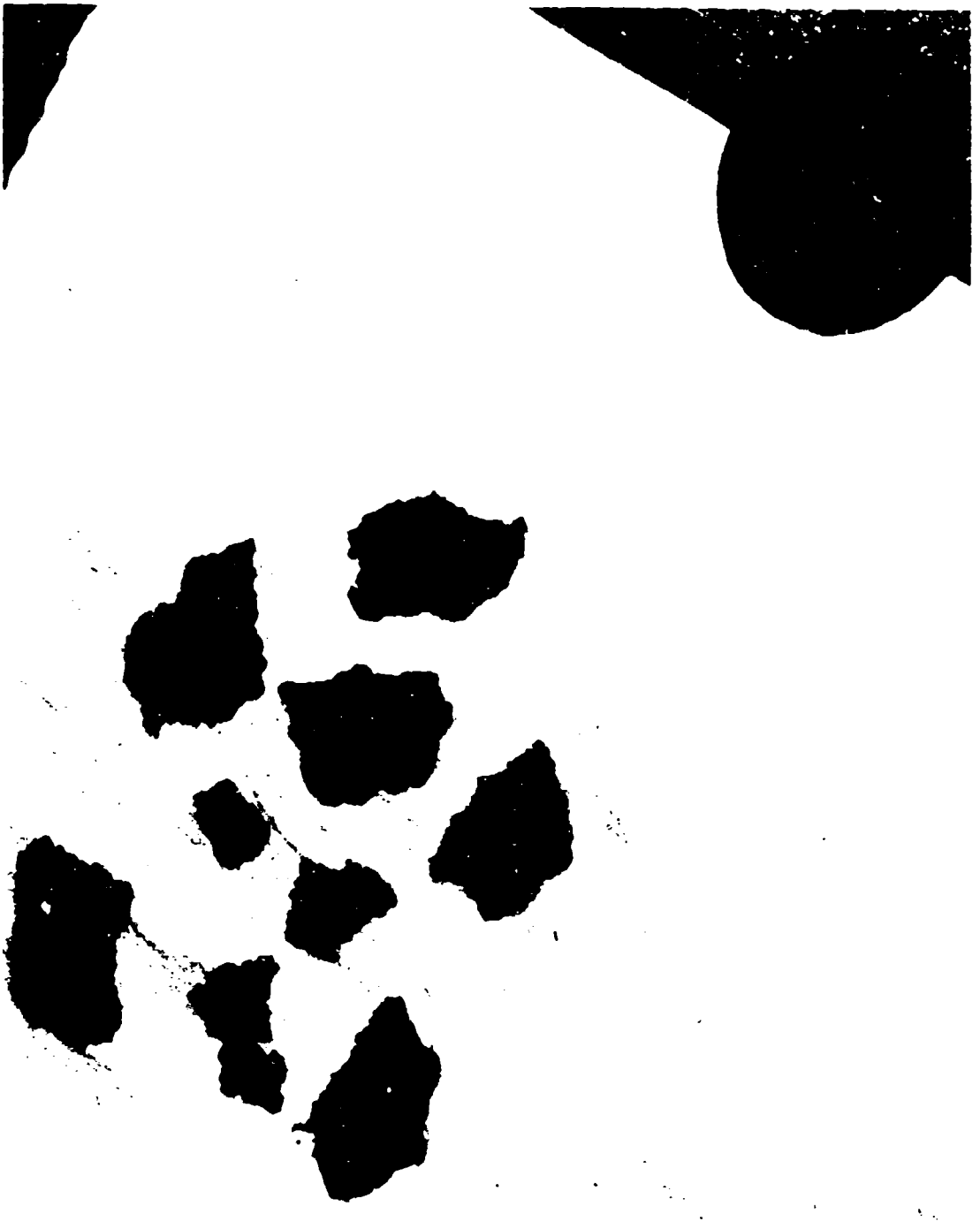

FIGURE 12. ALUMINUM OXIDE REMOVED FROM ABLATORS

FIGURE 13. HEATED SURFACE AFTER ALUMINUM OXIDE WAS REMOVED (SW5)

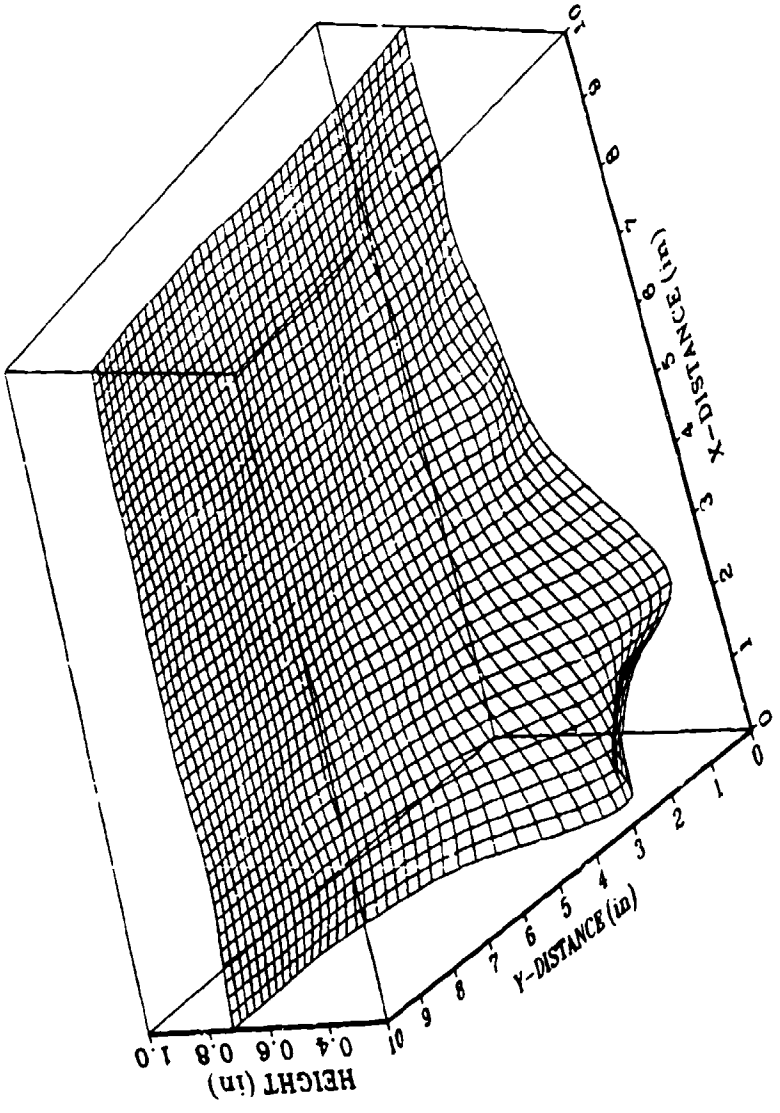

FIGURE 14. POSTTEST SURFACE OF MXBE350 (SW2)

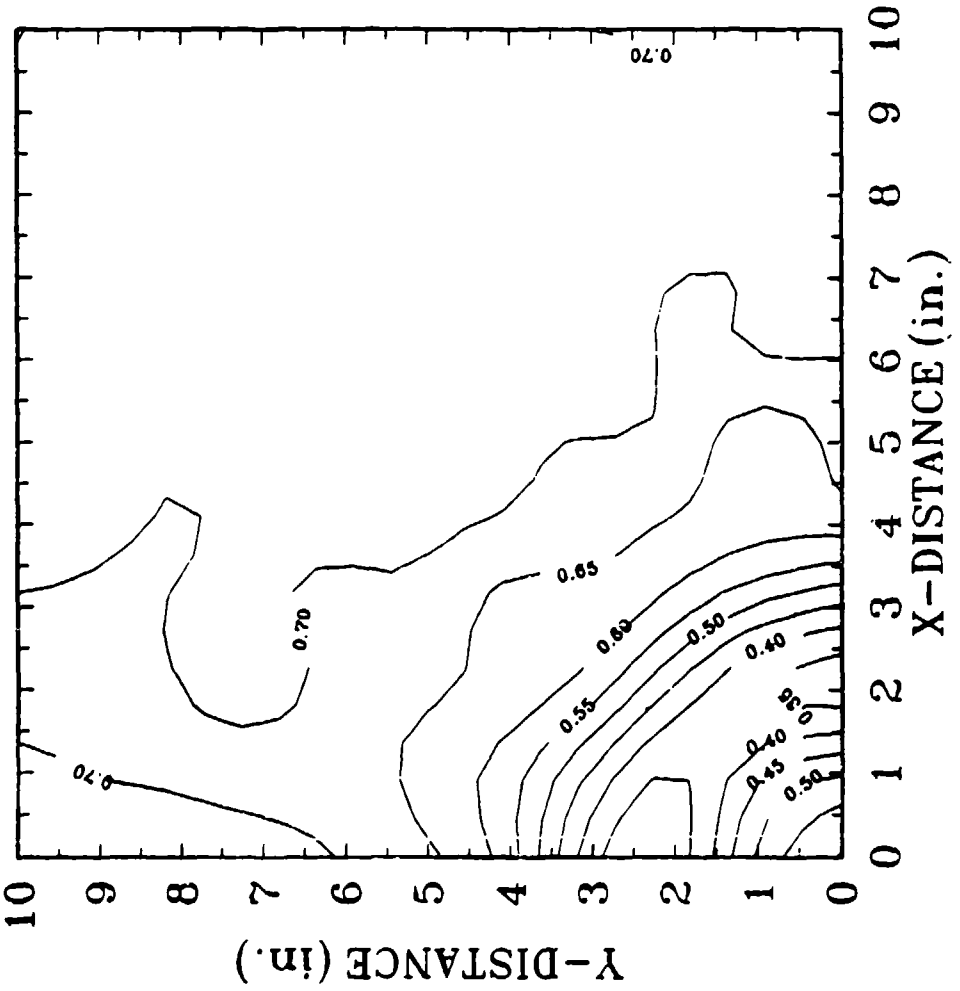

FIGURE 15. MXBE350 CONTOURS (SW2)

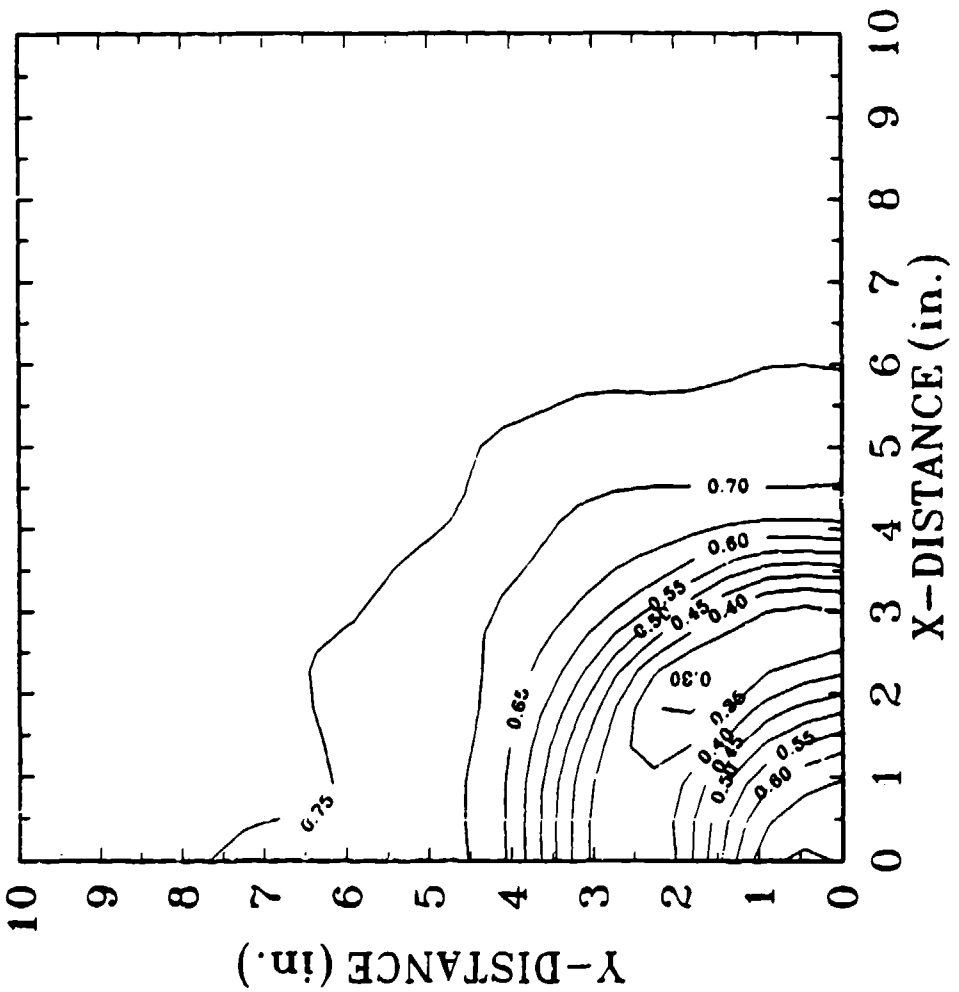

FIGURE 16. FM16771 CONTOURS (SW3)

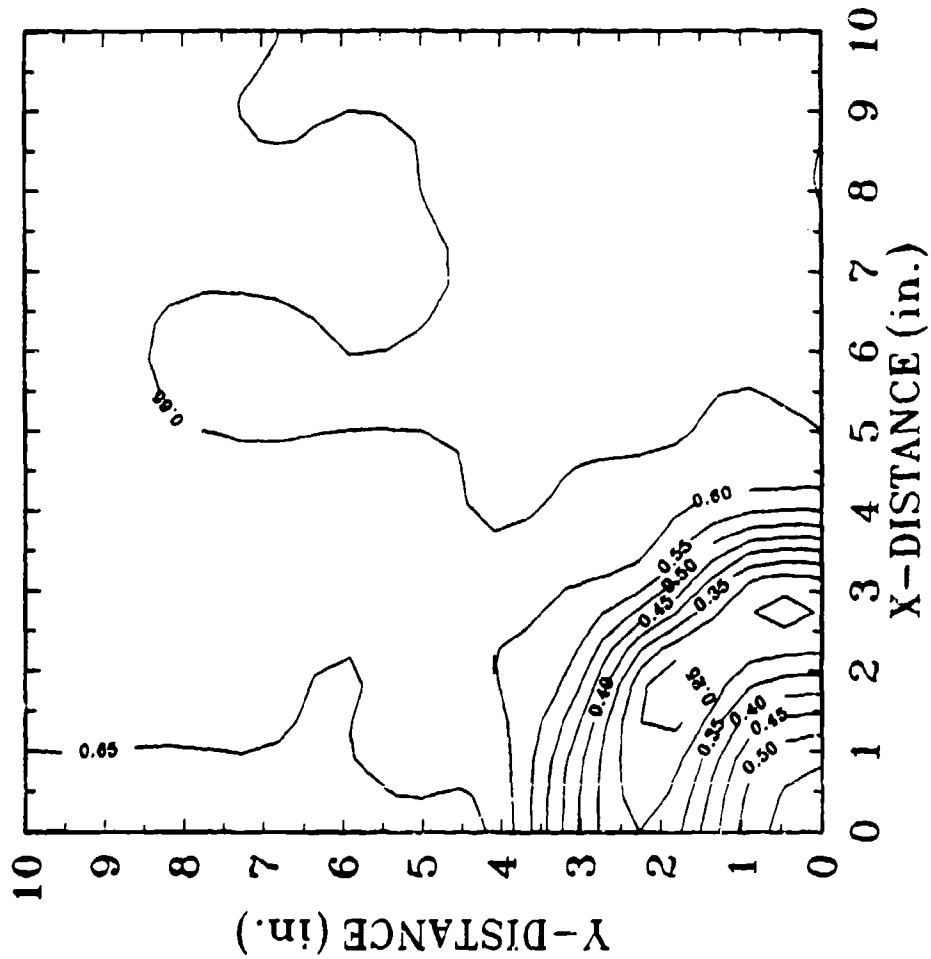

FIGURE 17. CA6304 CONTOURS (SW2)

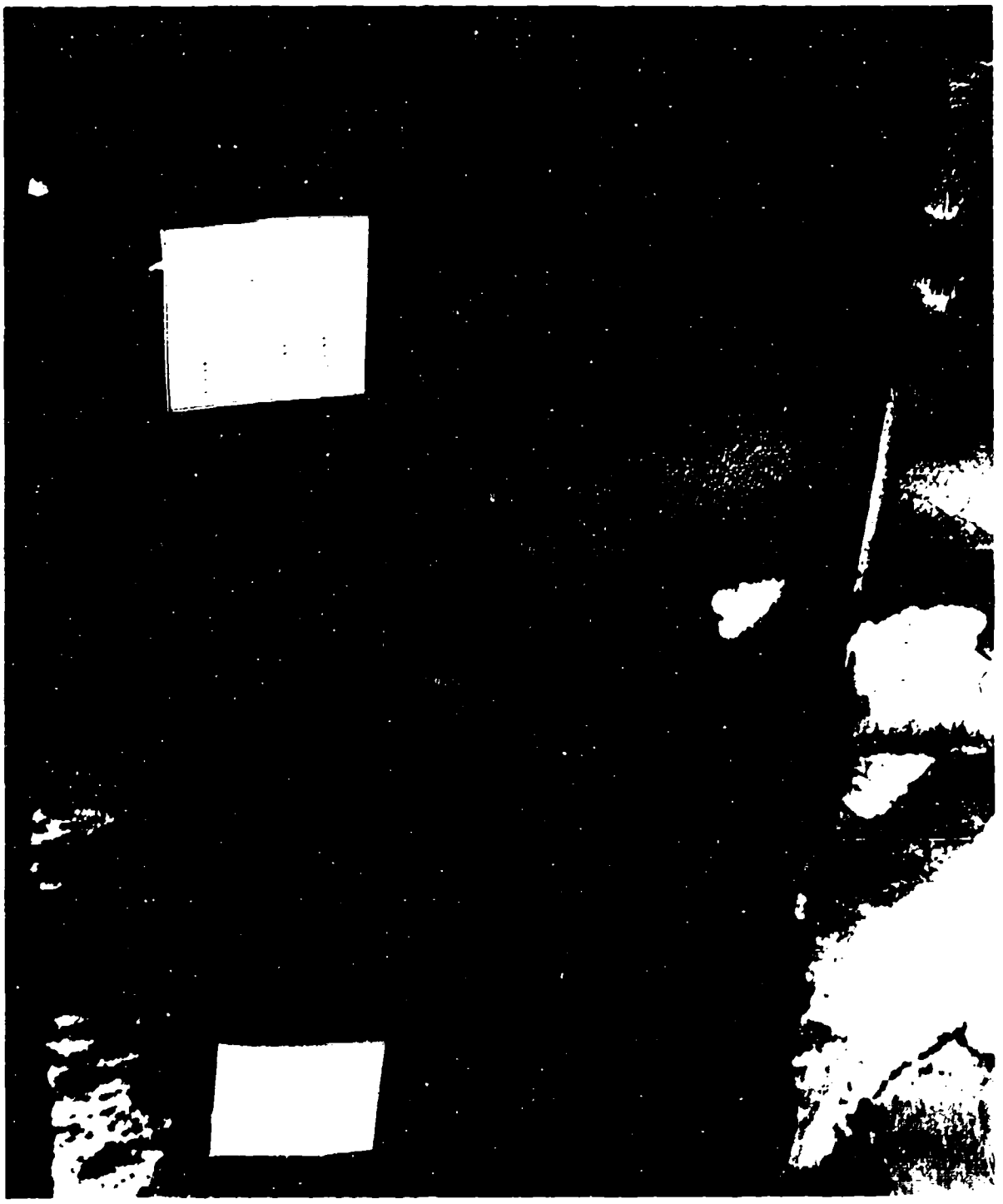

FIGURE 18. C³ DELAMINATION (UPPER RIGHT CORNER)

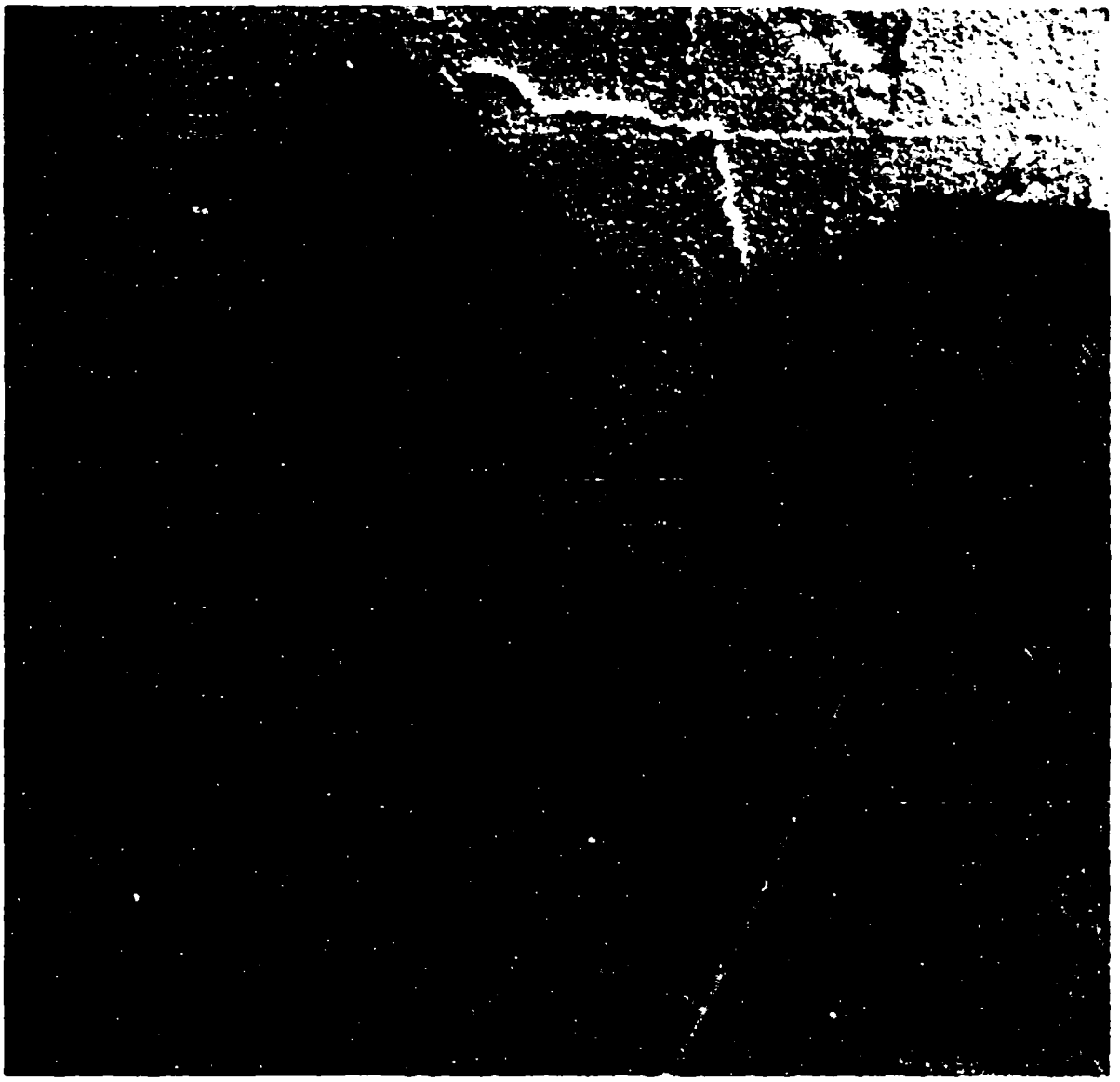

FIGURE 19. DELAMINATIONS RECOVERED AFTER TEST SW4

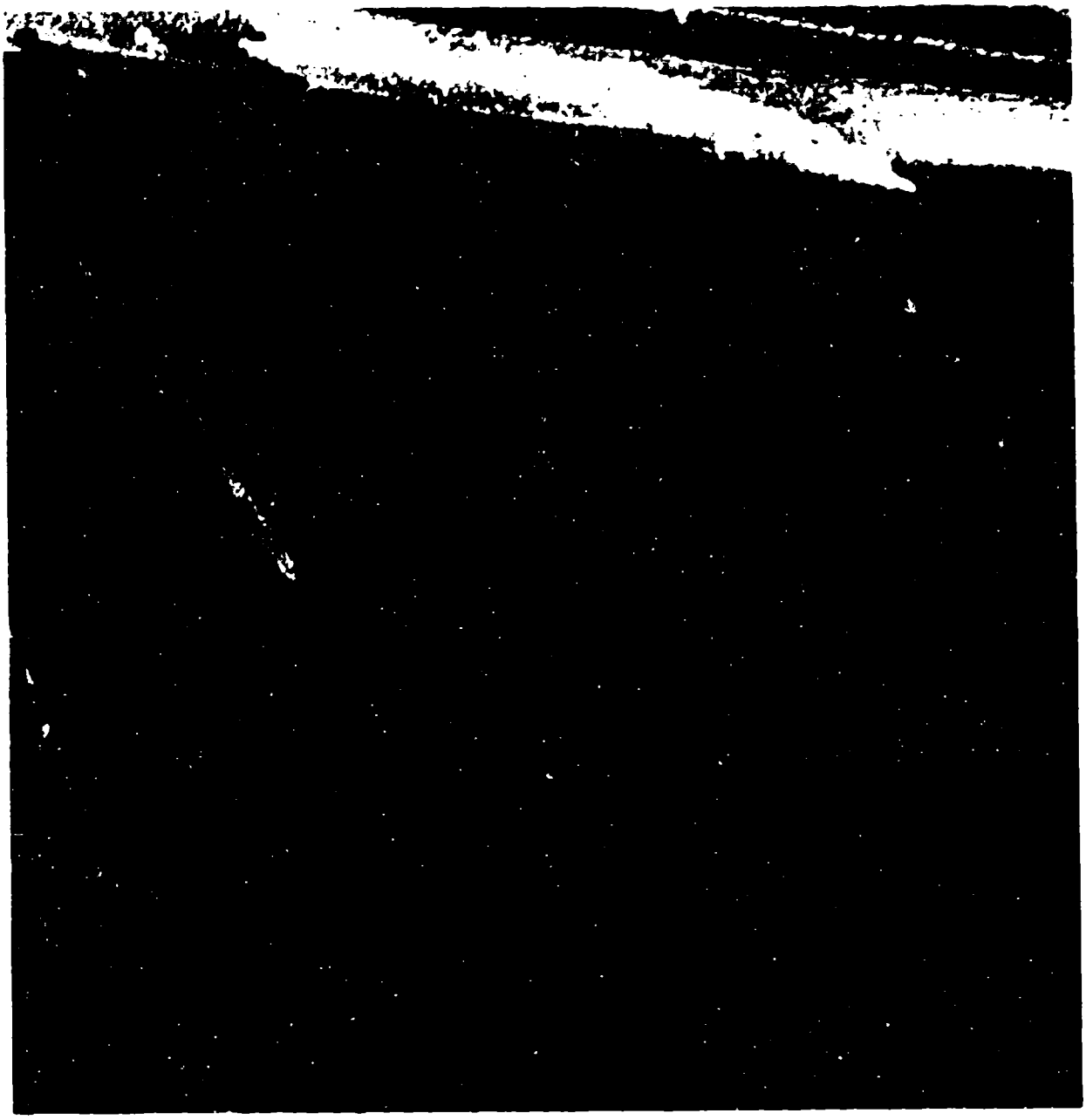

FIGURE 20. WARPED FR1 SAMPLE AFTER TEST SW2

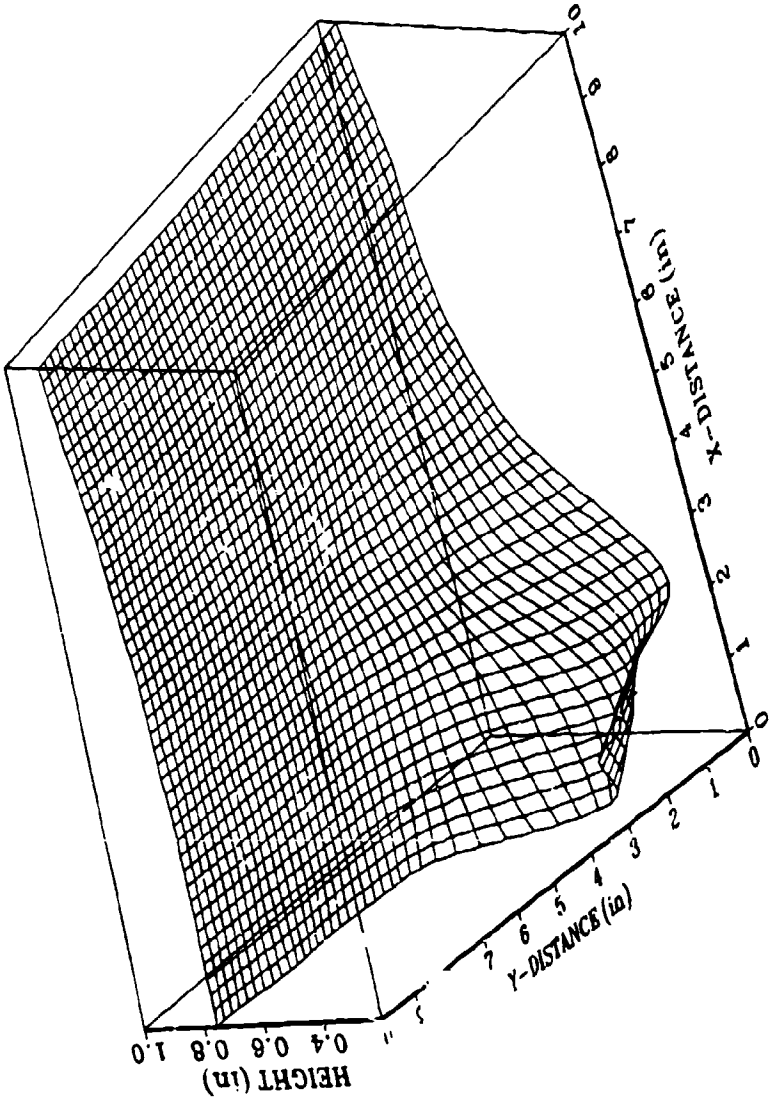

FIGURE 21. POSTTEST SURFACE OF FR1 (SW2)

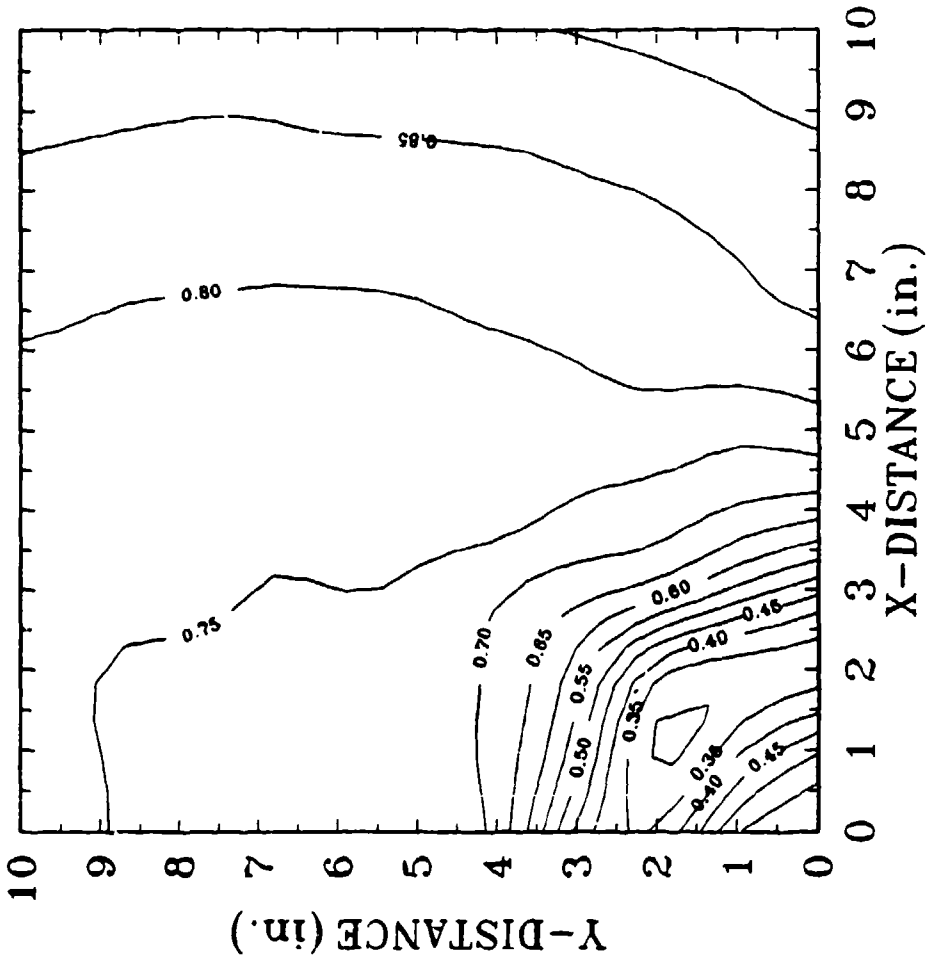

FIGURE 22. FR1 CONTOURS (SW2)

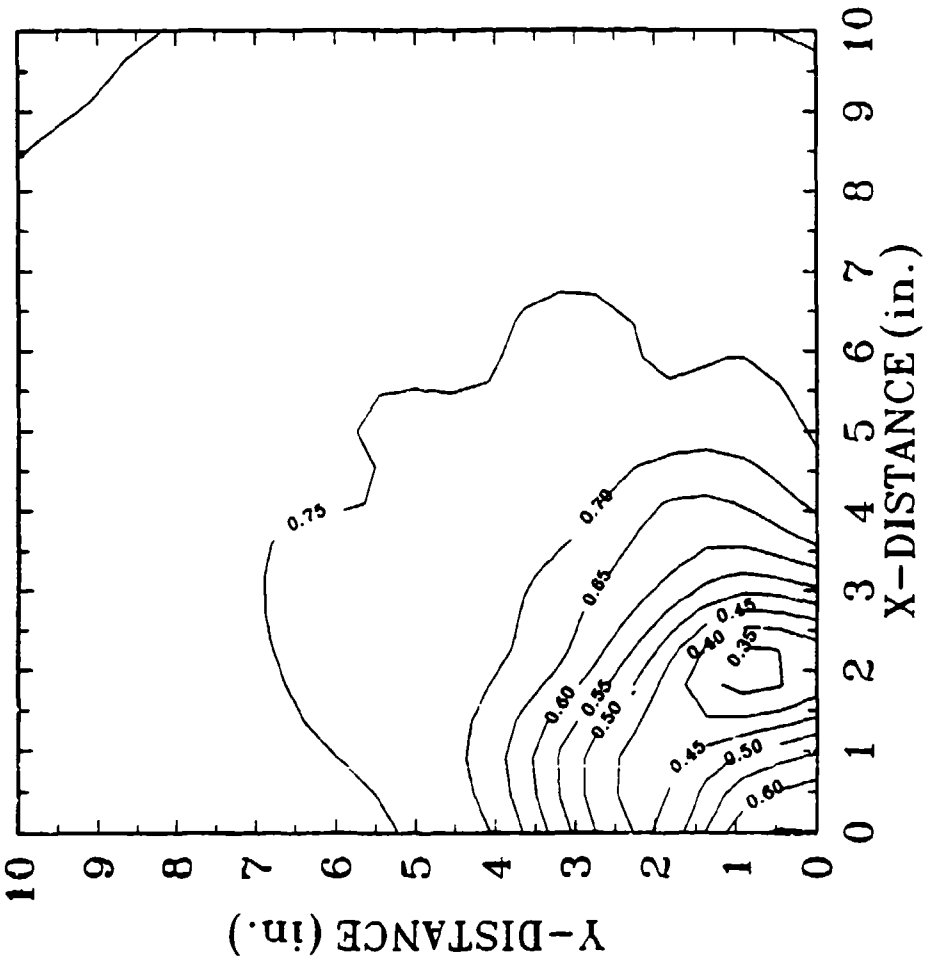

FIGURE 23. CD208 CONTOURS (SW5)

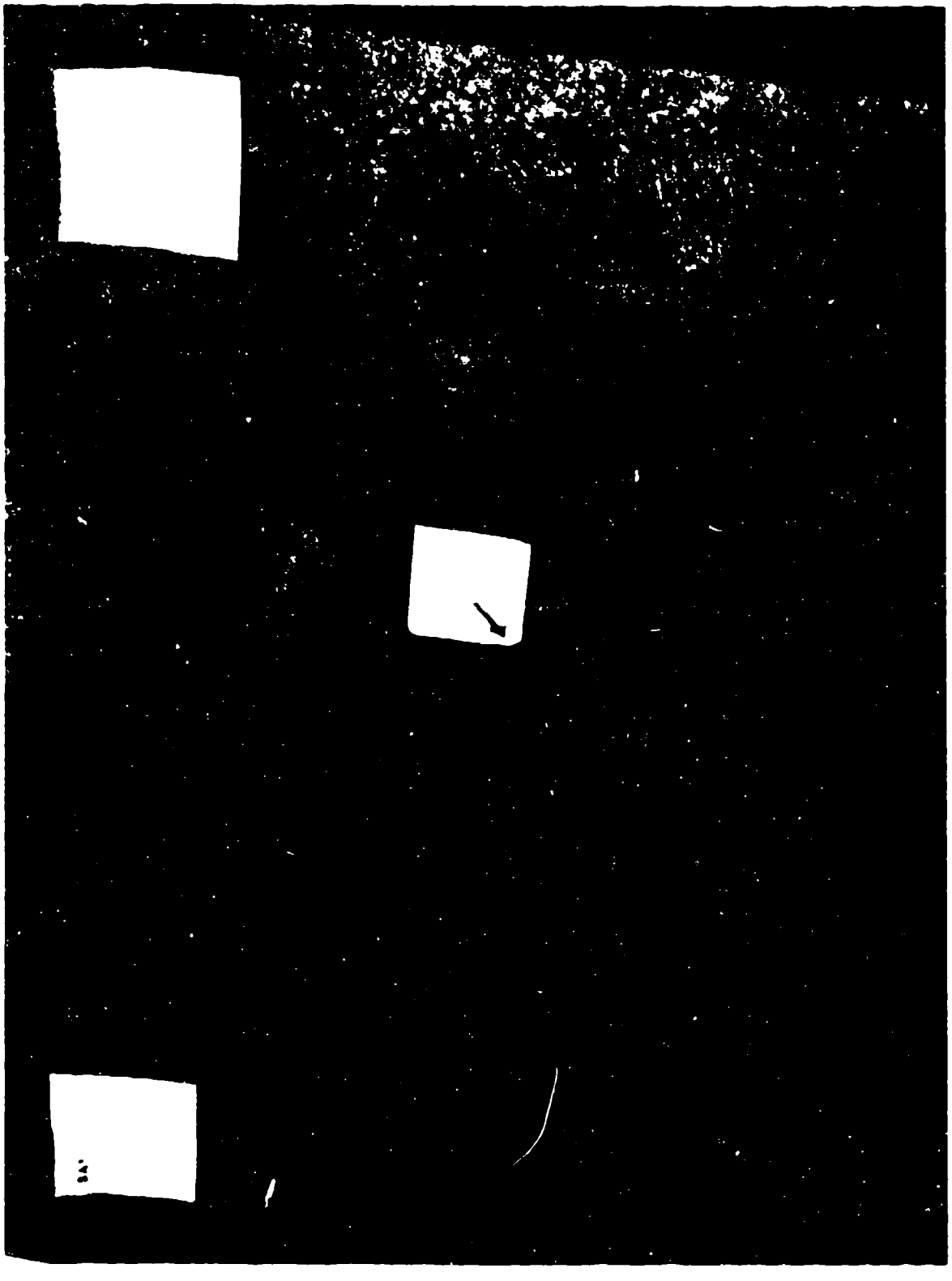

FIGURE 24. POSTTEST VIEW OF TEST SW3 ABLATORS

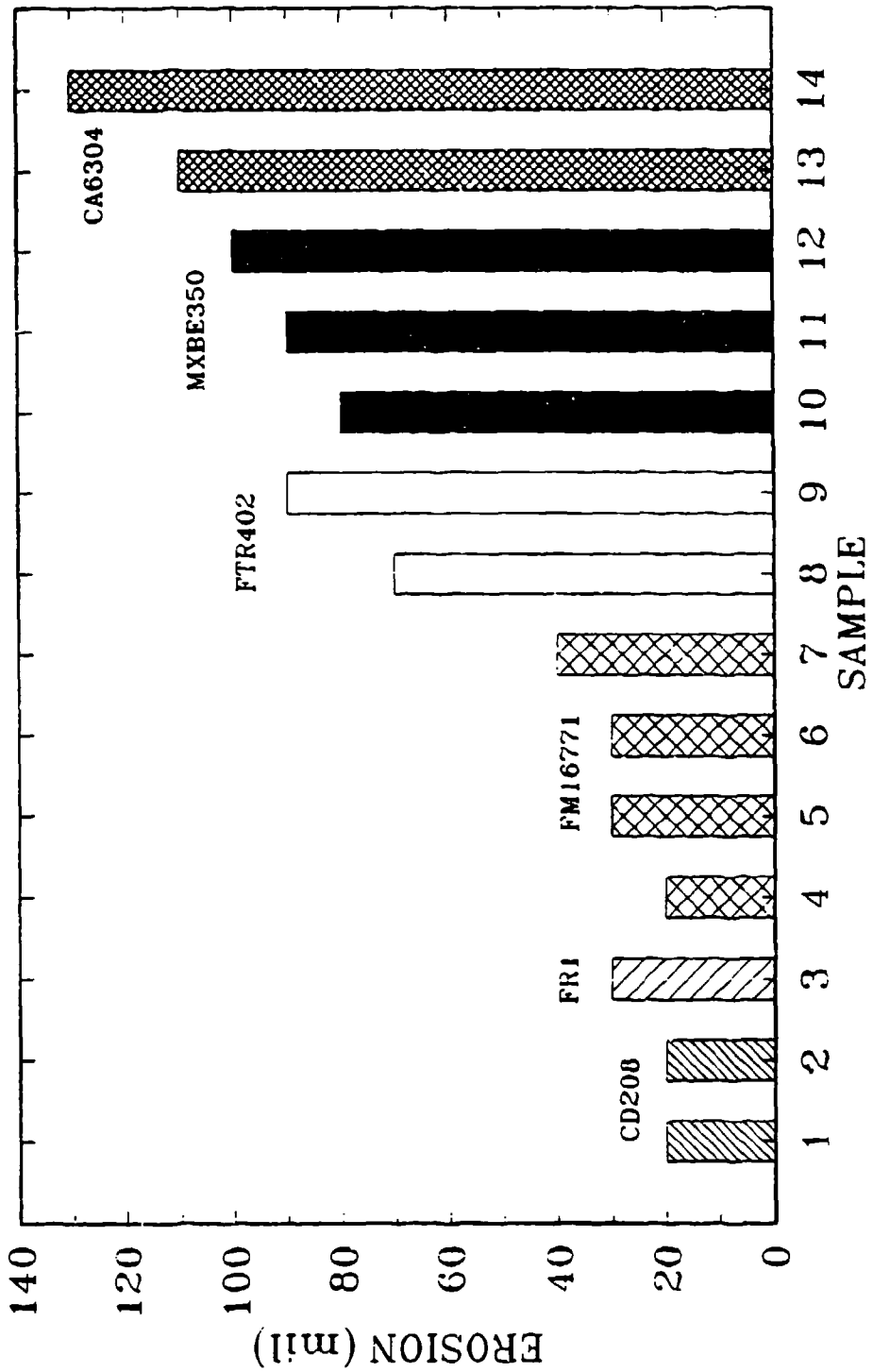

FIGURE 25. AVERAGE EROSION PRODUCED BY CONVECTIVE HEATING

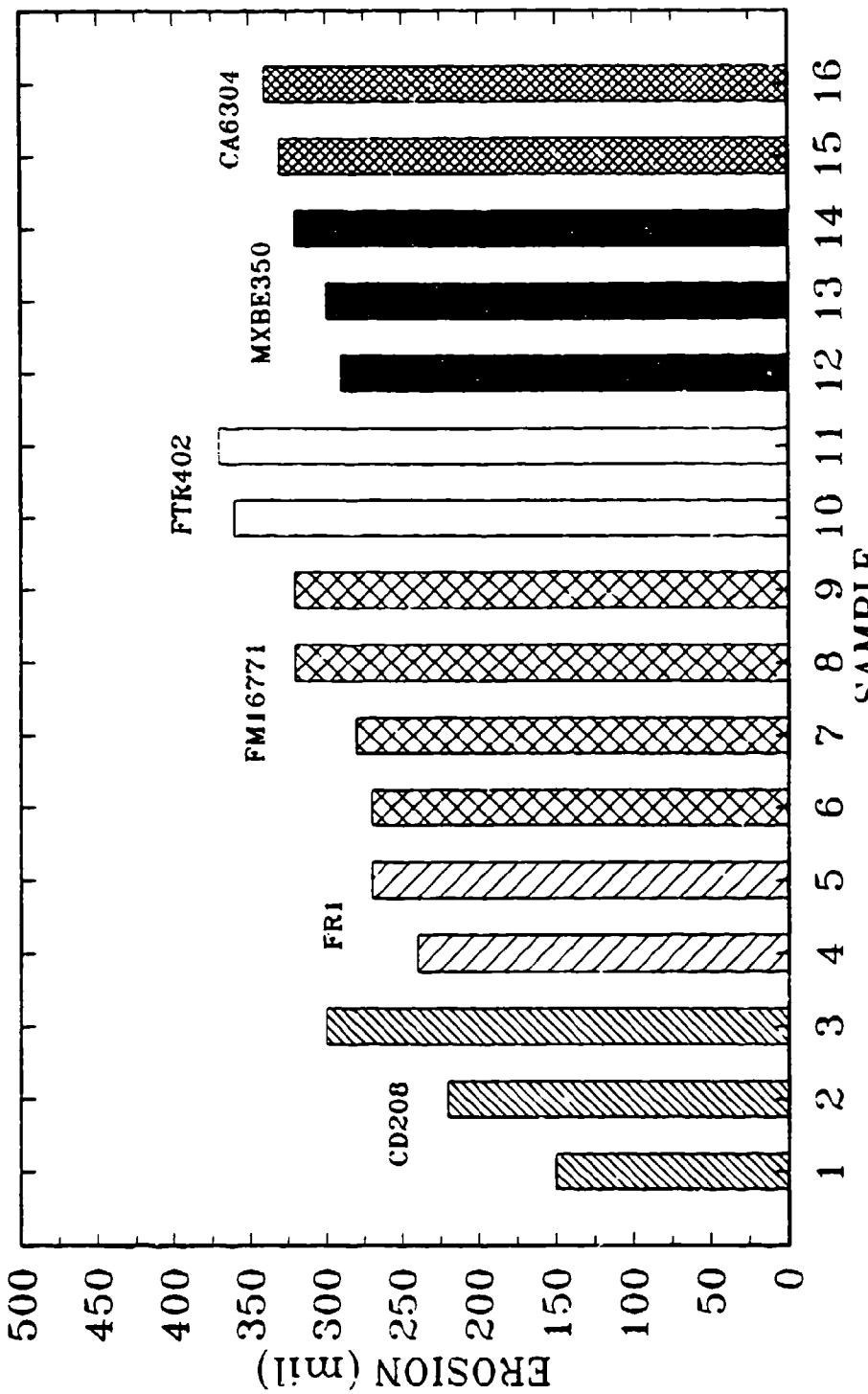

FIGURE 26. AVERAGE EROSION PRODUCED BY CONVECTIVE HEATING AND PARTICLE IMPINGEMENT

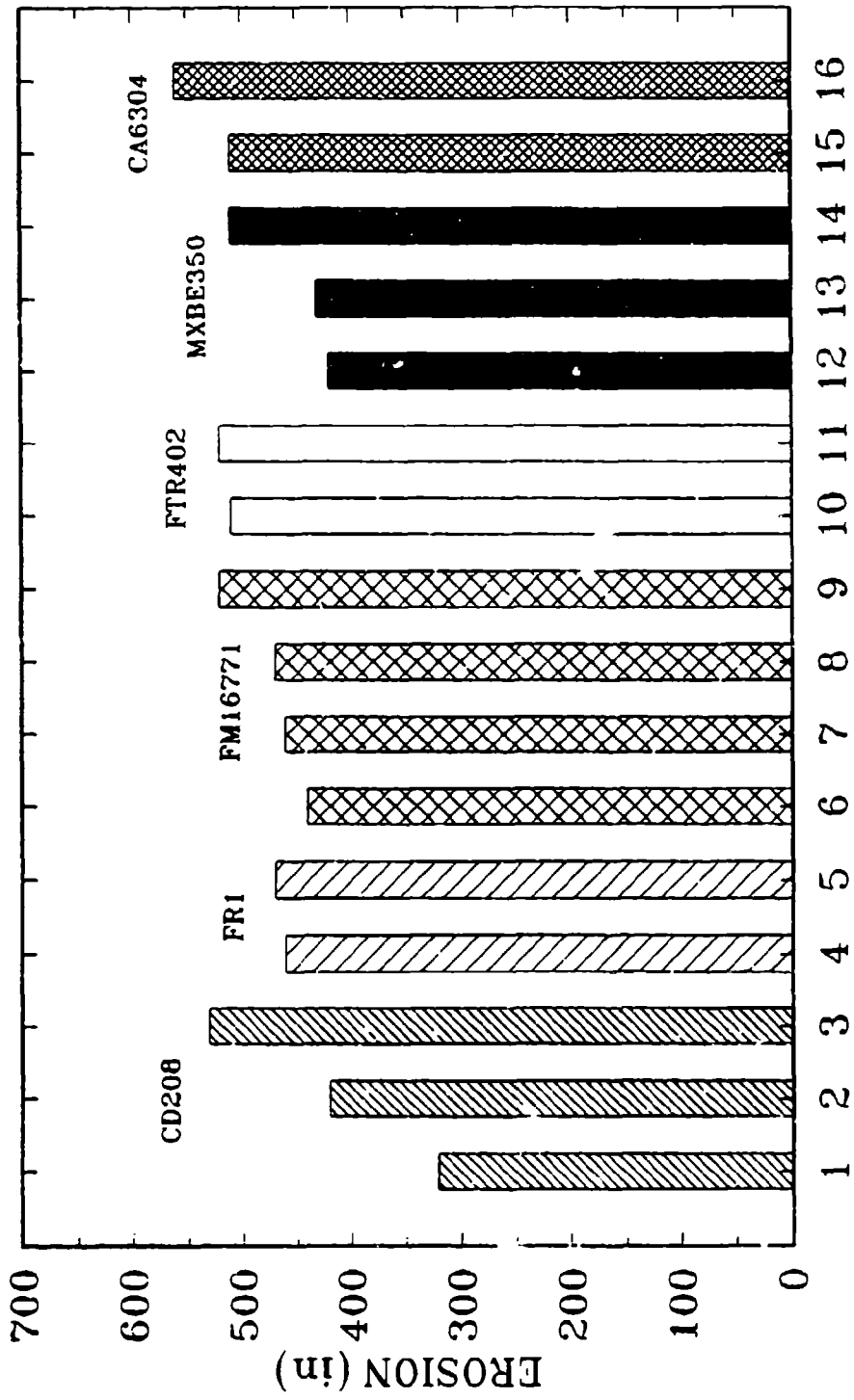

FIGURE 27. MAXIMUM EROSION PRODUCED BY CONVECTIVE HEATING AND PARTICLE IMPINGEMENT

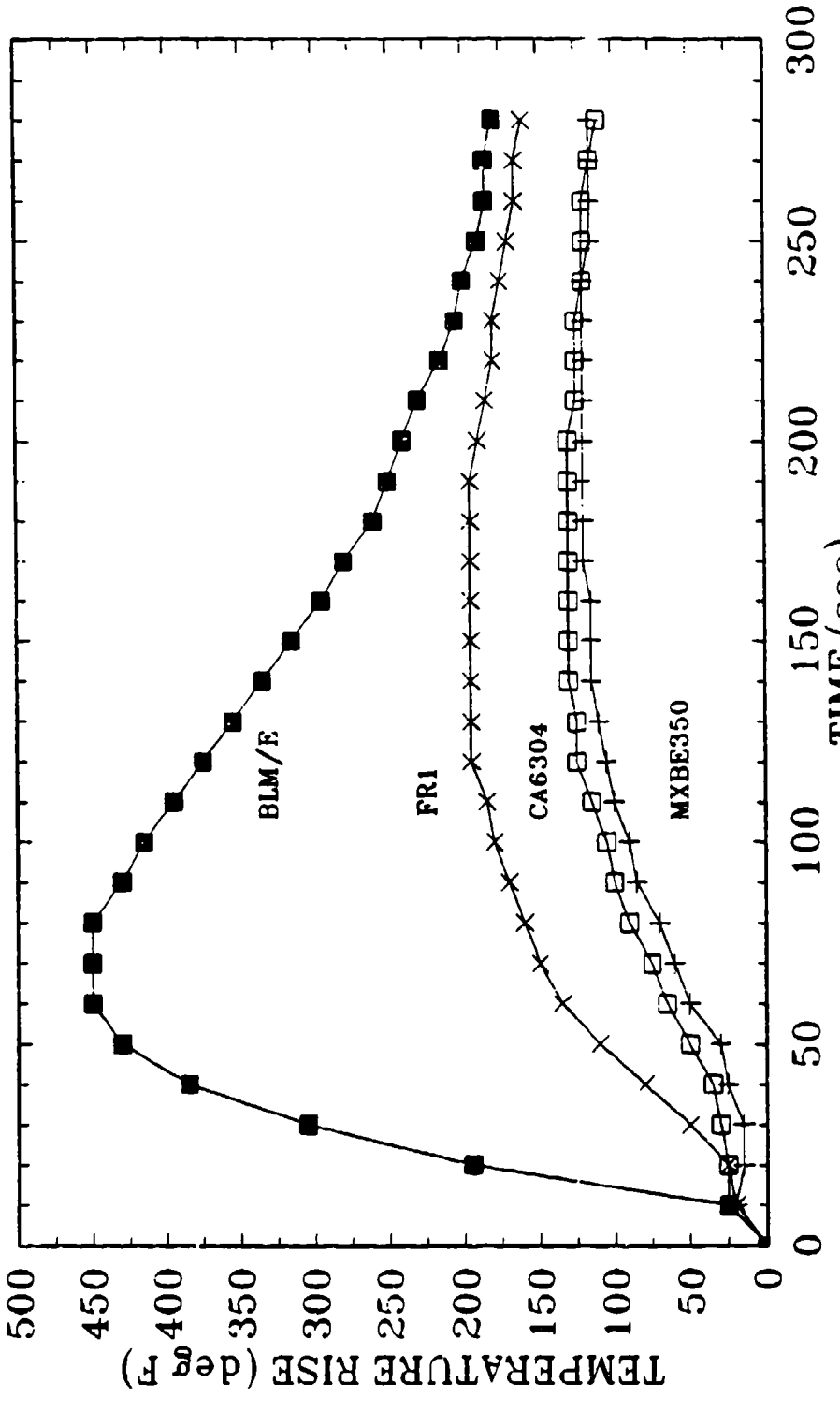

FIGURE 28. MEASURED BACK-WALL TEMPERATURE RISES (SW2)

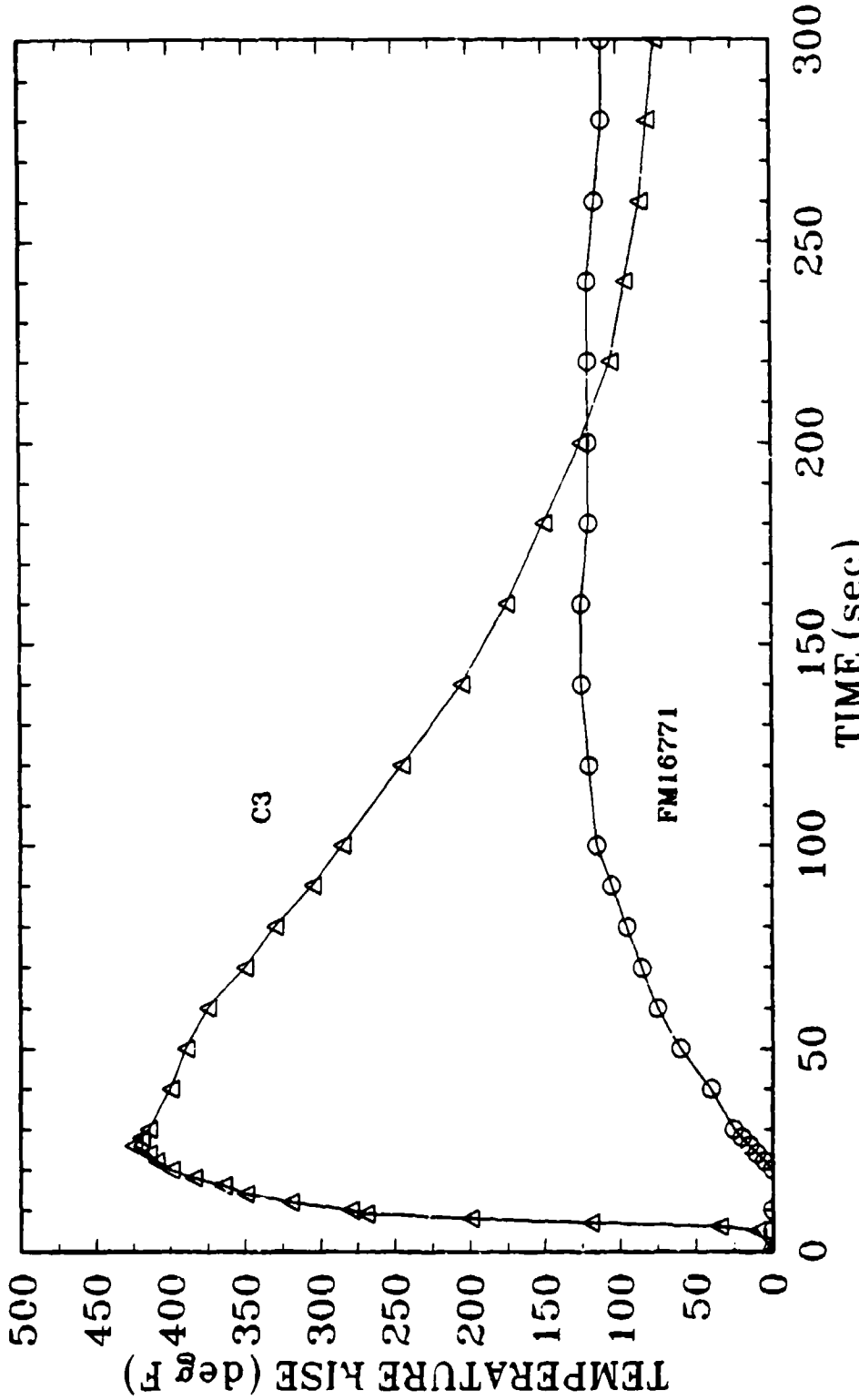

FIGURE 29. MEASURED BACK-WALL TEMPERATURE RISES (SW4)

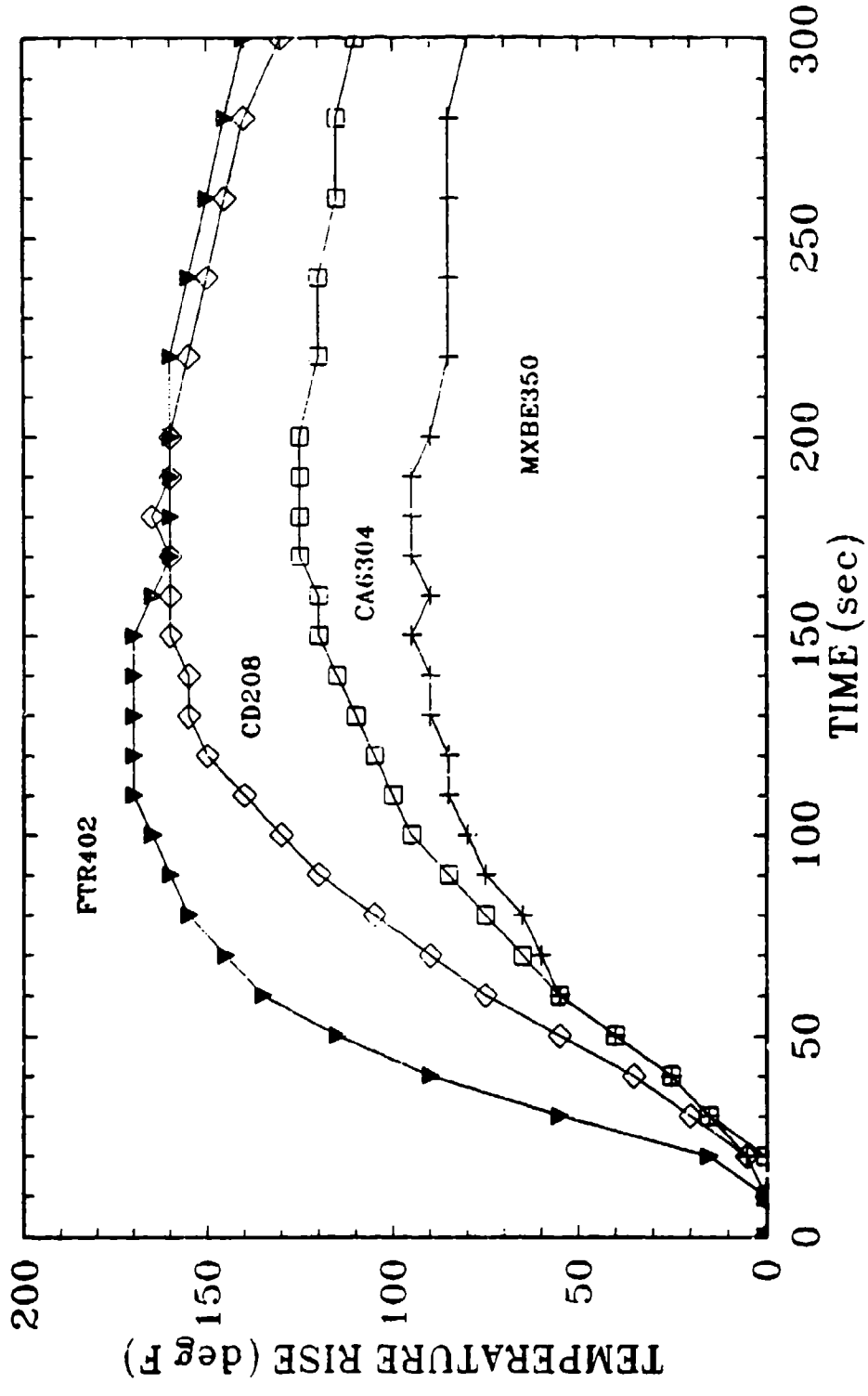

FIGURE 30. MEASURED BACK-WALL TEMPERATURE RISES (SW5)

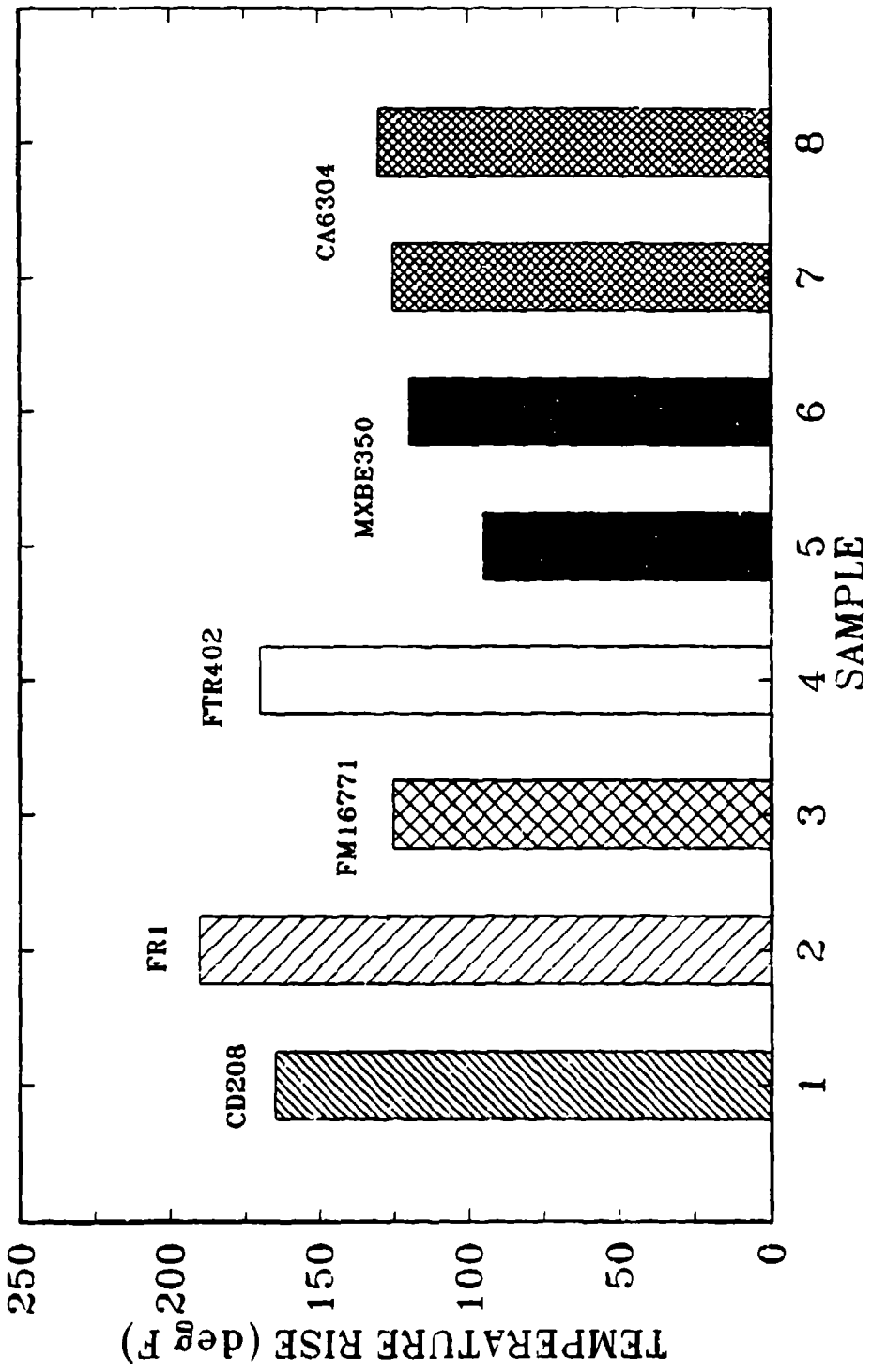

FIGURE 31. MAXIMUM BACK-WALL TEMPERATURE RISES

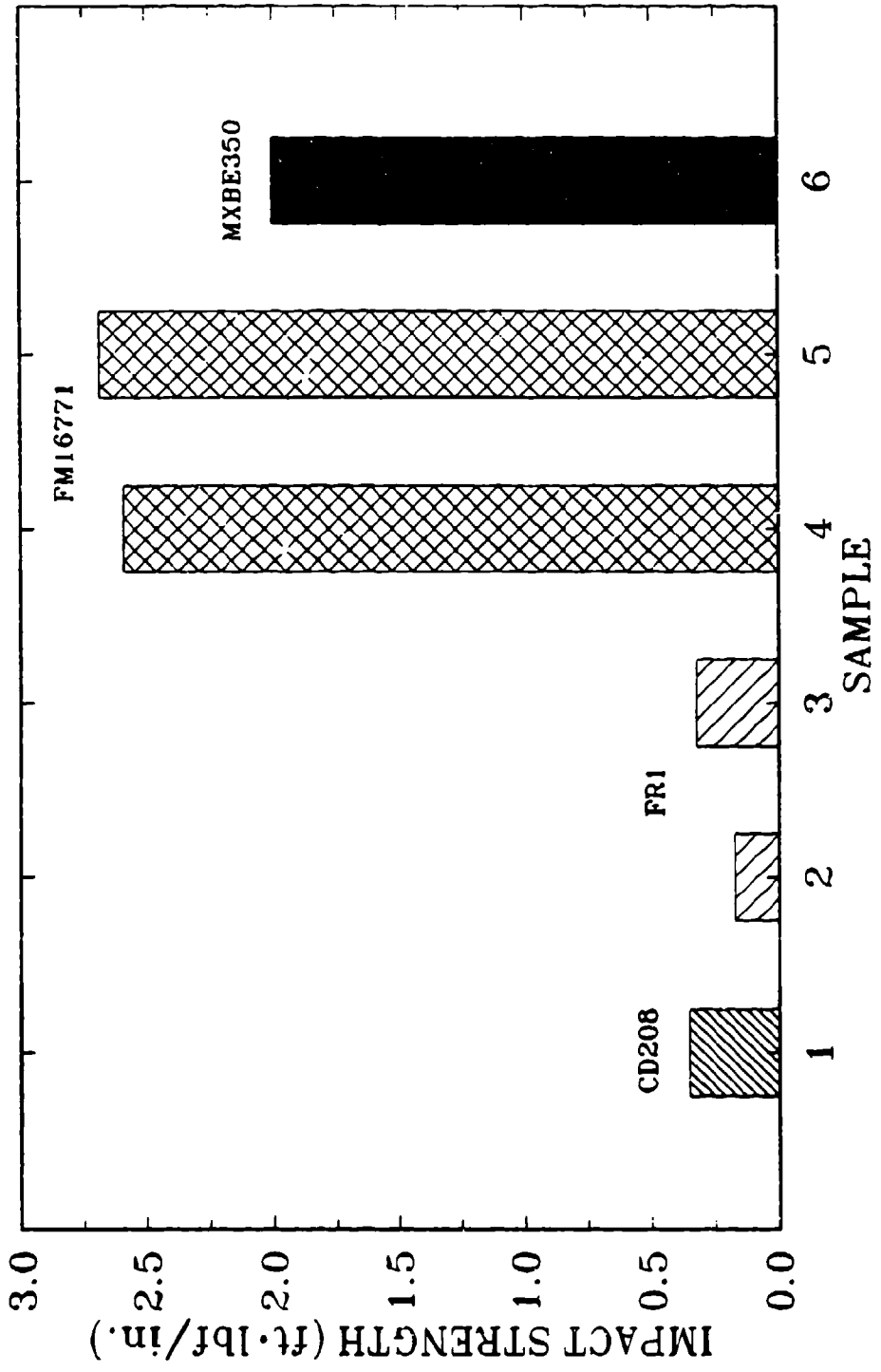

FIGURE 32. IZOD IMPACT STRENGTH

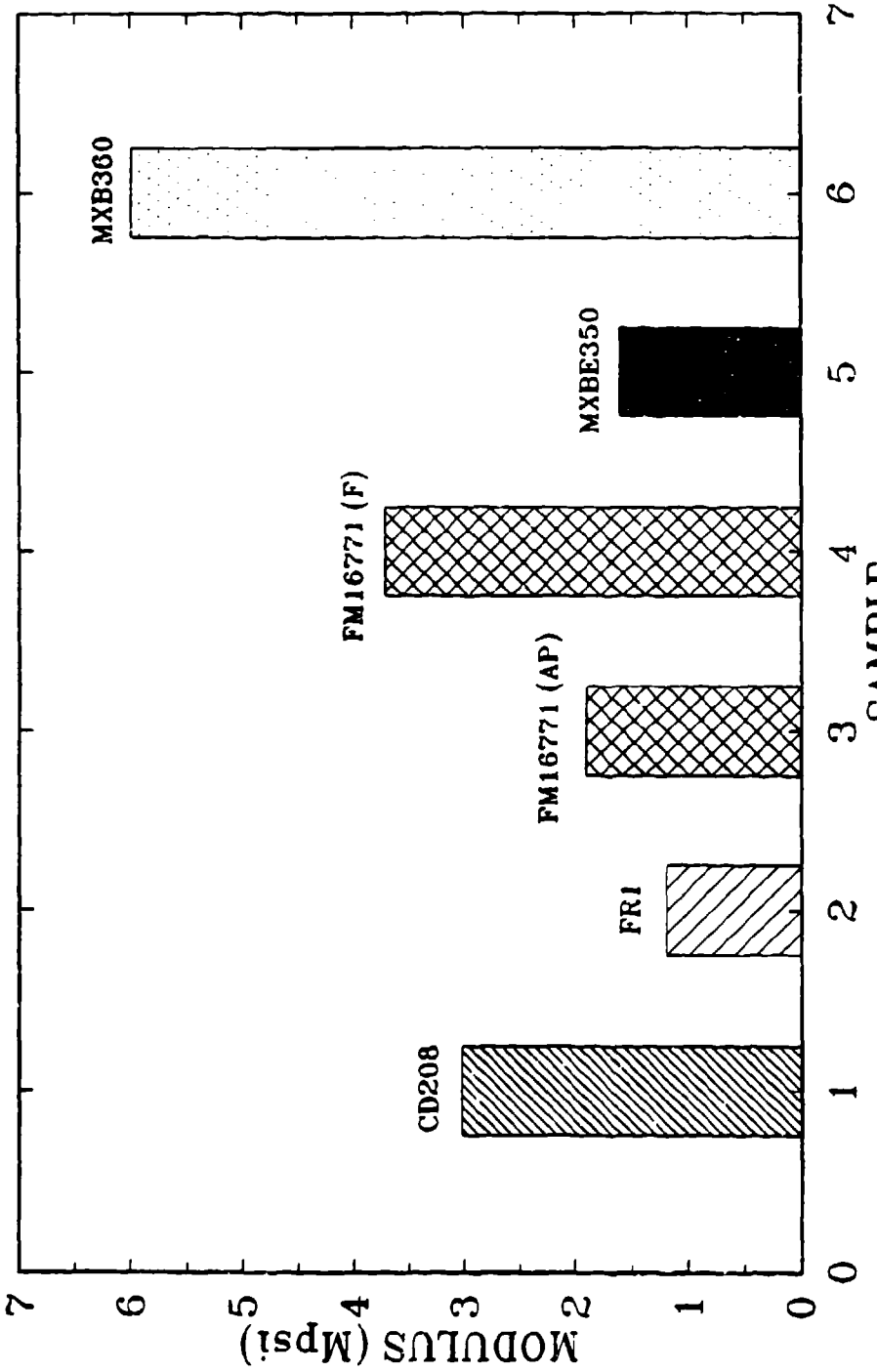

FIGURE 33. NSWCDD MEASURED COMPRESSION MODULUS

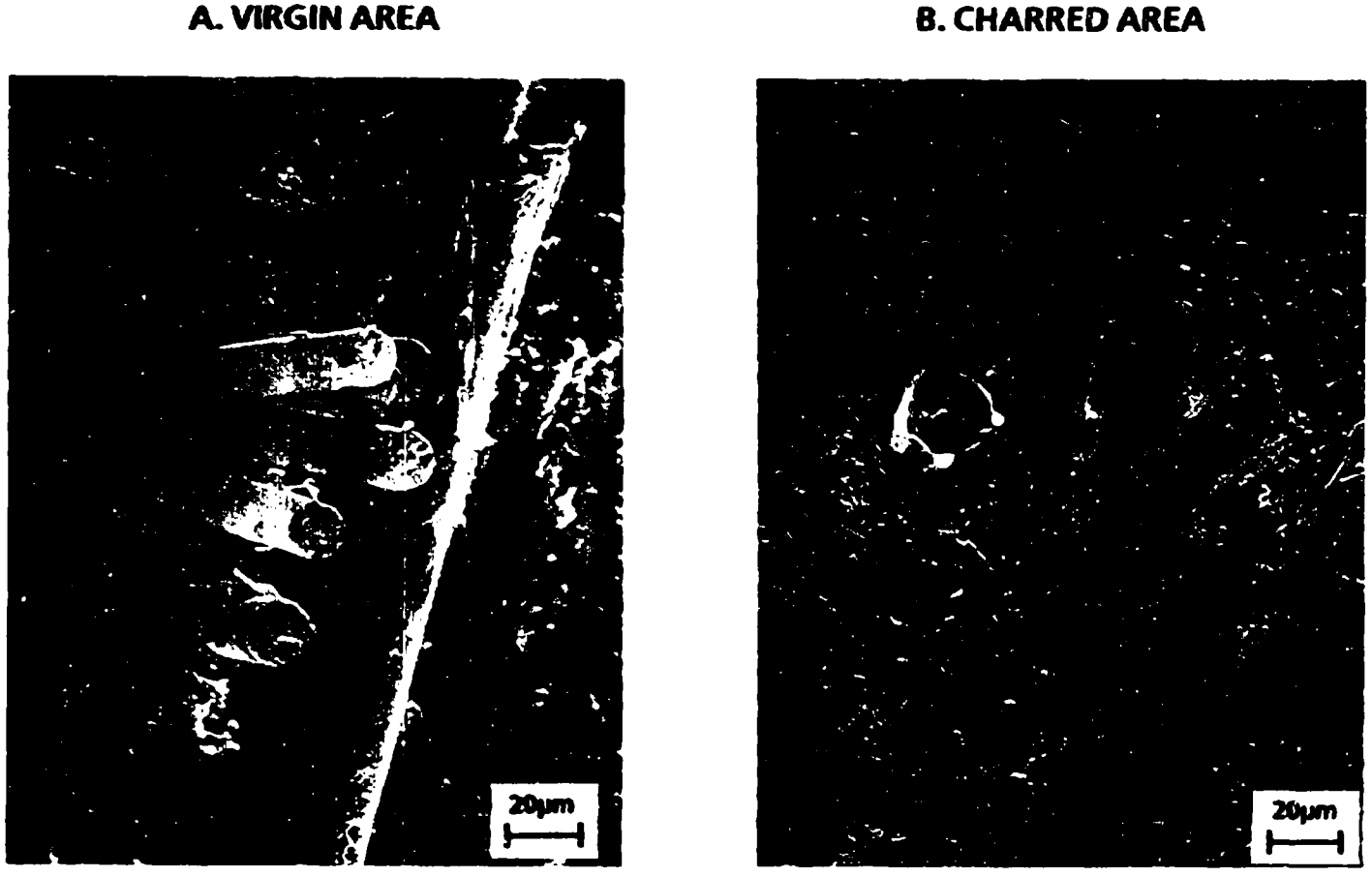

FIGURE 34. SEM MICROGRAPHS OF MXBE350 SAMPLE BEFORE AND AFTER NSWCDD TEST

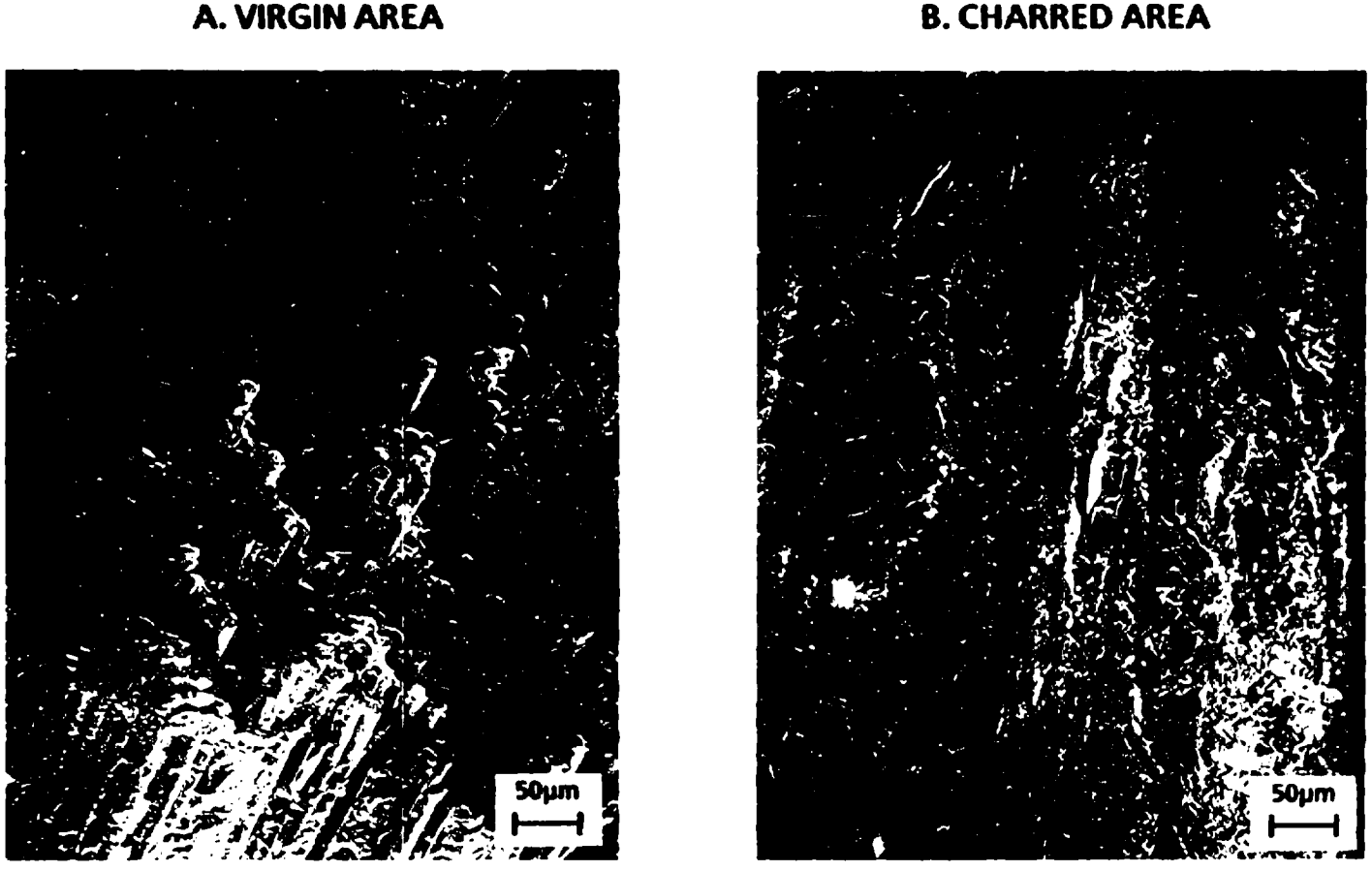

FIGURE 35. SEM MICROGRAPHS OF FM16771 (FIBERITE) SAMPLE BEFORE AND AFTER NSWCDD TEST

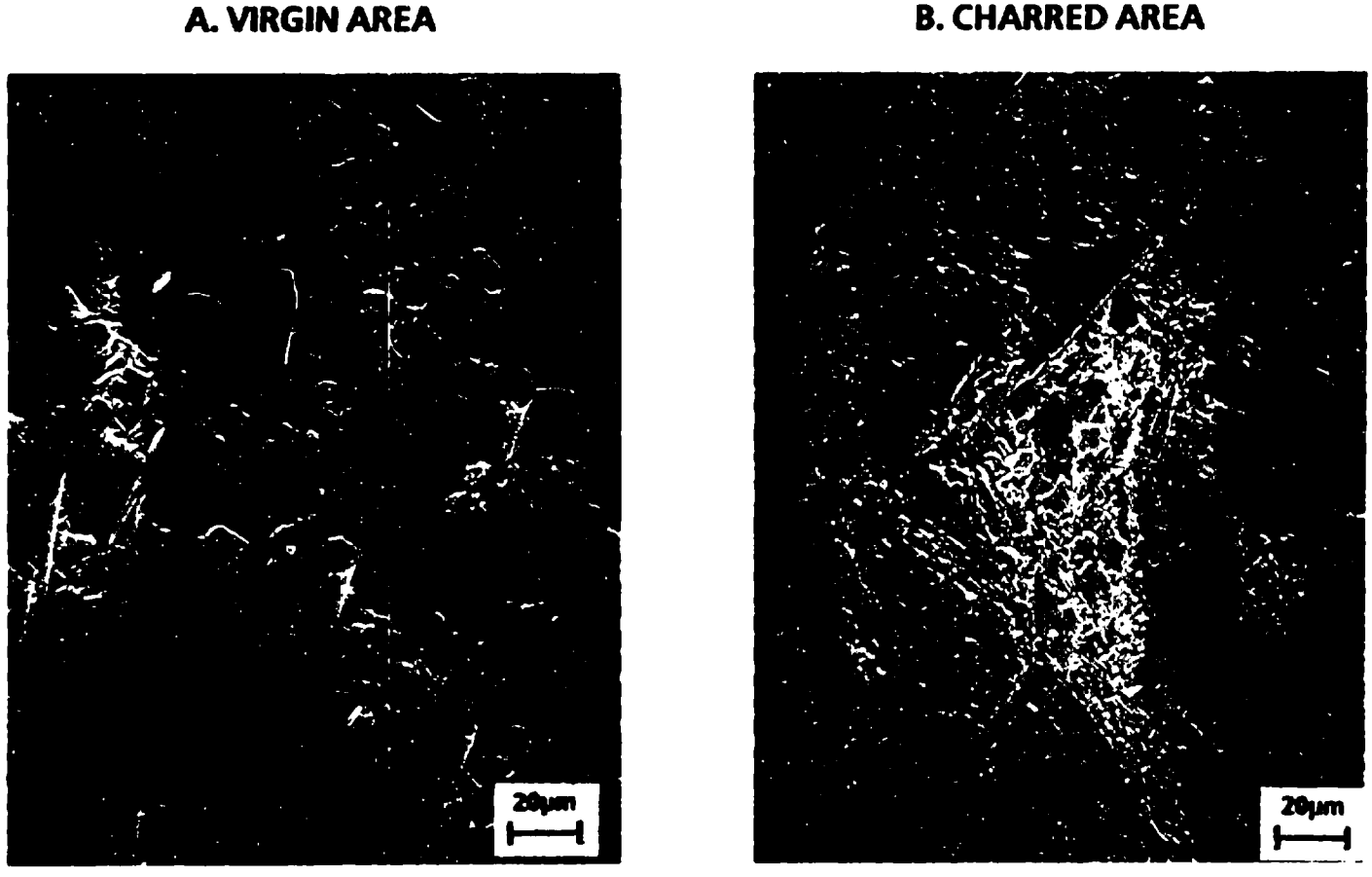

FIGURE 36. SEM MICROGRAPHS OF FM16771 (AMERICAN POLY-THERM) SAMPLE BEFORE AND AFTER NSWCDD TEST

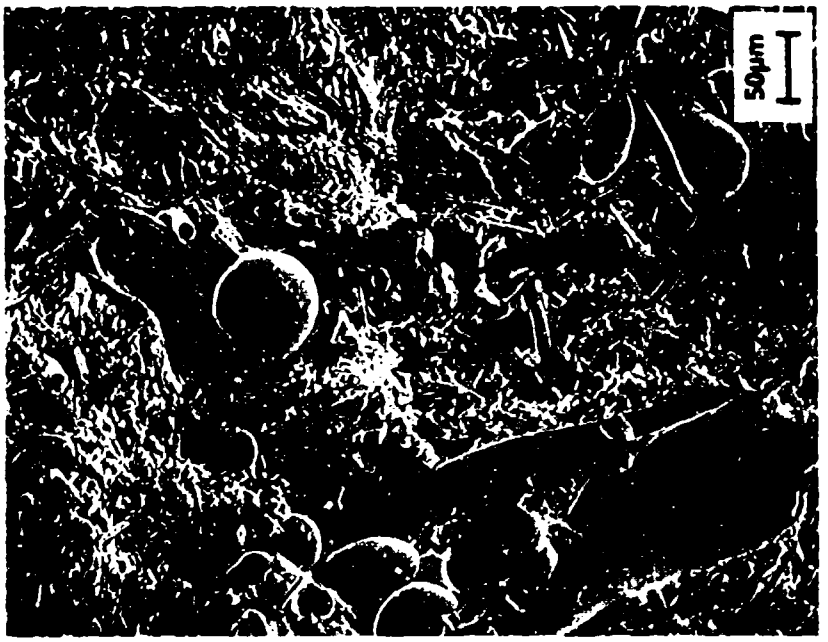

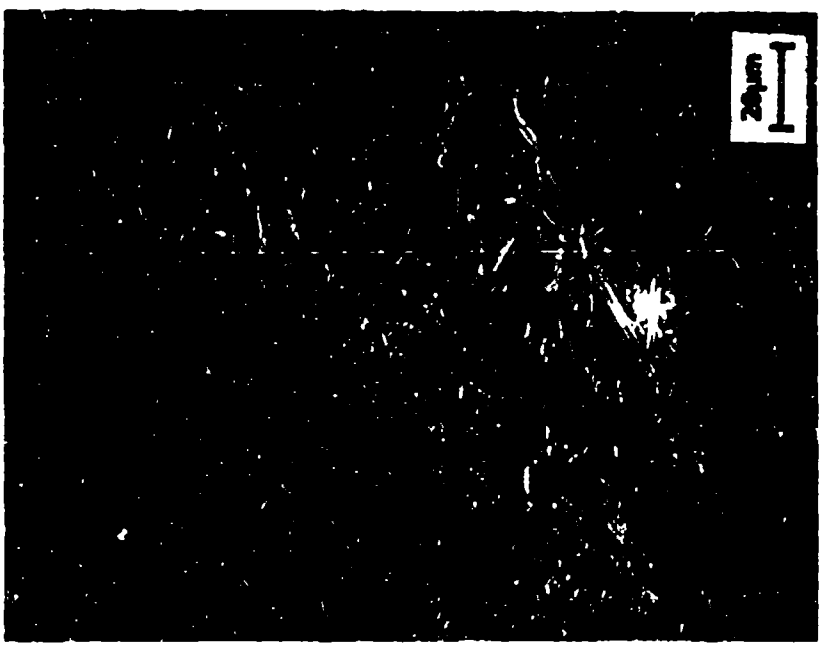

FIGURE 37. SEM MICROGRAPHS OF FR1 SAMPLE (VIRGIN AREA)

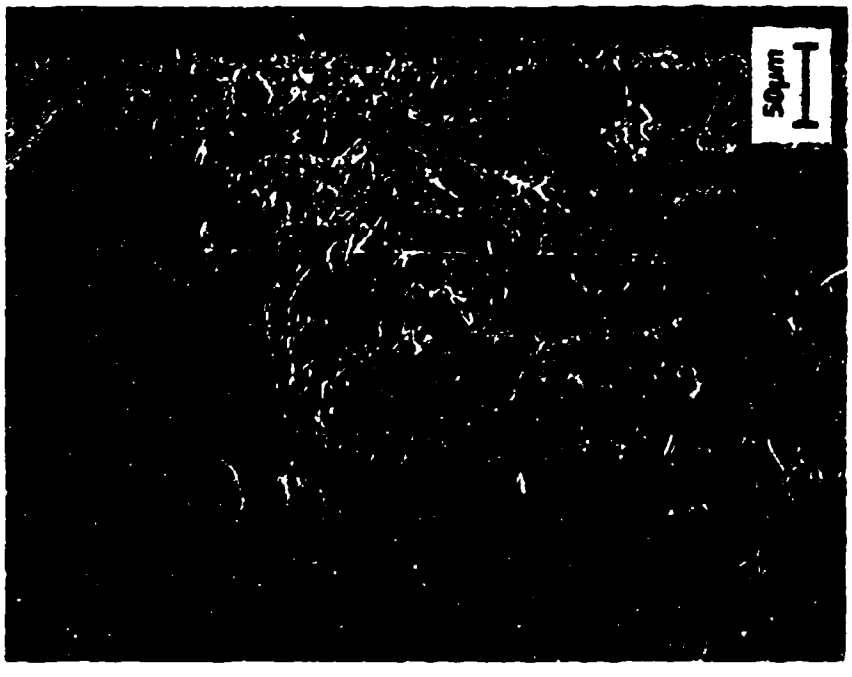

FIGURE 38. SEM MICROGRAPHS OF CD208 SAMPLE (VIRGIN AREA)

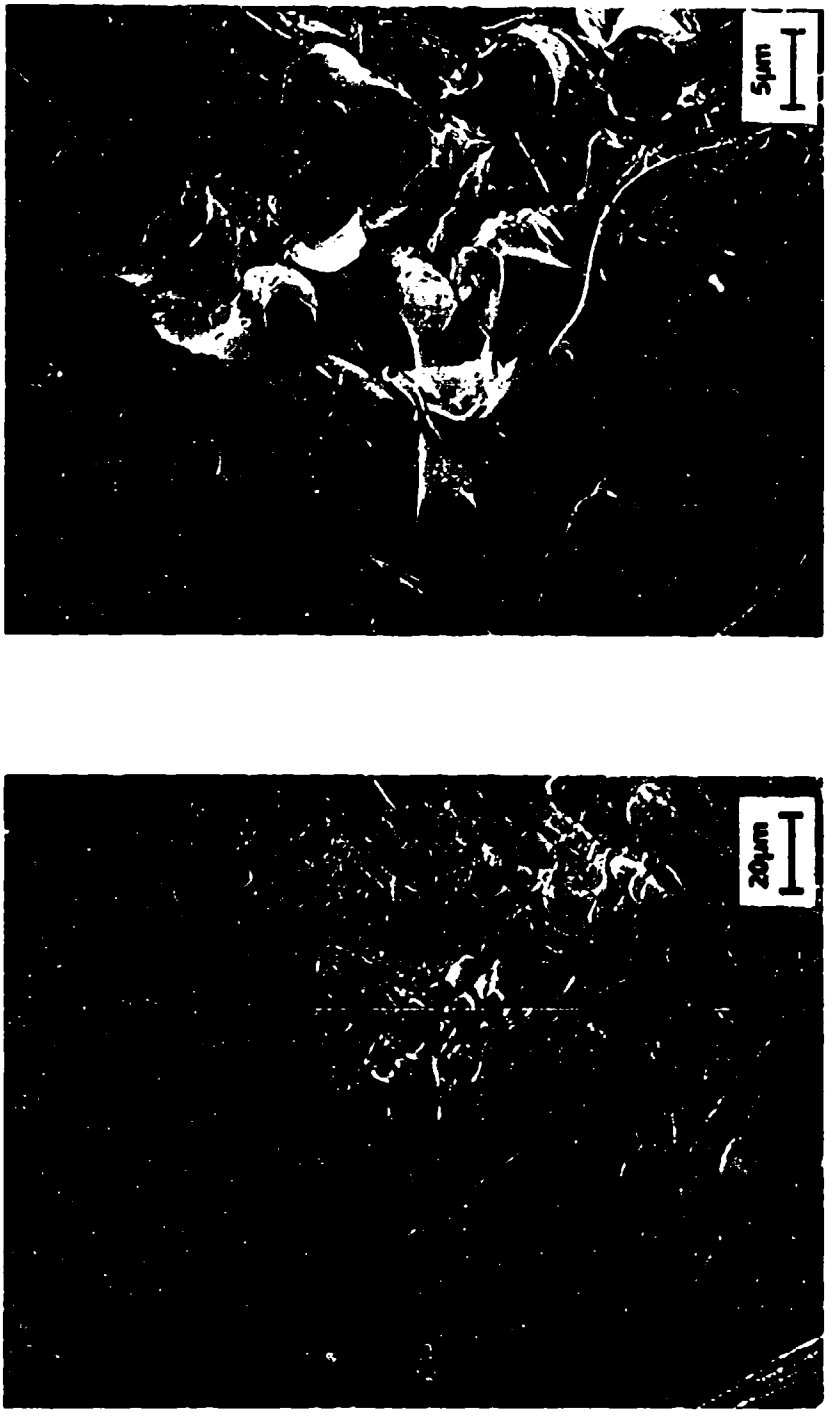

FIGURE 39. SEM MICROGRAPHS OF CD208 SAMPLE (CHARRED AREA)

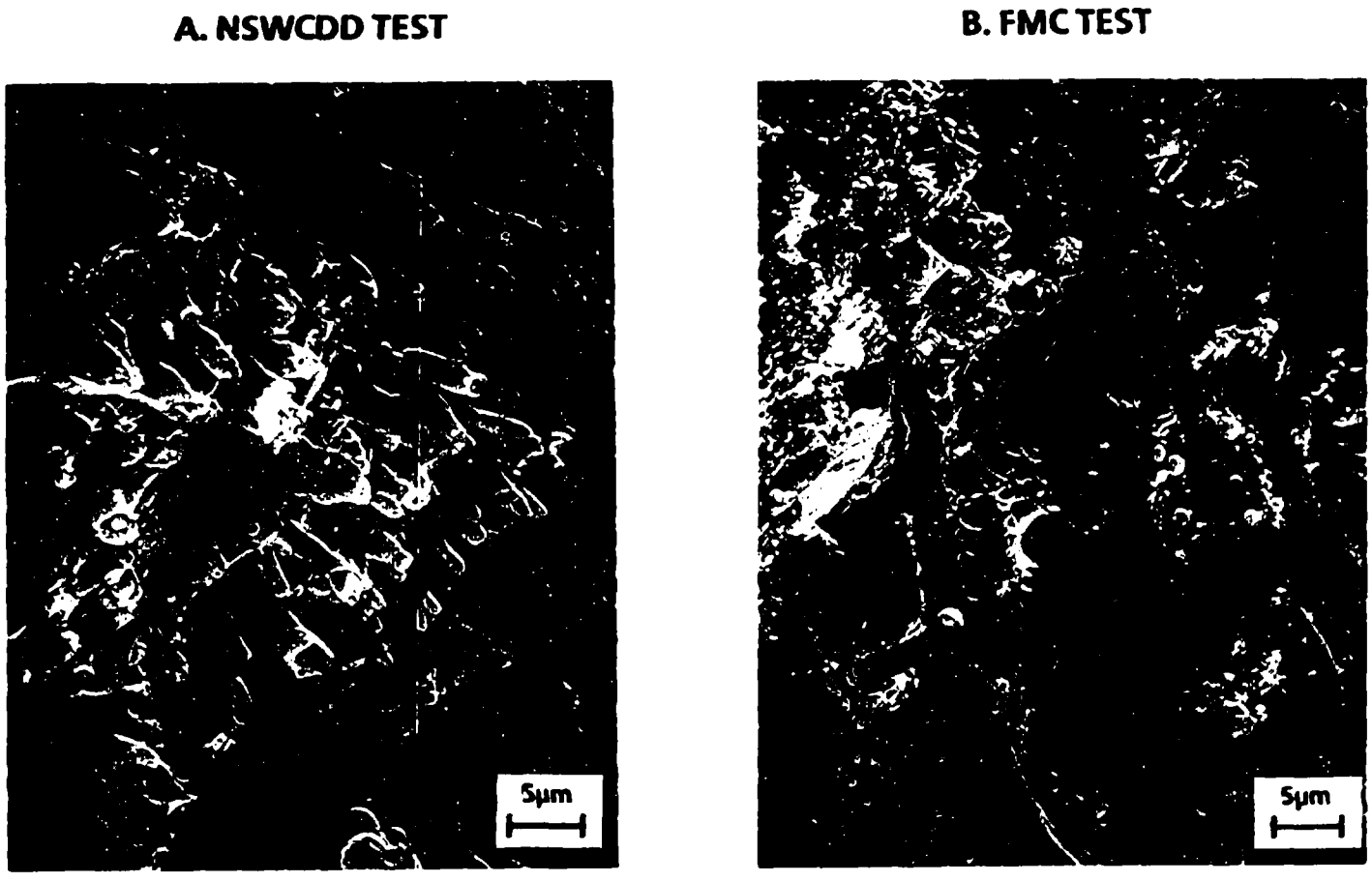

FIGURE 40. SEM MICROGRAPHS OF FR1 SAMPLE AFTER NSWCDD AND FMC TESTS

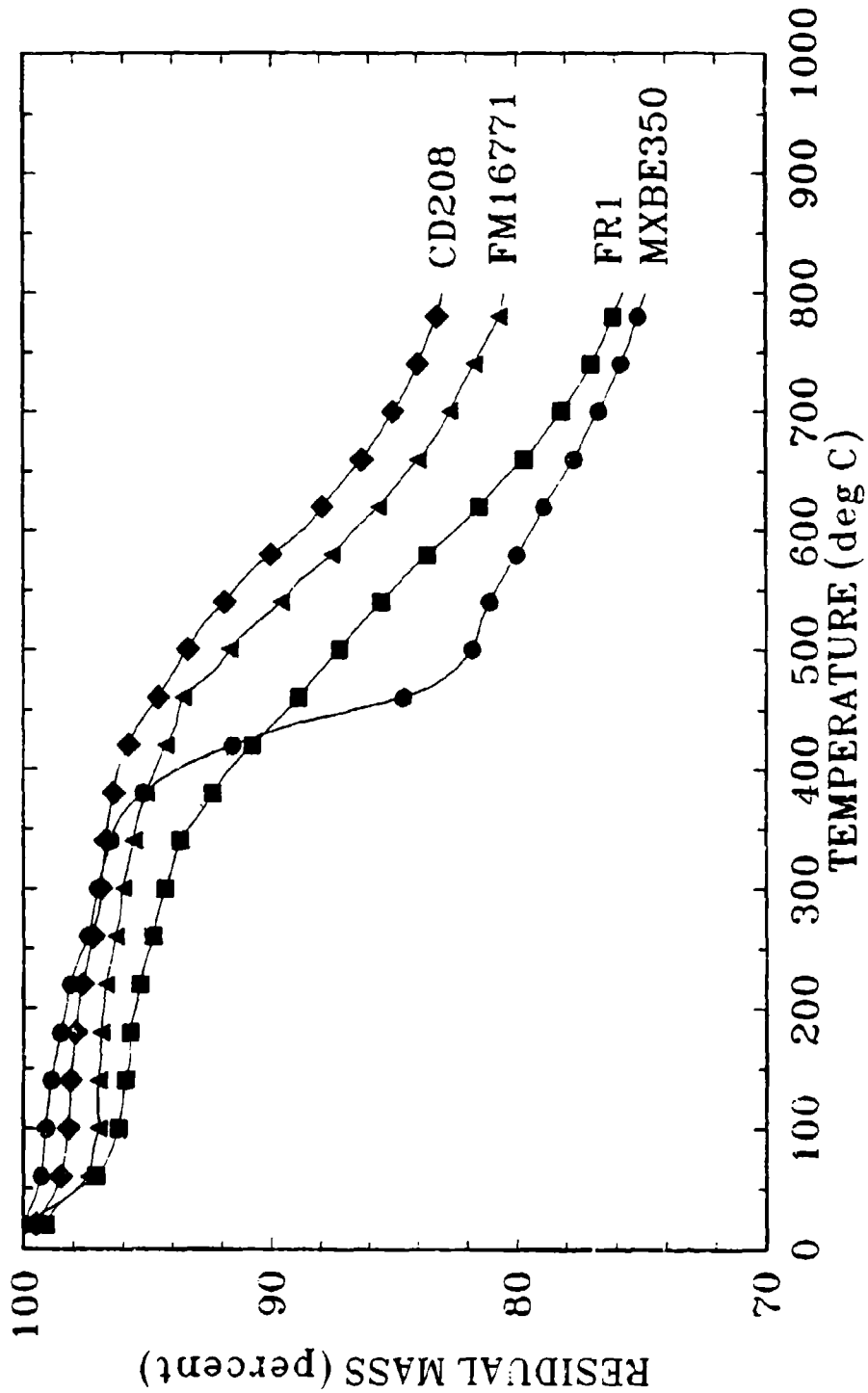

FIGURE 41. TGA IN HELIUM WITH 20°C/min HEATING RATE

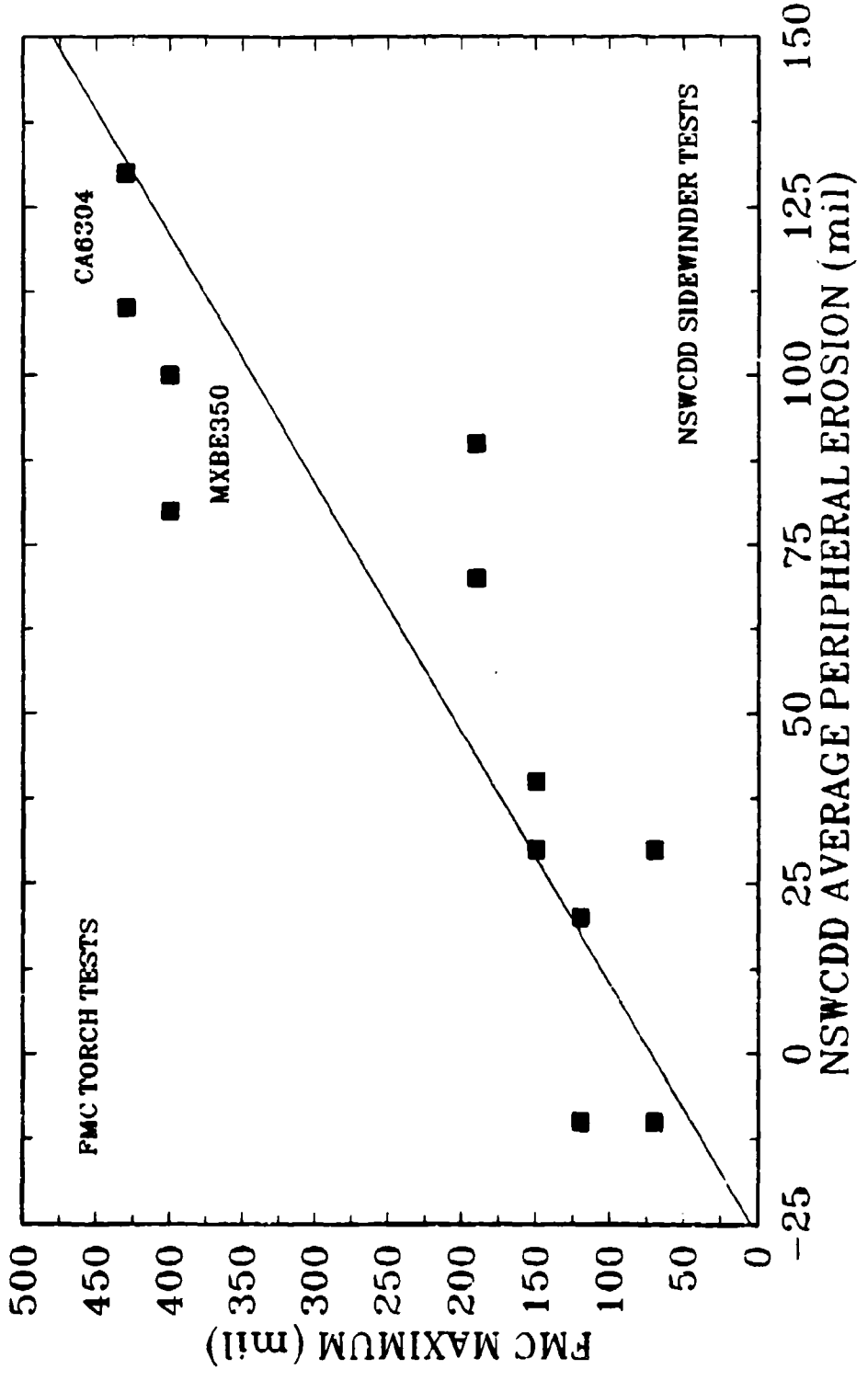

FIGURE 42. CORRELATION BETWEEN NSWCDD PERIPHERAL AND FMC MAXIMUM EROSION DATA

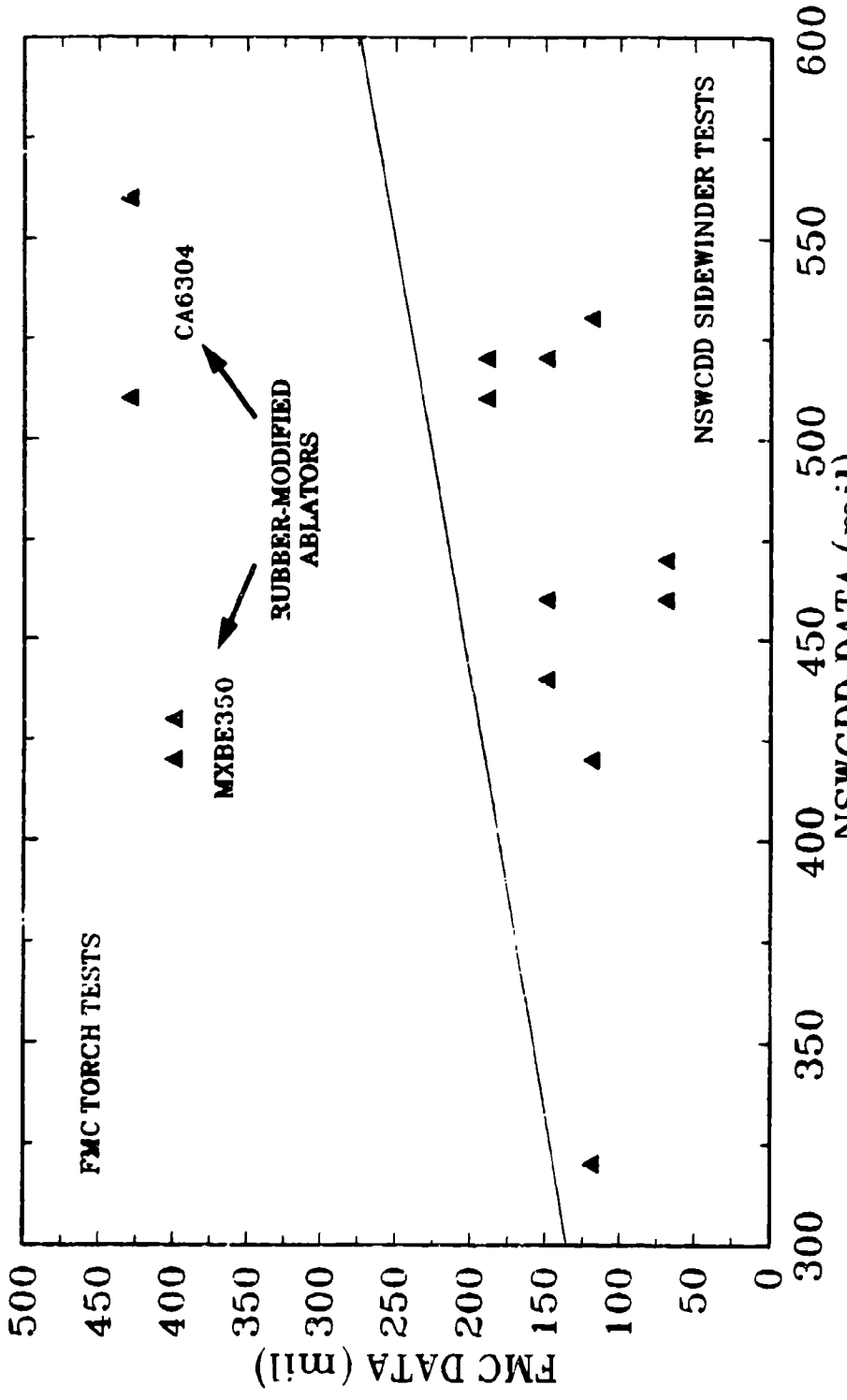

FIGURE 43. CORRELATION BETWEEN NSWCDD AND FMC MAXIMUM EROSION DATA

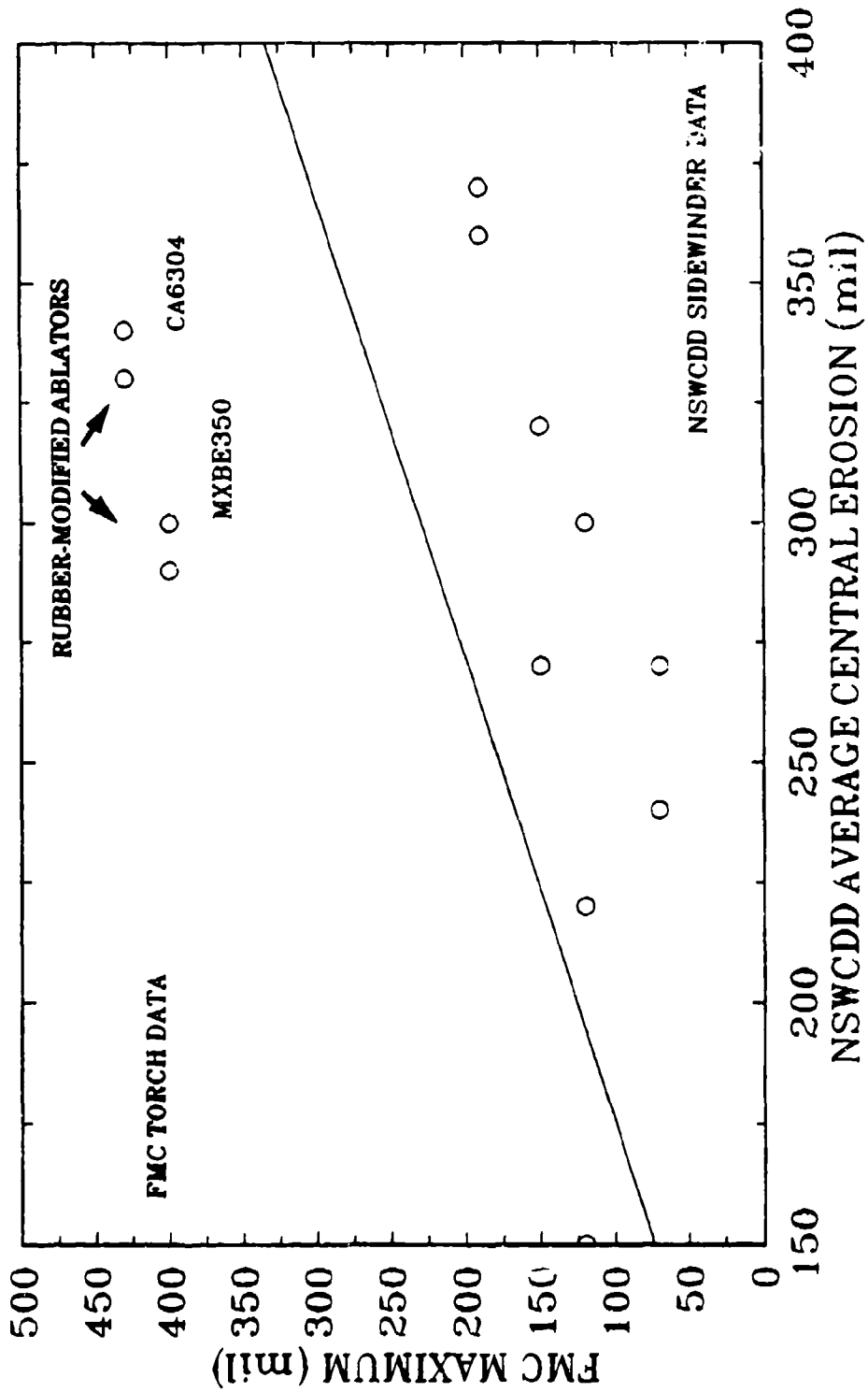

FIGURE 44. CORRELATION BETWEEN NSWCDD CENTRAL AND FMC MAXIMUM EROSION DATA

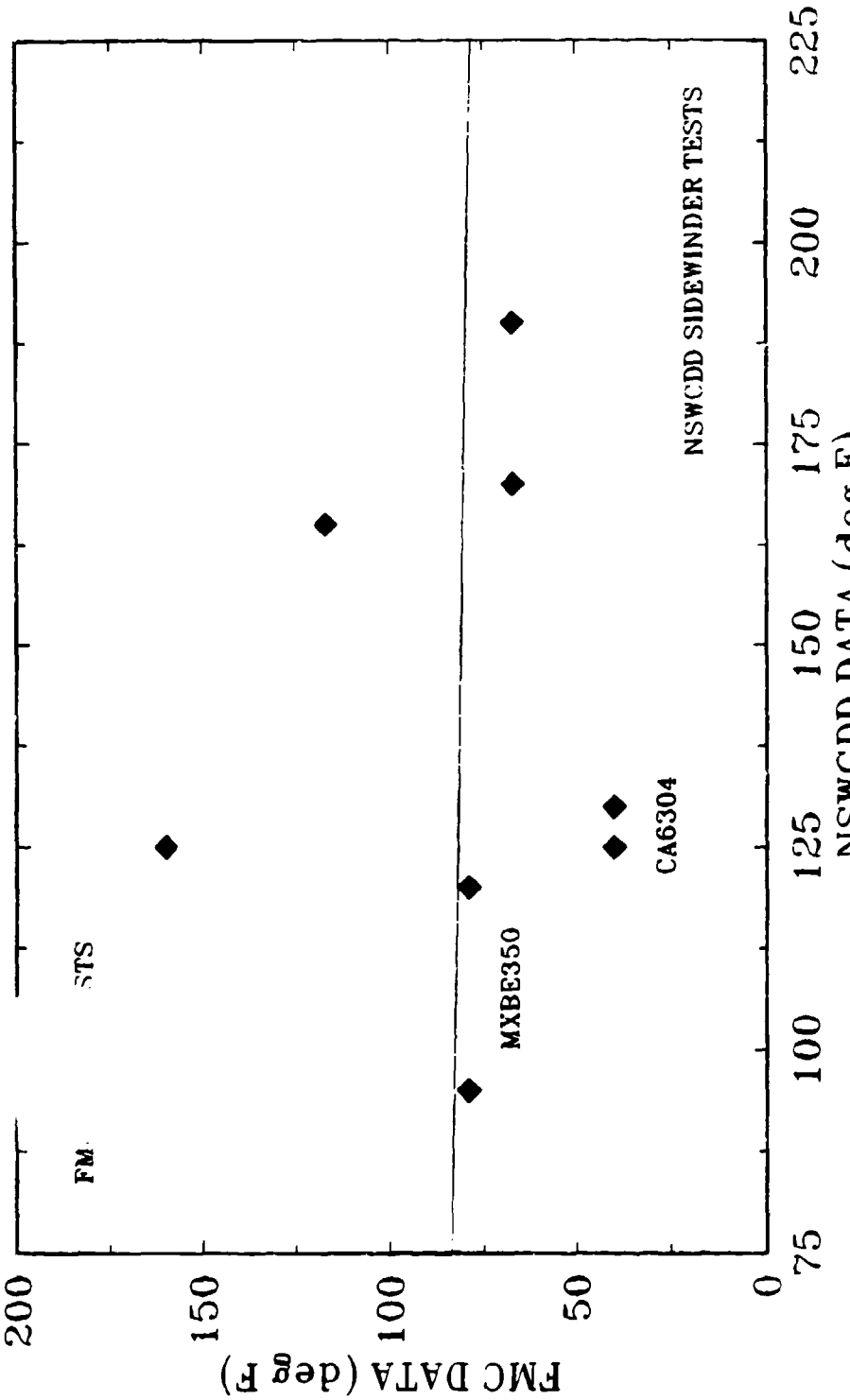

FIGURE 45. CORRELATION BETWEEN NSWCDD AND FMC MAXIMUM BACK-WALL TEMPERATURES

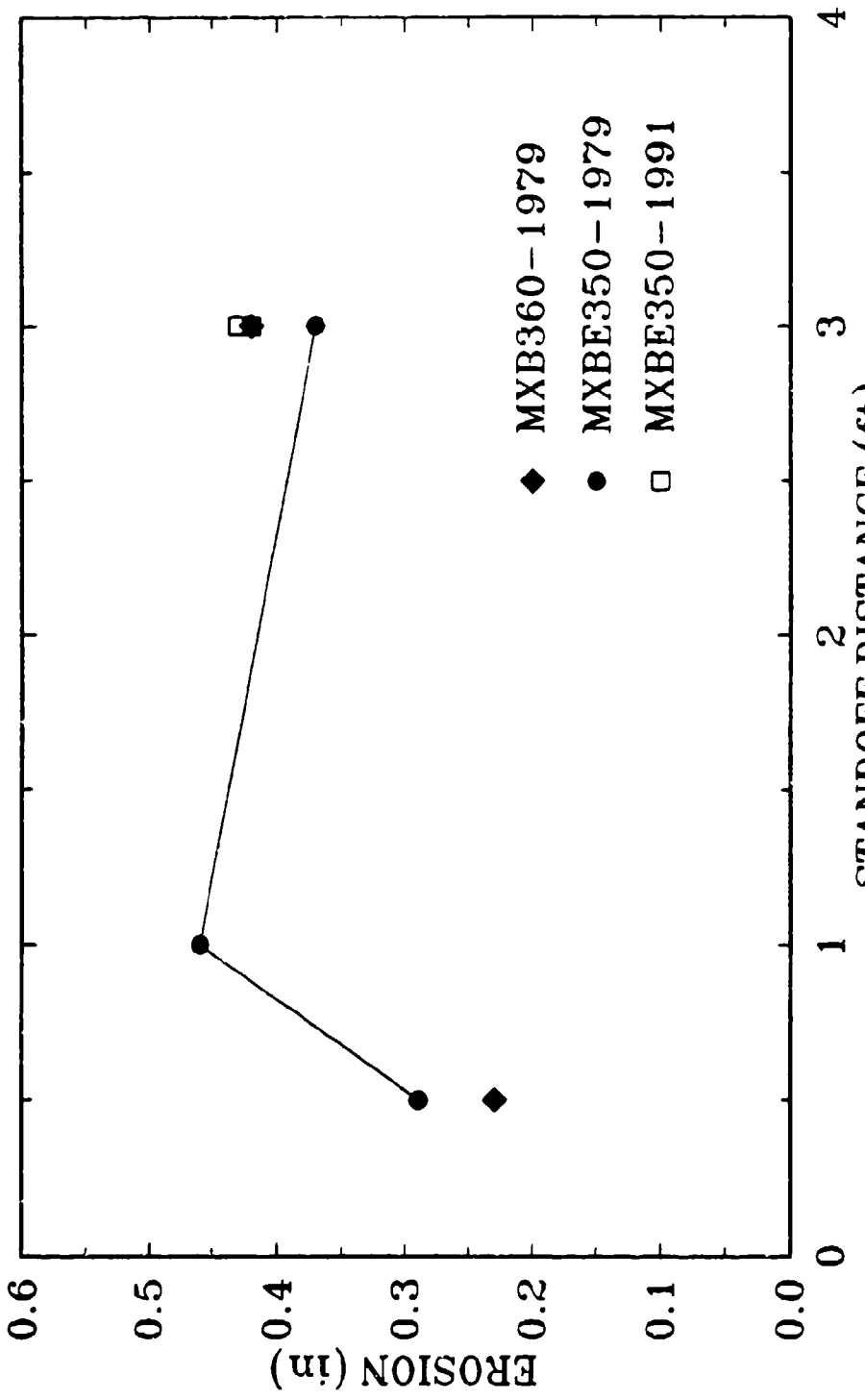

FIGURE 46. COMPARISON OF NSWCDD MAXIMUM EROSION MEASUREMENTS

TABLE 1. CANDIDATE ABLATORS FOR NSWCDD SIDEWINDER TESTS

ABLATOR	SOURCE	MATRIX	REINFORCEMENT	THICKNESS (IN)	THERMOCOUPLE	INCLUDED IN TEST				
						1	2	3	4	5
MXBE350	Swedlow	rubber-modified phenolic	continuous, glass -filament mat	0.74	yes	x	x			x
FM16771	Fiberite	phenolic	chopped glass, roving	0.75	yes	x		x		
FM16771	AP	phenolic	chopped glass, roving	0.75	yes			x	x	
CA6304	Ferro	rubber-modified phenolic	woven fiberglass	0.79	yes		x			x
FTR402	FMI	modified phenolic	2-D glass weave	0.75	yes	x				x
BLM/E	FMI	pyrolyzed phenolic & reimpregnated with structural epoxy	chopped carbon fibers	0.84	yes		x			
C^3	FMI	pyrolyzed phenolic	2-D carbon weave	0.76	yes				x	
FR1	FMI	modified phenolic	chopped ceramic fibers	0.76	yes		x	x		
Blackglas™	Allied Signal	ceramic (densified)	2-D weave of carbon-coated ceramic fibers	0.58-0.74 0.55-0.72	no no				x x	
CD208	Haveg	H41N phenolic	chopped ceramic, carbon, & glass fibers	0.75	yes	x		x		x

REFERENCES

1. Joseph H. Koo, Shan Lin, Michael J. Kneer, and Charles T. Boyer, *Performance of High-Temperature Composite Ablatives under a Hostile Environment*, 37th International SAMPE Symposium and Exhibition, Anaheim, CA, March 1992.

2. A. Chaboki, M.J. Kneer, M.E. Schneider, and J.H. Koo, *Supersonic Torch Facility for Ablative Testing*, AIAA-90-1761, AIAA/ASME 5th Joint Thermophysics and Heat Transfer Conference, Seattle, WA, June 1990.

3. J.H. Koo, M. Kneer, and M. Miller, *Comparison of Ablative Materials in a Simulated Solid Rocket Exhaust Environment*, AIAA- 91-0978, 32nd SDM Structures Structural Dynamics and Materials Conference, Baltimore, MD, April 1991.

4. J. Florio, Jr., *An Analytical and Experimental Investigation of the Decomposition of Glass-filled Polymer Composites*, Ph.D. Thesis, University of RI, 1989.

5. J.C. Glaser, Ablative Structural Characterization, TI F1007-051, FMC letter LS91148.ST of 16 December 1991.

6. Fiberite Product Data Sheet: FM 16771 Natural, 17 June 1991.

7. Ferro Product Data Sheet: FERROPREG CA-6304/1583 PHENOLIC/SILICA.

8. FMI Product Data Sheet: FTR 402 FIRE RESISTANT RESIN/PREPREG.

9. S. Stephenson, private conversation, FMI, 28 March and 21 May 1991.

10. Allied Signal Product Data Sheet entitled Blackglas™ TECHNOLOGY.

11. S. Gonczy, private conversation, Allied Signal, 8 May 1991.

12. J.G. Sakonia, Blackglas™, Allied Signal, Inc. letter of 1 November 1990.

13. Earle E. Biermann and A.B. Coates, *Rocket Motor Blast Effects and Proposed Ablative Protection for RAM Launching System EX 43*, NSWC TR 79-346, Naval Surface Warfare Center, Dahlgren, VA, October 1979.

14. G. Soo Hoo, G.R. Moore, and L.P. Anderson, *Supersonic Impingement Flow upon a Flat Plate*, CPIA Publication 332, Volume 1, JANNAF 12th Plume Technology Meeting, Colorado Springs, CO, November 1980.

15. Standard Operating Procedure Number G60-80-40 of 28 Sept 1990; subject: Restrained Rocket Firing Evaluation of Blast Protective Materials.

16. B. Hecht, private conversation, Haveg, 25 July 1991.

APPENDIX A

PROCEDURES FOR TESTING ABLATIVE SAMPLES WITH SIDEWINDER ROCKET MOTORS (01/15/92)

TEST NO ___
(___/___/___)
PLATE NO ___

Checklist

Procedures for Testing Ablative Samples
with Sidewinder Rocket Motors
(01/15/92)

Check out test stand and other ancillary equipment

____ 1. Verify pull test is current.

____ 2. Verify motor stand is all there.

____ 3. Verify dummy motor and laser are available and working.

____ 4. Verify MK 36 MOD 5, 6, 7, 8, or 10 Sidewinder motors are available.

____ 5. Prepare ammunition component request (for Sidewinder motors).

____ 6. Prepare Test Planning Record.

____ 7. Request firing date from range control.

____ 8. Verify there is enough FLEXFRAM 605TH for mounting and making a border.

____ 9. Verify there are enough Omega type-K foil thermocouples (CO1-K) for measuring back wall temperature.

____ 10. Verify the necessary instrumentation is available:

____ a. 6 Type-K thermocouple reference junctions (2 spares),

____ b. 6 Type-K thermocouple extension wire leads (2 spares) or 6 pair cable if reference junctions are near target,

____ c. lay cables and check for continuity and shorts,

____ d. NEXTEL fabric to wrap thermocouples wires directly behind the aluminum plate,

____ e. 6 amplifiers,

____ f. Tape recorder,

____ g. 2 VCR cameras, and

____ h. 35 mm camera with 2 rolls of 36 exp film.

PROCEDURES FOR SIDEWINDER ABLATOR TESTS page 2

Check out aluminum plates

____ 1. Locate the needed number of aluminum plates with thermocouple holes.

____ 2. Clean off mounting surface on plate.

____ 3. Make sure plates are flat.

Initial check of test samples

____ 1. Make an inventory card for each sample.

____ 2. Measure and record sample thickness and other dimensions.

____ 3. Check for two perpendicular sides (sides adjacent to other samples).

____ 4. Machine samples if necessary.

Gauge each ablator sample before mounting it on aluminum plate

____ 1. H13 will mark the left and bottom edges and front of each sample.

____ 2. Take the 4 samples to the gauge lab.

____ 3. Weigh each of the 4 samples separately.

____ 4. Measure the thickness of each ablator sample using a 1-inch grid in both vertical and horizontal directions.

____ a. **It is essential that the same grid locations be used used to gauge the ablators both before and after the test.**

____ b. **A sketch of the gauging grid will be provided to the gauge lab along with the appropriate data sheets.**

____ c. The grid is laid out on 1-inch intervals along both the left and bottom edges of the ablator sample.

____ d. There will be a minimum of 11 rows and 11 columns of grids, rows are parallel to the bottom edge and columns are parallel to the inside vertical edge.

Mount ablator samples onto aluminum plate

_____ 1. Locate center of plate relative to 4 thermocouple holes and scribe a horizontal line through the plate center midway between the upper holes and the lower holes.

_____ 2. Scribe a vertical line through the plate center midway between the right two holes and those on the left.

_____ 3. Notch the 4 edges of the plate with a file where the lines intersect the edges.

_____ 4. Power brush, with stiff-bristled wire brush, or glass peen entire front surface of aluminum plate **(do this outside away from assembly area).**

_____ 5. Wipe entire front surface of aluminum plate with fast drying solvent.

_____ 6. Identify the best two perpendicular sides of each ablator sample to be adjacent to other ablator samples.

_____ 7. Identify the flat side of each ablator for bonding to the aluminum plate (for uniform bondline thickness).

_____ 8. Remove tape, labels from the side of ablator to be bonded to plate.

_____ 9. Use sandpaper or wire brush to roughen bonding surface of each piece of ablator to remove glossy surface **(do this outside away from assembly area).**

_____ 10. Cover the heated surface of each sample with green ordnance tape to keep that face clean.

_____ 11. Wipe ablator bonding surface clean with water.

_____ 12. Thoroughly mix part A.

_____ 13. Add part A to part B mixing thoroughly and scraping can walls several times.

_____ 14. Use within 30 minutes.

_____ 15. Apply FLEXFRAM in center of aluminum plate and spread toward edges, **don't** fold over on self.

Mount ablator samples onto aluminum plate (continued)

____ 16. Spread the FLEXFRAM over the entire front surface of the aluminum plate with a notched trowel with all ridges running 90° to the bottom of the plate.

____ 17. Scribe a line in the soft FLEXFRAM between the 2 side notches, and through the center of the plate, then scribe a vertical line in the soft FLEXFRAM between the 2 top notches, and through the center of the plate.

____ 18. Apply FLEXFRAM in center of ablator and spread toward edges, **don't** fold over on self.

____ 19. Spread the FLEXFRAM over the entire bonding surface of the first ablator with a notched trowel, all ridges running parallel to the bottom of aluminum plate.

____ 20. Apply a coat of FLEXFRAM on the 2 inside edges of the first ablator sample, providing 'grout' between the samples.

____ 21. Lay the ablator sample down on the aluminum plate with the 2 square sides toward other ablator samples, making sure the corner of the ablator is at the center of the aluminum plate.

____ 22. Repeat this process for the 3 remaining ablator samples and insuring the FLEXFRAM 'grout' gap is about 30 mils thick and that FLEXFRAM oozes out of the gap, everywhere, between the samples.

____ 23. Squeeze the 4 samples together laterally.

____ 24. Clamp the 4 samples down on the aluminum plate with 2-2x4's and 4 C-clamps for 24 hours, to allow the FLEXFRAM to cure.

____ 25. Then scrape off any excess FLEXFRAM from the front of the 4 ablator samples **immediately**.

____ 26. Clean FLEXFRAM out of the thermocouple holes entirely so that the foil thermocouple can be bonded on to the back of each ablator sample.

____ 27. Form a 3/4-inch-thick FLEXFRAM border around the 4 ablative samples insuring the FLEXFRAM covers the sides of the samples entirely.

____ 28. Patch FLEXFRAM border under 2x4's later if necessary.

Instrumenting the 4 ablator samples

____ 1. Once the FLEXFRAM is thoroughly cured then take the green ordnance tape off the heated sample surfaces.

____ 2. Check each thermocouple for continuity before it is installed.

____ 3. The foil thermocouples will be applied to the back of each sample once the ablator samples have been gauged **(Omega type-K (CO1-K) foil gauges and high conductivity adhesive will be used to attach the thermocouples)** hold the gauge in place with a bent popsicle stick.

____ 4. After the gauge adhesive is cured, check the thermocouple for continuity.

____ 5. Heat each of the 4 thermocouple junctions with heat gun and check for output at ends of leads.

____ 6. Take close up photo of back of aluminum plate so you can see at least one thermocouple.

Test day installation of ablator samples and instrumentation checks

____ 1. Mount the dummy motor with laser in the restraint stand.

____ 2. Place the aluminum plate in the test stand and adjust its position so that the laser shines on the intersection of the 4 ablator samples.

____ 3. Secure the aluminum plate in place and verify the laser still shines on this intersection.

____ 4. Remove the dummy rocket motor with laser from restraint stand.

____ 5. Set up both VCR cameras to view the entire motor and the 4 ablator samples, 45° view angles from each side of the motor centerline.

____ 6. Take still photos of each of the ablator samples from one side and above **(make sure you can read the ablator label in the photo)** including the FLEXFRAM border.

____ 7. Take a still photo of the entire test including stand, motor and 4 ablator samples.

Test day installation of ablator samples and instrumentation checks (continued)

____ 8. **Insulate each thermocouple lead from the back of the aluminum plate to reference junction using 2 layers of NEXTEL adhesive-backed tape.**

____ 9. Connect the 4 thermocouples to the reference junctions, amplifiers, and leads back to the instrumentation shelter.

____ 10. Wrap the reference junctions in NEXTEL cloth and put them inside a steel ammo box.

____ 11. Place a 1-inch steel plate between the aluminum plate and the ammo box **(the steel plate completely fills the space between the inner angle iron supports)** being careful not to cut the thermocouple leads.

____ 12. Clamp the ammo box inside the center of the steel support grid behind the middle of the sample mounting plate.

____ 13. Mount the horizontal threaded rod in the slanting back supports of the stand holding the aluminum plate.

____ 14. Wrap the bundle of thermocouple leads in a NEXTEL cloth strip from the reference junctions all the way back to the sand bags behind the test stand.

____ 15. Check all 4 thermocouple circuits from the recorder back to the thermocouples by spraying compressed (cold) gas on each thermocouple.

____ 16. **Do a 500°F in-line pretest calibration of each thermocouple.**

____ 17. Replace any faulty instrumentation **including a bad foil thermocouple.**

____ 18. Take still photo of the instrumentation leads, reference junctions, and amplifiers.

____ 19. Start both VCR cameras at 5 minutes prior to test.

Posttest inspection and gauging of ablators

____ 1. **Do a 500°F in-line posttest calibration of each thermocouple.**

____ 2. Take a still photo of the entire test including stand, motor, and 4 ablator samples.

Posttest inspection and gauging of ablators (continued)

____ 3. Take still photos of each of the ablator samples from one side and above including the FLEXFRAM border.

____ 4. Take still photos of the instrumentation lead ference junction and amplifiers.

____ 5. Take VCR photos of test setup while walking back toward it and take close ups of: (1) the entire front of the 4 samples and border, (2) the back side of the aluminum plate, (3) the rocket motor, and (4) the instrumentation.

____ 6. Take the entire aluminum plate and 4 ablator samples to the building 278 before removing the samples (be careful not to drop the plate).

____ 7. Heat the back of the aluminum plate so the FLEXFRAM will decompose and release the samples from the aluminum plate (be careful not to crack the samples by bending them).

____ 8. This is an optional step and is used only when R31 needs to evaluate the char layer characteristics. Take the 4 samples to R31 at White Oak for analysis of a partial section of each of the 4.

____ a. Allow R31 to carefully cut a small triangular (1/2-inch side by 10-inch side) section from along one inside edge of each sample (taking care not to damage the char or aluminum oxide layers).

Note: an inside edge is one adjacent to another ablator sample.

____ b. R31 will evaluate the heat-effected zone of each sample, using scanning electron microscopy (SEM), to determine the character and thickness of the aluminum oxide and surface char layers on the small section removed from each sample (R31 will look at several radial distances from the center of impingement).

____ 9. H13 will carefully heat and scrape the FLEXFRAM from off of the back of each sample (taking care not to remove the char or aluminum oxide layers on the heated surface).

____ 10. H13 will carefully remove any loose aluminum oxide by hand (use NO tools or brushes) from the heated surface. Take care not to damage the char layer.

Posttest in . ion and gauging of ablators (continued)

11. Gauging with the **aluminum oxide** present.

____ a. Carefully remove the FLEXFRAM from the back of the sample.

____ b. Take the 4 samples to the gauge lab.

____ c. Weigh each of the samples separately.

____ d. **It is essential that the same grid locations always be used to gauge the ablators.**

____ e. The grid is laid out on 1-inch intervals along both the left and bottom edges of the ablator samples.

____ f. There may be some missing gauging points (some points may have been removed in the triangular section) **so be careful how measuring grid is set up and data is recorded.**

____ g. **A sketch of the gauging grid (the location of the missing triangular section will be indicated if it is missing) shall be provided to the gauge lab along with the appropriate data sheets.**

12. Gauging with the **aluminum oxide** removed.

____ a. Carefully remove the aluminum oxide coating by hand (do <u>not</u> use a wire brush).

____ b. Take the 4 samples to the gauge lab.

____ c. Weigh each of the samples separately.

____ d. **It is essential that the same grid locations always be used to gauge the ablators.**

____ e. The grid is laid out on 1-inch intervals along both the left and bottom edges of the ablator samples.

____ f. There may be some missing gauging points (some points may have been removed in the triangular section) **so be careful how measuring grid is set up and data is recorded.**

____ g. **A sketch of the gauging grid (the location of the missing triangular section will be indicated if it is missing) shall be provided to the gauge lab along with the appropriate data sheets.**

13. Gauging with the **char layer** removed (**optional**).

____ a. The char layer will be removed by vigorous scraping with a wire brush.

____ b. Take the 4 samples to the gauge lab.

____ c. Weigh each of the samples separately.

____ d. **It is essential that the same grid locations always be used to gauge the ablators.**

____ e. The grid is laid out on 1-inch intervals along both the left and bottom edges of the ablator samples

____ f. There may be some missing gauging points (some points may have been removed in the triangular section) **so be careful how measuring grid is set up and data is recorded.**

____ g. **A sketch of the gauging grid (the location of the missing triangular section will be indicated if it is missing) shall be provided to the gauge lab along with the appropriate data sheets.**

APPENDIX B

EROSION MEASURED IN NSWCDD SIDEWINDER TESTS

TABLE B-1. AVERAGE MEASURED PERIPHERAL[8] EROSION IN NSWCDD SIDEWINDER TESTS

MATERIAL TESTED	MANUFACTURER	TEST	NSWCDD AVERAGE MEASURED PERIPHERAL EROSION (IN)[3]	FMC MEASURED MAXIMUM EROSION (IN)[1]
FR1	FMI	SW3	-0.01[6]	0.07
CD208	Haveg	SW3	-0.01[9]	0.12
BLM/E	FMI	SW2	0.00	(note 5)
CD208	Haveg	SW1	0.02	0.12
CD208	Haveg	SW5	0.02	0.12
FM16771	Fiberite	SW1	0.02	—
FR1	FMI	SW2	0.03[2]	0.07
FM16771	AP	SW3	0.03	0.15
FM16771	Fiberite	SW3	0.03	—
FM16771	AP	SW4	0.04	0.15
FTR402	FMI	SW1	0.07	0.19
MXBE350	Swedlow	SW2	0.08	0.40
MXBE350[4]	Swedlow	SW1	0.09	—
FTR402	FMI	SW5	0.09	0.19
MXBE350	Swedlow	SW5	0.10	0.40
CAS304	Ferro	SW2	0.11	0.43
CA6304	Ferro	SW5	0.13	0.43
Blackglas™	Allied Signal	SW4	(no test)	(note 5)
Blackglas™	Allied Signal	SW4	(no test)	(note 5)
C[3]	FMI	SW4	0.56[7]	—

1 measured after FMC kerosene/oxygen torch tests with Al_2O_3
2 ablator/adhesive debonding precluded accurate erosion measurements
3 char removed by gently tapping it with a screwdriver
4 char removed by vigorous scraping with a wire brush
5 not available at the time of the FMC torch tests
6 negative erosion indicates the surface was higher after the test than before
7 surface recession is *not* erosion but delamination and layer blow away
8 peripheral region is an annulus with 4-in inner radius and 7-in outer radius
9 internal crack due to fabrication technique reduces 'apparent' erosion

TABLE B-2. AVERAGE MEASURED CENTRAL[6] EROSION IN NSWCDD SIDEWINDER TESTS

MATERIAL TESTED	MANUFACTURER	TEST	NSWCDD AVERAGE MEASURED CENTRAL EROSION (IN)[3]	FMC MEASURED MAXIMUM EROSION (IN)[1]
CD208	Haveg	SW3	0.15[7]	0.12
Blackglas™	Allied Signal	SW4	(no test)	(note 2)
Blackglas™	Allied Signal	SW4	(no test)	(note 2)
BLM/E	FMI	SW2	0.21	(note 2)
CD208	Haveg	SW5	0.22	0.12
FR1	FMI	SW3	0.24	0.07
FM16771	AP	SW3	0.27	0.15
FR1	FMI	SW2	0.27	0.07
FM16771	Fiberite	SW3	0.28	—
MXBE350	Swedlow	SW2	0.29	0.40
MXBE350	Swedlow	SW5	0.30	0.40
CD208	Haveg	SW1	0.30	0.12
FM16771	AP	SW4	0.32	0.15
FM16771	Fiberite	SW1	0.32	—
MXBE350[4]	Swedlow	SW1	0.32	—
CA6304	Ferro	SW2	0.33	0.43
CA6304	Ferro	SW5	0.34	0.43
FTR402	FMI	SW1	0.36	0.19
FTR402	FMI	SW5	0.37	0.19
C[3]	FMI	SW4	0.49[5]	(note 2)

1 measured after FMC kerosene/oxygen torch tests with Al_2O_3
2 not available at the time for FMC to test
3 char removed by gently tapping it with a screwdriver
4 char removed by vigorous scraping with a wire brush
5 surface recession is *not* erosion but delamination followed by layer lift off
6 central region is inside a circle with a 4-in radius
7 internal crack due to fabrication technique reduces 'apparent' erosion

TABLE B-3. MAXIMUM MEASURED CENTRAL[6] EROSION IN NSWCDD SIDEWINDER TESTS

MATERIAL TESTED	MANUFACTURER	TEST	NSWCDD MEASURED MAXIMUM CENTRAL EROSION (IN)[3]	FMC MEASURED MAXIMUM EROSION (IN)[1]
Blackglas™	Allied Signal	SW4	(no test)	(note 2)
Blackglas™	Allied Signal	SW4	(no test)	(note 2)
CD208	Haveg	SW3	0.32[7]	0.12
BLM/E	FMI	SW2	0.36	(note 2)
MXBE350	Swedlow	SW2	0.42	0.40
CD208	Haveg	SW5	0.42	0.12
MXBE350	Swedlow	SW5	0.43	0.40
FM16771	AP	SW4	0.44	0.15
FM16771	AP	SW3	0.46	0.15
FR1	FMI	SW2	0.46	0.07
FR1	FMI	SW3	0.47	0.07
FM16771	Fiberite	SW3	0.47	—
CA6304	Ferro	SW2	0.51	0.43
FTR402	FMI	SW5	0.51	0.19
MXBE350[4]	Swedlow	SW1	0.51	—
FM16771	Fiberite	SW1	0.52	0.15
FTR402	FMI	SW1	0.52	0.19
CD208	Haveg	SW1	0.53	0.12
CA6304	Ferro	SW5	0.56	0.43
C[3]	FMI	SW4	0.61[5]	—

1 measured after FMC kerosene/oxygen torch tests with Al_2O_3
2 not available at the time for FMC to test
3 char removed by gently tapping it with a screwdriver
4 char removed by vigorous scraping with a wire brush
5 surface recession is *not* erosion but delamination and layer blow away
6 central region is inside a circle with a 4-in radius
7 internal crack due to fabrication technique reduces 'apparent' erosion

APPENDIX C

BACK WALL HEATING MEASURED IN NSWCDD SIDEWINDER TESTS

TABLE C-1. MAXIMUM MEASURED BACK-WALL TEMPERATURE IN NSWCDD SIDEWINDER TESTS

MATERIAL TESTED	MANUFACTURER	TEST	MEASURED BACK-WALL TEMPERATURE RISE (°F)	
			NSWCDD	FMC[1]
MXBE350	Swedlow	SW5	95	79
MXBE350	Swedlow	SW2	120	79
FM16771	AP	SW4	125	160
CA6304	Ferro	SW5	125	40
CA6304	Ferro	SW2	130	40
CD208	Haveg	SW5	165	117
FTR402	FMI	SW5	170	67
FR1	FMI	SW2	190	67
C[3]	FMI	SW4	425	(note 2)
BLM/E	FMI	SW2	450	(note 2)

1 measured during FMC kerosene/oxygen torch tests with Al_2O_3
2 not available at the time for FMC to test

DISTRIBUTION

	Copies
ATTN PMS4003B (K. PAYNE)	1
PMS420-11 (M. MILLER)	1
PMS422-11	1
PMS422-12	1
PMS422-31	1
062ZN1	1
062ZN2	1
COMMANDER	
NAVAL SEA SYSTEMS COMMAND	
2531 NATIONAL CITY	
BLDG 3	
WASHINGTON DC 20362-5160	
ATTN CODE 3276 ALLEN GEHRIS	1
COMMANDER	
NAVAL WEAPONS CENTER	
CHINA LAKE CA 93555-6001	
ATTN CODE 4L24 FORREST SICKLER	1
NAVAL SHIP WEAPON SYSTEMS	
ENGINEERING STATION	
PORT HUENEME CA 93043-5007	
CENTER FOR NAVAL ANALYSES	
4401 FORD AVE	
ALEXANDRIA VA 22302-0268	1
DEFENSE TECHNICAL	
INFORMATION CENTER	
CAMERON STATION	
ALEXANDRIA VA 22304-6145	12
ATTN GIFT AND EXCHANGE	
DIVISION	
LIBRARY OF CONGRESS	
WASHINGTON DC 20540	4

	Copies
ATTN AL PUHL	1
NATHAN RUBINSTEIN	1
JOHNS HOPKINS UNIVERSITY	
APPLIED PHYSICS	
LABORATORY	
JOHNS HOPKINS ROAD	
LAUREL MD 20707	
ATTN KENNETH A TAYLOR	1
RAYTHEON COMPANY	
EQUIPMENT DIVISION	
430 BOSTON POST ROAD	
WAYLAND MA 01778	
ATTN JOSEPH H KOO	1
MARK SCHNEIDER	1
DAVID HEIM	1
WINSTON CHUCK	1
SHAN LIN	1
MIKE MILLER	1
MIKE KNEER	1
FMC CORPORATION	
NAVAL SYSTEMS DIVISION	
4800 EAST RIVER ROAD	
PO BOX 59043	
MINNEAPOLIS MN 55459-0043	
ATTN CASS LAUX	1
DAVID ADAMS	1
MARTIN MARIETTA AERO AND	
NAVAL SYSTEMS	
103 CHESAPEAKE PARK PLACE	
BALTIMORE MD 21220	

DISTRIBUTION (Continued)

	Copies
ATTN JACK SIKONIA	1
STEVE GONZY	1
ALLIED SIGNAL RESEARCH AND TECHNOLOGY	
PO BOX 1021R	
MORRISTOWN NJ 07962-1021	
ATTN HAL WEATHERLY	1
AMERICAN POLY-THERM CO INC	
2000 FLIGHTLINE DR	
LINCOLN CA 95648	
ATTN BERT HECHT	1
ARCADY CHECHIK	1
AMETEK INC	
HAVEG DIVISION	
900 GREENBANK RD	
WILMINGTON DE 19808	
ATTN FRED SEIBERT	1
DON BECKLEY	1
BP CHEMICALS (HITCO) INC	
700 E DYER RD	
SANTA ANA CA 92705-5611	
ATTN CHIP ROTH	1
JERRY HARTMAN	1
HEMANT GUPTA	1
SP SYSTEMS	
MONTECATINI ADVANCED MATERIALS	
5915 RODEO ROAD	
LOS ANGELES CA 90016	
ATTN SCOTT STEPHENSON	1
FIBER MATERIALS INC	
5 MORIN ST	
BIDDEFORD INDUSTRIAL PARK	
BIDDEFORD ME 04005-4497	

	Copies
ATTN ED HEMMELMAN	1
DAN DALENBERG	1
ICI FIBERITE	
501 WEST THIRD ST	
WINONA MN 55987	
ATTN CLINT JUHL	1
RAY WILLIAMS	1
ICI FIBERITE	
23271 VERDUGO DR	
SUITE A	
LAGUNA HILLS CA 92653	
ATTN BILL GRAHAM	1
GERHARD SCHIROKY	1
LANXIDE CORP	
1300 MARROWS RD	
PO BOX 6077	
NEWARK DE 19714-6077	
ATTN JIM WHITE	1
SWEDLOW INC	
12122 WESTERN AVE	
GARDEN GROVE CA 92645	
ATTN WILHELM BETZ	1
BRANDENBERGER-ISOLIERTECHNIK GMBH & CO KG	
POSTFACH 1164 + 1165	
TAUBENSUHLSTRASSE 6	
D-6470 LANDAU/PFALZ	
WEST GERMANY	
ATTN KLAUS MEYER	1
FRATHERM ISOLIERUNGS GMBH	
POSTFACH 90 03 69	
FRAUENLOBSTRASSE 2	
D-6000 FRANKFURT/MAIN 90	
WEST GERMANY	

DISTRIBUTION (Continued)

	Copies
ATTN DANIEL QUENTIN SNPE US OPERATIONS 1111 JEFFERSON DAVIS HWY SUITE 700 ARLINGTON VA 22202	1
ATTN JACKEY PATTEIN SNPE ARMOR COMPOSITES 29590 POINT-DE-BUIS FRANCE	1
ATTN ETIENNE SUBRENAT SEP SOLID PROPULSION AND COMPOSITES DIV LE HAILLAN BP 37 33165 SAINT-MEDARD EN JALLES FRANCE	1
ATTN CLAUDE BONNET SEP INC 1100 17TH ST NW SUITE 320 WASHINGTON DC 20036	1
TPRL CINOAS BUILDING 2595 YEAGER RD WEST LAFAYETTE IN 47906	1
INTERNAL DISTRIBUTION	
B02	1
B05 MOORE	1
D04	1
E281 WAITS	1
E231	3
E232	2
G205 LONG	1
G205 MILLER	1
G205 PUIG	1
G21 ATKINSON	1
G21 MILLS	1
G21 PRITCHETT	1
G22 WAGGENER	1
G91 BULLOCK	1
GH0	1
GH1 BOWEN	1
GH1 GESSLER	1
GH3	1
GH3 ANDERSON	1
GH3 BOWEN	1
GH3 BOYER	25
GH3 BURGESS	1
GH3 CHESTER	1
GH3 DELOACH	1
GH3 FREDERICK	1
GH3 KORDICH	1
GH3 MILLER	1
GH3 POWERS	1
GH3 SOO HOO	1
GH3 VENDETTUOLI	1
K22 OPEKA	1
K22 VARICK	1
L11 HARMAN	1
N74 GIDEP	1
N84	1
R07 MESSICK	1
R31	1
R31 DUFFY	1
R31 HAUGHT	1
R31 TALMY	1
R31 WELLER	1
R31 ZAYKOSKI	1
R34 LIU	1
R34D	1

REPORT DOCUMENTATION PAGE

Form Approved
OMB No. 0704-0188

1. AGENCY USE ONLY (Leave blank)	2. REPORT DATE	3. REPORT TYPE AND DATES COVERED
	October 1992	

4. TITLE AND SUBTITLE
Performance of Reinforced Polymer Ablators Exposed to a Solid Rocket Motor Exhaust

5. FUNDING NUMBERS

6. AUTHOR(S)
C. Boyer, T. Burgess, J. Bowen, K. Deloach, I. Talmy, D. Haught, J. Duffy, & J. Zaykoski

7. PERFORMING ORGANIZATION NAME(S) AND ADDRESS(ES)
Naval Surface Warfare Center
Dahlgren Division (Code GH3)
Dahlgren, VA 22448-5000

8. PERFORMING ORGANIZATION REPORT NUMBER
NAVSWC TR 91-645

9. SPONSORING/MONITORING AGENCY NAME(S) AND
NSWCDD VLS Program Office, Mr. Mike Puig (G205)
NSWCDD IED Program Office, Dr. Glen Moore (H023)

10. SPONSORING/MONITORING AGENCY REPORT NUMBER

11. SUPPLEMENTARY NOTES

12a. DISTRIBUTION/AVAILABILITY
Approved for public release; distribution is unlimited.

12b. DISTRIBUTION CODE

13. ABSTRACT *(Maximum 200 words)*

Summarized in this report is the effort by the Naval Surface Warfare Center Dahlgren Division (NSWCDD) and FMC Corporation (a launcher manufacturer) to identify new high performance ablators suitable for use on Navy guided missile launchers (GML) and ships' structures. The goal is to reduce ablator erosion by 25 to 50 percent compared to that of the existing ablators such as MXBE350 (rubber-modified phenolic containing glass fiber reinforcement). This reduction in erosion would significantly increase the number of new missiles with higher-thrust, longer-burn rocket motors that can be launched prior to ablator refurbishment. In fact, there are a number of new Navy missiles being considered for development and introduction into existing GML: e.g., the Antisatellite Missile (ASM) and the Theater High-Altitude Area Defense (THAAD) Missile.

The U.S. Navy experimentally evaluated the eight best fiber-reinforced, polymer composites from a possible field of 25 off-the-shelf ablators previously screened by FMC Corporation. They were tested by the Navy in highly aluminized solid rocket motor exhaust plumes to determine their ability to resist erosion and to insulate. Izod impact tests were conducted to characterize their flexibility and resistance to cracking. Finally, these materials were studied using scanning electron microscopy (SEM) and thermogravimetric analysis (TGA) to better understand the macroscopic behavior they demonstrated. Each of these new ablators tested at NSWCDD was only comparable to or significantly inferior to the existing in-service ablator MXBE350 when it came to erosion resistance in the presence of flows producing high convective heating and also heavily laden with aluminum-oxide particles. Hence the Navy and FMC are working with both domestic and foreign composite developers to modify existing ablator designs in hopes of achieving the desired performance improvements in 1992.

14. SUBJECT TERMS			15. NUMBER OF PAGES
ablator	Guided Missile Launchers	erosion	98
tactical missiles	convective heating	solid rocket motors	16. PRICE CODE
aluminum oxide particles			

17. SECURITY CLASSIFICATION OF REPORT	18. SECURITY CLASSIFICATION OF THIS PAGE	19. SECURITY CLASSIFICATION OF ABSTRACT	20. LIMITATION OF ABSTRACT
UNCLASSIFIED	UNCLASSIFIED	UNCLASSIFIED	SAR